Continental Margin Sedimentation

From Sediment Transport...

Edited by
C.A. Nittrouer
J.A. Austin
M.E. Field
J.H. Kravitz
J.P.M. Syvitski
and P.L. Wiberg

...to Sequence Stratigraphy

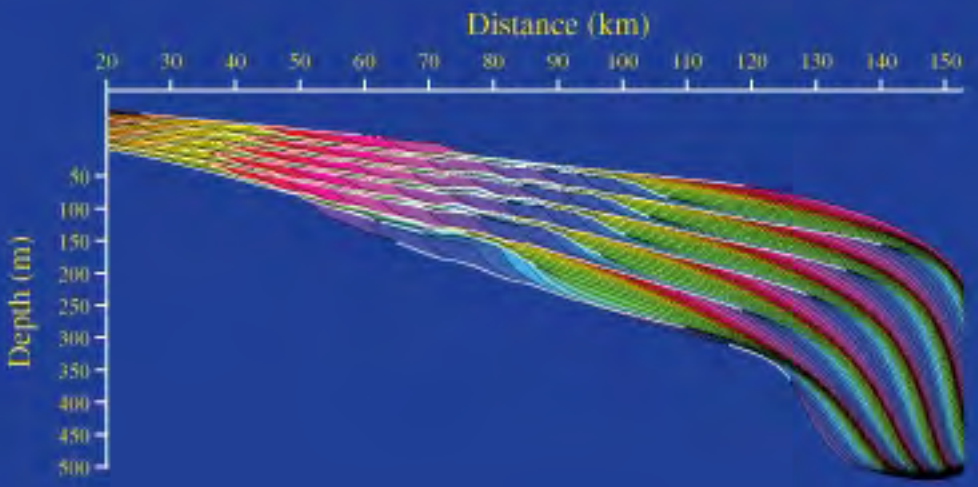

Special Publication
Number 37
of the International
Association of
Sedimentologists

Blackwell
Publishing

BLACKWELL PUBLISHING
350 Main Street, Malden, MA 02148-5020, USA
9600 Garsington Road, Oxford OX4 2DQ, UK
550 Swanston Street, Carlton, Victoria 3053, Australia

First published 2007 by Blackwell Publishing Ltd

1 2007

Library of Congress Cataloging-in-Publication Data
Continental margin sedimentation : from sediment transport to sequence stratigraphy / edited by C.A. Nittrouer . . . [*et al.*].
p. cm. – (Special publication number 37 of the International Association of Sedimentologists)
Includes bibliographical references and index.
ISBN 978-1-4051-6934-9 (hardback : alk. paper)
1. Sedimentation and deposition. 2. Sedimentology. 3. Sequence stratigraphy. 4. Sediment transport. 5. Continental margins. I. Nittrouer, Charles A.

QE571.C57 2007
551.3'53–dc22

2007007166

A catalogue record for this title is available from the British Library.

Set in 10.5/12.5pt Palatino
by Graphicraft Limited, Hong Kong
Printed and bound in Singapore
by Markono Print Media Pte Ltd

For further information on
Blackwell Publishing, visit our website:
www.blackwellpublishing.com

The long-term stratigraphic record on continental margins

GREGORY S. MOUNTAIN*, ROBERT L. BURGER†, HEIKE DELIUS‡, CRAIG S. FULTHORPE§, JAMIE A. AUSTIN§, DAVID S. GOLDBERG¶, MICHAEL S. STECKLER¶, CECILIA M. McHUGH**, KENNETH G. MILLER*, DONALD H. MONTEVERDE*, DANIEL L. ORANGE†† *and* LINCOLN F. PRATSON‡‡

*Rutgers, the State University of New Jersey, Piscataway, NJ 08854, USA (Email: gmtn@rci.rutgers.edu)
†Yale University, New Haven, CT 06520, USA
‡Task Geoscience, Ltd, Aberdeen AB23 8GX, UK
§University of Texas Institute for Geophysics, Austin TX 78759-8500
¶Lamont-Doherty Earth Observatory, Palisades, NY 10964, USA
**Queens College, Flushing, NY 11367, USA
††AOA Geophysics, Inc., Moss Landing, CA 95039, USA
‡‡Duke University, Durham, NC 27708, USA

ABSTRACT

Processes that build continental-margin stratigraphy on time-scales of > 20 kyr have been investigated. Eustatic sea-level exerts a major influence on sedimentation, but the Eel River margin shows that its effects can be interwoven with those of tectonism. Rapid Oligocene subsidence along the Cascadia subduction zone resulted in a foundered forearc basin. Regression and sedimentary reconstruction began in the Pliocene, and up to 1 km of sediment has accumulated since then, with rotating faults, synclines, anticlines and regional uplifts marking plate interactions. Fourteen seismic unconformities along structural highs can be traced into synclines. Many are ravinements formed during rising sea level, and ~70–100 kyr cyclicity suggests a glacio-eustatic signal. Incised channels formed during regressions over the past ~360 kyr, when rivers drained into Eel Canyon. In contrast, the New Jersey margin has long been dormant tectonically, providing clearer access to a eustatic imprint. Lack of Paleogene sediment supply resulted in a carbonate ramp prior to development of Oligocene deltas. With little accommodation space to allow aggradation, clinoforms prograded ~100 km seaward, reaching the shelf break by Late Pleistocene. Coastal-plain drilling recovered ~15 Oligocene and Miocene highstand deposits, which correlate with glacio-eustatic oscillations. Beneath the mid-to-outer shelf, incised valleys have been preserved, and clinoform strata suggest reworking of lobate deposits. Four Late Pleistocene sequences reveal no hiatuses at sequence boundaries, and no correlations between glacio-eustatic oscillations and stratal architecture. Stratal discontinuities are a common feature in margin sediments and provide objective means of interpreting the geological record. Continuous coring is essential to understand the processes that create stratal architecture.

Keywords Eustatic sea level, forearc basin, unconformities, tectonism, accommodation space, shelf valleys, sequence stratigraphy, clinoforms.

INTRODUCTION

This paper describes the production of the long-term stratigraphic record on continental margins. Concepts and analytical techniques are presented first, and then two diverse margins (Eel and New Jersey) are described and contrasted. The goal is to provide a general understanding of the long-term stratigraphic record, reinforced by specific examples of distinctly different continental margins.

Distinguishing time-scales

While there is no generally accepted distinction between long- and short-term sedimentary records, and furthermore, no standardization as to what constitutes the briefest of all – the event-scale record – the following criteria are adopted here. **Events** are processes lasting minutes to days that include (but are not limited to) ash falls, massive storms and floods, abrupt tectonic disturbances, tsunamis and extraterrestrial impacts. Each can leave a distinct imprint on the sedimentary record at a regional and global scale and may provide the ability to establish near-synchroneity to the origin of widely separated stratigraphic features. Many papers in this volume exploit event-scale processes recorded in cores or monitored in the water column above the seabed during observations that span months to years. These processes combine to create the **short-term** sedimentary record, defined here as sediments deposited since the **Last Glacial Maximum** (LGM; ~20 ka).

The **long-term** record pertains to sediments older than ~20 ka, and contains the history of shorter term processes. Typically, events are aperiodic and unpredictable, in contrast to long-term processes that are either the integrated sum of individual events, or occur with measurable periodicities. For example, earthquakes and resultant debris flows constitute events that, if adequately preserved, can provide a correlation marker. Such events are short-lived and unpredictable, but if they occur often enough their net effect is an important control on sediment distribution, and is relevant to analysing the long-term record. Therefore, this paper will touch on some parts of the short-term record that provide a context for better understanding of the long-term record.

The importance of the long-term record

If well-preserved, aperiodic events can provide distinct stratigraphic markers, and the 'short-term' record can yield information on time-scales relevant to human activities; why should the 'long-term' record be considered valuable? There are several answers.

First, the long-term record documents behaviour of the complex Earth system under boundary conditions that may be very different from those of today. Monitoring active processes or consulting the short-term record simply cannot capture the complete range of Earth system activity. For example, to understand fully the role of sea level in the delivery of sediment to a continental shelf and beyond, only the long-term record provides the opportunity to examine this process during glacial maxima, when sea level was as much as 120 m below present. At these times, rivers were downcutting and flushing previously sequestered sediment from floodplains; but how much and by what processes did this sediment remain on an exposed shelf, or how much and by what processes did it bypass the shelf entirely? This cannot be determined by examining either the modern world or the short-term record. As another example, global temperatures during the late middle Eocene were as high as at any time in the past 100 Myr (Savin, 1977; Miller *et al*., 1987a); what effects on precipitation/weathering/runoff can be ascribed to this extreme state, and what insight does this provide to understanding changes that may be developing today as global warming becomes increasingly significant? To begin answering these questions, the long-term record must be analysed.

Second, consulting the long-term record provides the chance to evaluate numerical models that are intended to duplicate real-world phenomena (see Syvitski *et al*., this volume, pp. 459–529). This model-checking confirms or refutes that the Earth system works in the manner described by the model. For example, it is known that rifted lithosphere becomes more rigid with time, but is this actually manifested (as the rigid-plate model predicts; e.g. Watts *et al*., 1982) in a long-term onlap of the craton, measured in hundreds of kilometres over tens of millions of years? Model-checking also provides sensitivity tests concerning the significance of various parameters to the working of the whole system. For example, does a doubling in the rate of sea-level rise double the rate of shoreline retreat?

Third, many fundamental processes that drive the Earth system, or allow us to monitor it, act on time-scales far longer than the short term (~20 kyr). Late Pleistocene glaciers advanced and retreated on 100-kyr cycles (Imbrie *et al*., 1984); total magnetic-field reversals occur at ~0.1–1 Myr intervals (Lowrie & Kent, 2004); spreading-rate changes at mid-ocean ridges can occur on 10-Myr

time-scales with significant impact on global sea level (Hays & Pitman, 1973); even evolutionary change itself, providing one of the most fundamental yardsticks for measuring geological time, proceeds too slowly for the past 20 kyr to detect meaningful change. In sum, only studies based on the long-term record can capture the full range of fundamental processes that characterize and shape continental margins.

Long-term geochronology: dating continental-margin records

Radiometric dating is generally not applicable to the study of long-term continental-margin records because suitable material is not available. Consequently, time equivalency (correlation) is usually established through **biostratigraphy** using fossils, **magnetostratigraphy** using reversals of the Earth's magnetic field, and **chemostratigraphy** using variations in isotope ratios ($^{18}O/^{16}O$, $^{14}C/^{12}C$ and $^{87}Sr/^{86}Sr$). Dates are then assigned by tying the fossil, magnetic and isotopic records to a standard time-scale. Pleistocene sediments older than 40–60 ka (the extent of the radiocarbon technique) are the most difficult to date due to sparse biostratigraphic events as well as to the length of the most recent epoch of normal magnetic polarity (0–790 ka; Lowrie & Kent, 2004). Tertiary sediments are frequently dated by integrating biostratigraphy with Sr-isotopic stratigraphy (Miller *et al*., 1998a). Age resolution for Tertiary strata varies; it can be as fine as ±0.5 Myr, but in some cases age uncertainties may reach many millions of years.

Planktonic foraminifera, coccolithophores, diatoms and pollen are the taxa most commonly used to establish the biostratigraphy of the continental-margin successions considered in this paper (i.e. 20 ka to 40 Ma). Most studies from the submerged subsurface utilize core samples or drill cuttings, and consequently they depend on microfossils and fragments of mollusc shells. The resolution of dates derived from fossil content depends ultimately on the rate of evolution, the state of fossil preservation and the ability to identify changes in morphology from one stratigraphic level to the next. At any given position in the rock record, the ability of fossils to provide an age determination requires the appearance or disappearance of key index fossils. There are times of rapid evolutionary change that provide temporal resolution approaching ±0.5 Myr (e.g. the early to middle Eocene) and others in which resolution remains ±1–2 Myr (e.g. the late Oligocene) (Berggren *et al*., 1995).

The application of magnetogeochronology relies on measuring the direction of remanent magnetization in sediments. Total field reversals appear to be aperiodic, with time between reversals varying from 0.1 to 1 Myr for the interval considered in this paper (e.g. Berggren *et al*., 1995; Lowrie & Kent, 2004). Consequently, when coupled with other dating tools, the identification of remanent direction can potentially narrow the probable age by a factor of two or more.

Four types of geochemical dating are commonly used in the study of continental-margin sediments: $^{87/86}Sr$, $^{18/16}O$, $^{14/12}C$ and amino acid racemization. The first two depend on an independently derived curve of isotopic change, to which a measured value is compared. The latter two depend on knowing a time-dependent rate of change that needs no independent information; the value of the sample itself provides its age. A variety of post-depositional processes can degrade the reliability of these measurements because they depend on a geochemical system remaining closed since the time of deposition.

ANALYSING THE LONG-TERM RECORD

Basin-wide surfaces and long-term processes

The development of sequence stratigraphy

Despite all that has been learned in the past 200 yr about stratigraphy (Nystuen, 1998), controversy over what controls the long-term sedimentary record still focuses on eustasy versus tectonism. One observation that has endured, however, is that widespread **unconformities** divide the rock record into distinct sedimentary packages. Debate may continue as to what caused these breaks, but their existence is universally accepted.

Lateral changes in facies were described by Walther (1894), when he recognized the critical aspect of time-transgressive deposition that results in horizontal facies changes repeated in vertical successions. Therefore, the physical character of rocks can be unreliable for evaluating time equivalency

between widely separated units, and bounding unconformities may be extremely valuable in establishing stratigraphic correlation. However, using stratal discontinuities has serious shortcomings, because local response to a global process can mask the true sequence of events. For example, glacial cycles have long been recognized as a mechanism for the origin of boundaries in sedimentary rocks (Agassiz, 1840; Maclaren, 1842), but large ice sheets can depress the Earth's surface, and, as they melt, the crust progressively rebounds to create a purely local regression (Jamieson, 1865).

The debate regarding the cause for widespread unconformities continued into the mid-20th century (Stille, 1924; Grabau, 1940), but many scientists accepted evidence of ocean water periodically spilling onto the continents to form widespread marine deposits, and receding to form long-period, continent-wide unconformities. For example, six unconformably bounded units of Cambrian to Tertiary age were traced across North America by Sloss (1963). These rock-stratigraphic units were termed **sequences** and their significance lay in the unifying processes invoked to explain such widespread distribution.

The digital revolution of the 1970s dramatically improved the quality of seismic-reflection data, revealing the geometry of buried strata with previously unseen clarity. These improvements, coupled with the search for fossil fuels, accelerated the pace of seismic surveying on continental margins, and soon a community of classically trained stratigraphers began to develop new ways of applying reflection profiles to the interpretation of basin history. The technique, termed **seismic stratigraphy** (Payton, 1977), was quickly accepted, and with some refinements remains the most widely used approach to study the long-term record of continental margins.

Seismic stratigraphy exploits the fact that physical contrasts across bedding planes or between packages of beds lead to acoustic reflections. Consequently, patterns of seismic reflections in the subsurface closely match buried stratal geometry. To be detected, these contrasts must be vertically abrupt at the scale of metres to tens of metres, and must persist laterally for tens to hundreds of metres. Hence, gradual velocity/density changes that coincide with lateral (time-transgressive) facies changes are typically too subtle to be detected acoustically.

Mitchum *et al*. (1977a,b) described patterns of buried geometries revealed by seismic profiles, and demonstrated that strata could be grouped into unconformably bounded units. Vail *et al*. (1977) identified many more unconformities than were known from previous studies of the rock record. For example, the two youngest units described by Sloss (1963) were divided into more than two dozen unconformity-bounded subunits, and these were later revealed to contain still more subunits (Haq *et al*., 1987). The underlying approach to these studies, whether based on outcrops, boreholes or seismic profiles (e.g. Van Waggoner *et al*., 1988), held to the same tenet: stratal discontinuities comprise an imprint of global processes on the long-term record of depositional systems.

Basin-wide stratal gaps spanning similar time intervals suggested the possibility of a common cause operating on a 1–2 Myr time-scale associated with changes in global sea level (**eustasy**; Vail *et al*., 1977; Posamentier *et al*., 1988). This explanation has generated controversy for a variety of reasons (e.g. Christie-Blick, 1991; Miall, 1991; Karner & Driscoll, 1997). Although the utility of analysing the geological record in terms of unconformably bound stratal units is widely accepted, many scientists are unwilling to accept that synchrony in widely separated basins can be established with sufficient confidence to prove a single cause. Numerical models also indicate that the stratigraphic imprint of eustatic change would be asynchronous in basins having different tectonic histories. Furthermore, variations in deltaic sedimentation, even in the absence of eustatic change, can build stratigraphic architecture that is very difficult to distinguish from those imposed by true changes in global sea-level. Eustatic changes every 1–2 Myr strongly suggest the growth and decay of polar ice sheets (no other mechanism is known to be of sufficient amplitude or frequency, see Harrison, 1990), but there is no geological or isotopic evidence to support their unbroken, cyclic occurrence over the past 200 Myr as Haq *et al*. (1987) proposed.

Current stratigraphic models

Despite the lack of consensus as to cause, there is general agreement that the sedimentary record is discontinuous at a wide range of scales. These pervasive breaks are expressed as abrupt changes

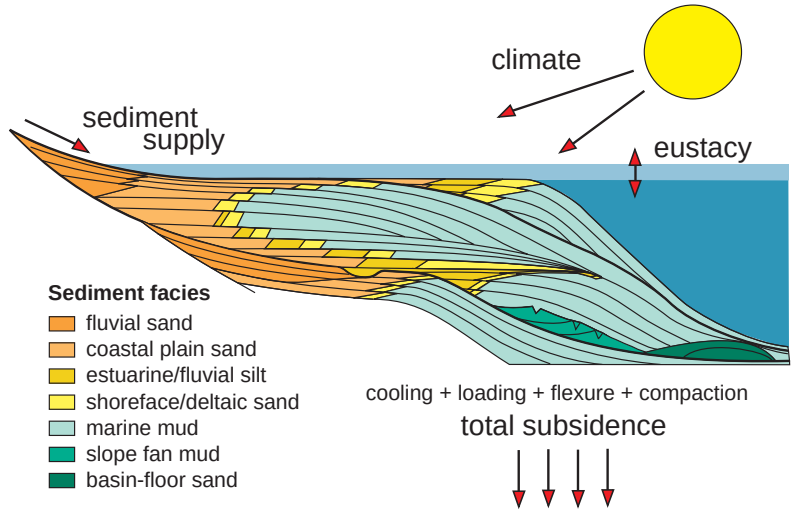

Fig. 1 An idealized clinoform, comprising a fundamental stratigraphic element of detrital sediment deposited adjacent to a point source flowing into standing water. It has been proposed that the influences of sediment supply, total subsidence, climate and eustasy control the distribution of facies as indicated. (After Mitchum, 1977a; Vail *et al*., 1977.)

in biofacies, lithofacies, and/or the angular termination of stratal surfaces. Seismic profiles can reveal in a single cross-section the arrangement of stratal surfaces that cannot be resolved by outcrops or boreholes. The basic unit of seismic stratigraphic analysis is the **depositional sequence**, defined as a genetically related package of sediments bounded above and below by unconformities and their correlative conformities (Mitchum, 1977a). On continental margins, a prominent type of sequence develops an overall sigmoidal shape (Fig. 1), and is termed a **clinoform**. These are characterized by relatively gently dipping strata at their landward (**topset**) and basinward (**bottomset**) extremes, and more steeply dipping (**foreset**) strata between these locations. The transition between topset and foreset beds is termed the **rollover**.

Clinoforms are a fundamental stratigraphic element of continental margins, and develop wherever detrital sediments are transported from shallow to deeper water (Posamentier *et al*., 1988). Vertical dimensions range from centimetres to hundreds of metres, and horizontal dimensions from metres to hundreds of kilometres. Although a clinoform resembles the cross-sectional shape of sediments comprising an entire continental margin (Posamentier & Vail, 1988), it is incorrect to equate these structures and conclude that they record the action of similar processes. Bottomsets of a typical sequence lie immediately basinward of foresets of the previous sequence, and, with time, onlap the clinoform and completely bury it. The height of typical continental slopes places any 'bottomset' strata hundreds to thousands of metres below the 'topset' strata of the shelf. This amount of topographic relief cannot be accounted for within time spans represented by sequences. Clinoform rollovers and continental shelf breaks may coincide spatially, but they are the result of different processes (Steckler *et al*., 1993).

Clinoforms typically stack one above the other, and despite complexities (see Christie-Blick & Driscoll, 1995), each sequence is distinguished by its bounding unconformities. Three principal types of angular discordance are recognized: **onlap**, **downlap** and **toplap** (Mitchum, 1977b) (Fig. 2). The first describes an angular termination of strata building landward against the basal unconformity of a sequence. The second describes angular terminations building basinward across an underlying unconformity. The third describes stratal terminations caused by an unconformity that defines the top of a sequence, created either by sediment bypassing or erosion. Pre-existing topography, local tectonism, ocean currents and localized sediment sources are some of the many processes and features that lead to complex three-dimensional stratal geometries, and make it possible for one surface to exhibit all three classes of termination in the same basin. Hence, the complexity of a basin dictates how many profiles must be examined before identifying basin-wide sequence boundaries (see Karner & Driscoll, 1997).

An important concept that is still being evaluated is that sequence boundaries possess a time-stratigraphic significance (Vail *et al*., 1977): all strata

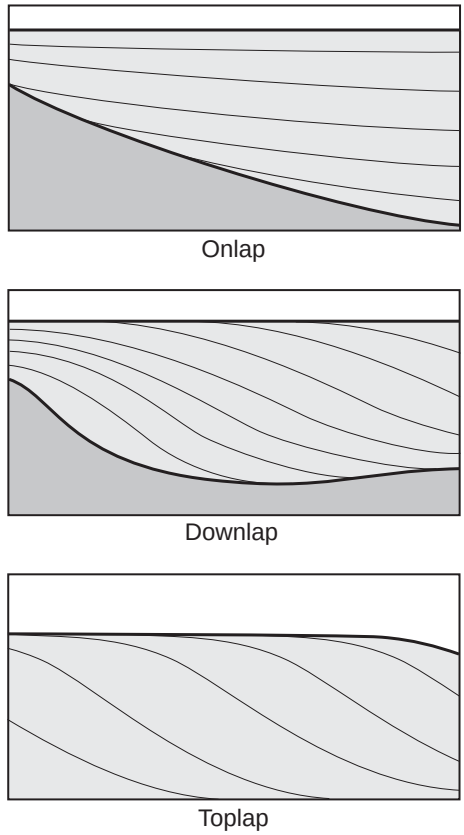

Fig. 2 Three principal types of angular discordance between reflectors (thin lines) and bounding unconformities (bold lines) interpreted as sequence boundaries. (After Mitchum *et al*., 1977b.)

above a sequence boundary are younger than all strata below. Once identified in this manner, the strata confined to a given sequence can be interpreted in a chronostratigraphic context distinct from that of other sequences in that same basin.

The arrangement of strata within a sequence usually follows one of two patterns, depending on the type of basal sequence boundary. A **Type I** boundary is the result of subaerial erosion across the entire upper surface of the previous sequence (Van Waggoner *et al*., 1988). Consequently, the strata show evidence of erosion (including valley incision) into the previous sequence, abrupt upward shoaling of facies across the basal sequence boundary, and shallow-water sediments deposited in a deep-water turbidite system basinward of the clinoform. **Type II** boundaries develop without subaerial exposure of marine sediment, submarine-fan deposition, or abrupt upward shoaling (Van Waggoner *et al*., 1988). Regardless of the type of basal unconformity, all sequences show an upward progression from onlap to toplap, and the downlap surface that divides these patterns represents a major intrasequence feature termed the **maximum flooding surface** or MFS (Fig. 3). Some workers consider this to be the most readily recognized and useful marker within siliciclastic, continental-margin settings. This approach to basin analysis, termed **genetic stratigraphy** (Galloway, 1989), exploits the ease of identifying a MFS over the occasional difficulty of locating a basin-wide unconformity (sequence boundary) in an up-dip setting where there are many other hiatuses.

Detecting intrasequence geometry attests to sharp changes in physical properties that coincide with bedding or groups of beds within a single unconformably bounded sequence. The most common change in detrital sediments along a continental margin is for relatively coarse-grained sediment to be overlain by finer-grained sediment. In turn, the fine sediments typically coarsen upwards in a gradual manner, without abrupt contrasts that could otherwise generate reflections, until replaced at a sharp contact by finer-grained sediment. These coarsening upward units are termed **parasequences** and are the building blocks of sequences (Van Waggoner *et al*., 1988). The geometric relationships of parasequences define **system tracts** (Posamentier *et al*., 1988).

The major influences on stratigraphic succession are sediment supply, global sea level (eustasy) and **total tectonism** (the sum of basin subsidence/uplift, thermal subsidence, sediment loading and sediment compaction). Both physical and numerical models predict the effects of these factors individually (Parker *et al*., 1986; Reynolds *et al*., 1991; Steckler *et al*., 1993; Niedoroda *et al*., 1995; Syvitski *et al*., 1999). However, the interactions among factors also exert significant control on the long-term record. For example, the manner in which a large supply of fluvial sediment will disperse and accumulate on the shelf is determined by the space available below wavebase (i.e. **accommodation space**), which in turn is controlled by the balance between eustasy and total subsidence. Choosing among these factors presents a daunting challenge to the geologist attempting to extract the history of events that produce the geometries revealed in seismic profiles.

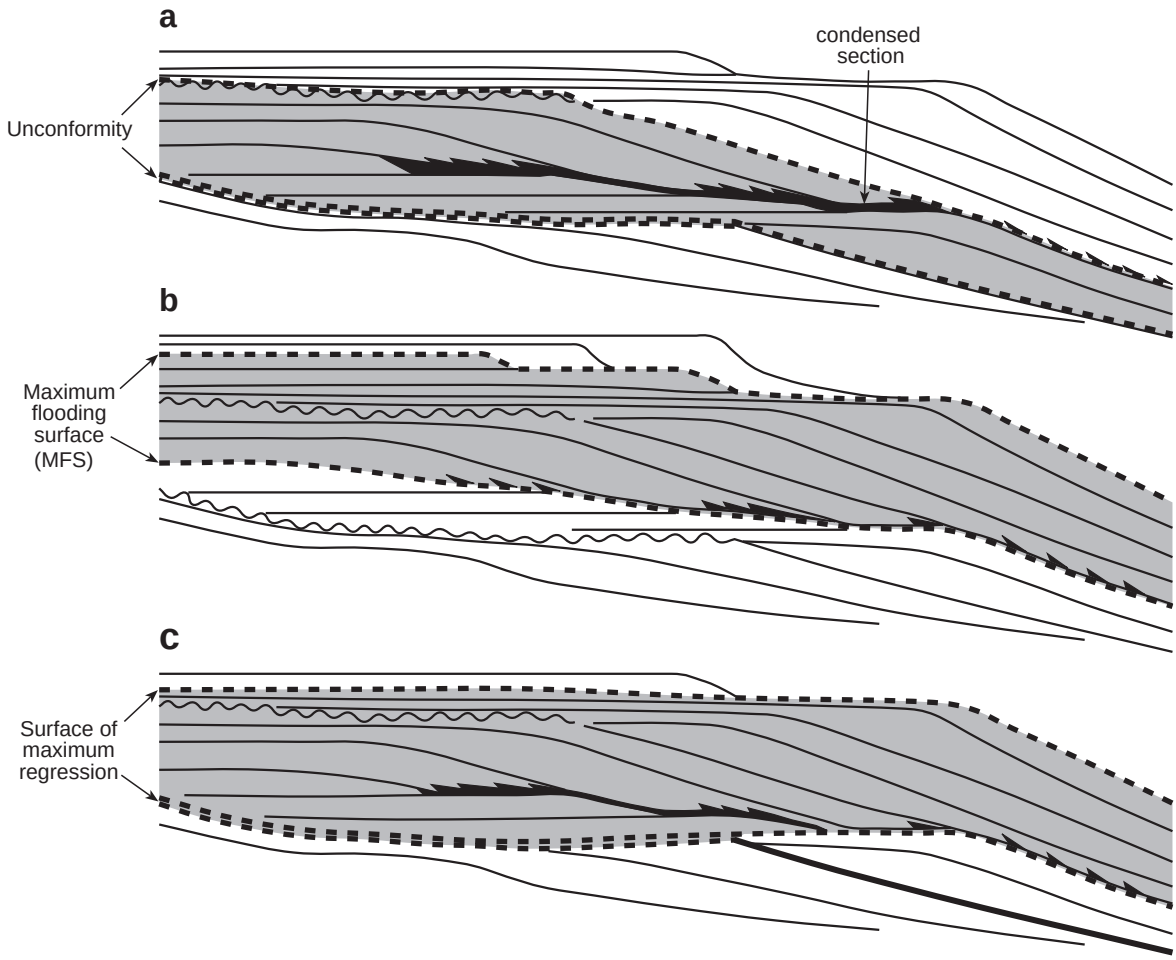

Fig. 3 Three ways of defining sequences based on stratal relationships. (a) Sequences are bounded by unconformities or their correlative conformities. (b) Sequences are bounded by maximum flooding surfaces. (c) Sequences are bounded by surfaces of maximum regression. (From Posamentier & Allen, 1999.) Reproduced with permission from SEPM (Society for Sedimentary Geology).

Tools for accessing the long-term record

Seismic stratigraphy

Seismic reflections are the result of downgoing acoustic energy encountering abrupt vertical changes in sound velocity and/or bulk density beneath the seafloor. The product of velocity and density is defined as **acoustic impedance** and, in general, the greater the vertical change in impedance, the larger the amplitude of the reflected energy. However, sound energy decreases as the square of the distance travelled. Particle-to-particle friction reduces energy further (as a function of frequency, distance, velocity and absorption coefficient of the medium). Low frequencies and slow velocities allow energy to propagate the greatest distance. For this reason, reflected wavelets can be appreciably different from those that enter the subsurface (e.g. Tucker & Yorston, 1973).

The reliability of interpretations based on weak reflections depends on the ability to distinguish true reflected energy from noise. Common sources of noise include rough sea state and poor towing characteristics of the sound receiver (streamer) and sound source. Artefacts that generate unwanted reflections include, but are not limited to: seafloor and internal ('peg-leg') multiples, diffracted arrivals and out-of-plane reflections. Although each can be minimized with appropriate acquisition

techniques or specially designed data processing, their occurrence cannot be eliminated.

The practical limits to vertical seismic resolution have been thoroughly studied and shown to depend largely on the frequency of the seismic source (Widess, 1973; Neidell & Poggiagliolmi, 1977; Sheriff, 1977, 1985; Mahradi, 1983). High frequencies resolve more closely spaced reflectors than do low frequencies, but they are unable to penetrate as far into the seabed. Hence, the desirable seismic source is as broadband as practical; the higher frequencies provide optimum resolving power in the shallow part of the section, and lower frequencies penetrate to greater depth and return reflected energy (but with reduced resolution). Experiments and numerical models show that reflections from two surfaces can be clearly resolved when separated by a distance of at least one wavelength of the downgoing acoustic pulse. As the vertical separation narrows, the two reflections begin to interfere, but can be resolved down to separations of one-eighth wavelength. At still narrower distances, the contribution of reflected energy from the two surfaces can no longer be distinguished, despite the fact that some sort of surface or group of surfaces can be detected (Widess, 1973).

Acoustic energy travels as spherically spreading waves, and each impedance change acts as a secondary source of these waves. As a result, reflections that appear to come from directly beneath the streamer may originate at a different location. The distance ahead, behind or to either side of the shortest path to a point on a buried reflector gives rise to the concept of a **Fresnel Zone** (Sheriff, 1977), or acoustic footprint. The smaller the footprint, the better one can distinguish features separated by a narrow horizontal distance (see Sheriff (1985) for details). The size of the footprint is governed by velocity and frequency of the seismic pulse, and the distance to the reflector.

Backstripping

Seismic profiles provide information about how continental-margin strata are arranged in space (i.e. through conversion from travel-time), but identifying the effects of tectonism, climate change, sea-level change and sediment supply in building that record presents a significant challenge (see additional discussion in Syvitski *et al*., this volume, pp. 459–529). Backstripping is frequently used to estimate tectonic subsidence by accounting for and removing the effects of other causes of subsidence, such as loading due to the weight of the sedimentary column. However, where tectonic subsidence can be estimated, as is the case for the New Jersey margin, the backstripping approach can be used instead to calculate the palaeobathymetry (e.g. Kominz *et al*., 1998) and, from there, to reconstruct the stratigraphy through time (Steckler *et al*., 1988, 1999). The rate of tectonic subsidence on this old passive margin is low (0–4 m Myr^{-1}), and can be readily estimated from previous tectonic analyses (e.g. Steckler *et al*., 1988; Keen & Beaumont, 1990). In contrast, the subsidence of active margins such as the Eel River basin is complex (Clarke, 1992; Gulick *et al*., 2002) and cannot be estimated sufficiently for backstripping.

Reconstructing sedimentation on a continental margin using the backstripping technique comprises several steps (Fig. 4a–f) (Steckler *et al*., 1993) that sequentially remove the accumulated effects of subsidence or deformation. The first step is to strip off all sediment above the horizon of interest (Fig. 4b). The weight of sediment corresponding to the removed interval is then calculated, and the remaining layers are flexurally unloaded (Fig. 4c). However, the correct value for **flexural rigidity** of continental margins is a matter of debate (Watts, 1988; Fowler & McKenzie, 1989; Karner, 1991; Kooi *et al*., 1992). To estimate its value on the New Jersey margin, for example, a parameterization has been used that accounts for the influence of large variations in sediment and crustal thickness at the margin, as well as other factors (Lavier & Steckler, 1997). This model predicts that the Miocene elastic thickness on the New Jersey margin varies between 23 and 30 km, and this range has been used to compute the **isostatic rebound** of the underlying layers (Steckler *et al*., 1999).

Backstripping is an iterative process, and the next step is to correct for the **compaction** that occurred due to the weight of overlying sediments removed in the previous step (Fig. 4d). For this decompaction at the New Jersey margin, an exponential decrease in porosity with depth (e.g. Sclater & Christie, 1980) has been assigned, based on lithologies known from wells drilled in the region. The layers have then been decompacted to their

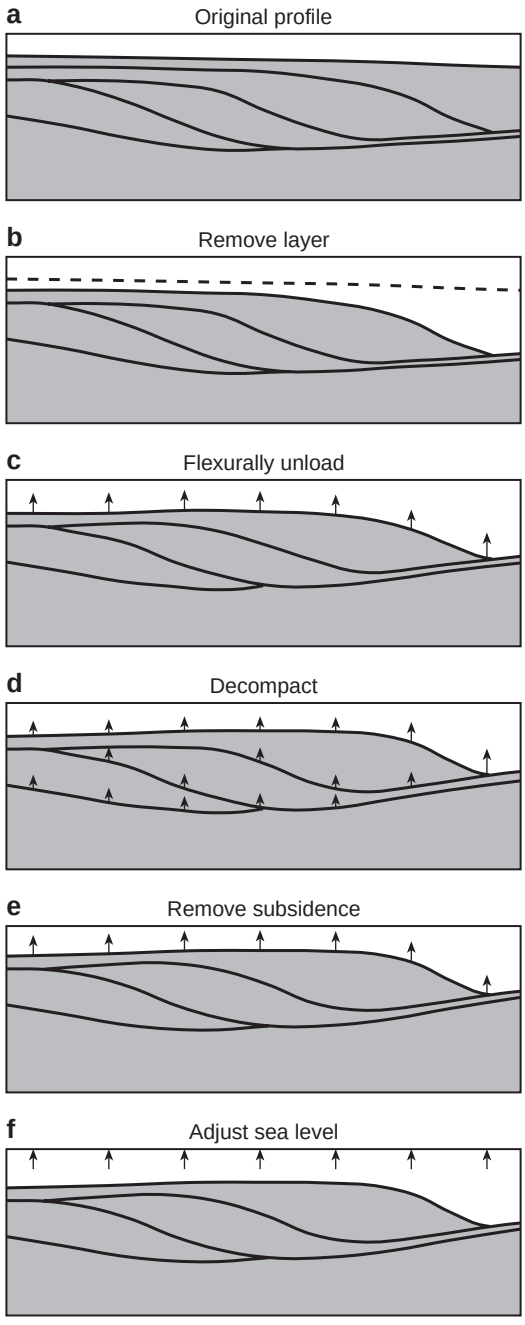

Fig. 4 Diagram illustrating steps used in reconstructing stratigraphy and palaeobathymetry using backstripping. See text for details. (From Steckler *et al*., 1999.)

original porosities and their depths adjusted. In a margin as old as the USA Atlantic margin, the observed tectonic subsidence during the Tertiary follows a smoothly decaying exponential curve. Knowledge of the sedimentary and lithospheric structure (Diebold *et al*., 1988; Grow *et al*., 1988; Sheridan *et al*., 1988; Holbrook & Kelemen, 1993; Klitgord *et al*., 1994) provides an estimate of the overall tectonic subsidence (Fig. 4e; Watts & Thorne, 1984; Steckler *et al*., 1988; Keen & Beaumont, 1990). Thermal subsidence has been calculated for the interval between the Oligocene and the present, using a two-dimensional thermal model for the New Jersey margin similar to that of Steckler *et al*. (1988). The last step in backstripping a profile is adjusting for the change in sea level since the time of the reconstruction (Fig. 4f). The effect of water loading is removed using the long-term estimates of Kominz (1984) for the sea-level history, which does not include high-frequency glacio-eustatic fluctuation. A different sea-level curve would cause vertical shifts of the palaeodepths across the entire reconstruction. The final result is a reconstruction of the palaeobathymetry and underlying horizons across a continental-margin profile for the sequential time intervals of the reconstruction.

Uncertainties in the reconstructions can be assessed by varying the flexure and compaction used for the reconstruction. Compaction errors arise from uncertainties in the lithology and the **compaction coefficients** of those lithologies, and are generally proportional to the thicknesses of sediments removed. Consequently, backstripping errors on a continental margin decrease in the landward direction. Uncertainties of 25% in compaction parameters, for example, can produce errors of up to 65 m for a 1300-m-thick section at the shelf–slope transition. However, similar uncertainties for clinoform rollovers 300–500 m beneath the New Jersey shelf lead to errors of only 5–15 m. The compaction depends upon the local overburden removed, thus it influences the height of the reconstructed clinoforms. Uncertainties from varying the flexural rigidity are up to ~100 m for the deepest reflectors beneath the outer shelf, decrease for younger surfaces, and taper to zero beneath the modern coastal plain. Flexural unloading produces a smooth isostatic response, and thus primarily affects the clinoform depth to ±30 m.

Drilling and logging

Recovering samples of the long-term record buried more than a few tens of metres in continental margins is expensive, technically challenging and,

therefore, is rarely attempted by the research community. Although cuttings and sidewall samples are routinely collected in oil or gas wells, commercial interests generally do not take the time and expense to recover continuous drill cores. **Downhole measurements** in commercial wells provide a substitute. Unlike measurements made directly on fragmented and incomplete drill cores, downhole data provide continuous information and sample a larger volume of rock (Goldberg, 1997). There are three general categories of downhole logging devices: electrical, nuclear and acoustic (see Doveton, 1986; Ellis, 1987; Paillet *et al*., 1992; Goldberg, 1997). In addition, borehole imaging, temperature and various *in situ* properties can be measured with wireline tools. Most devices have a vertical resolution better than 0.5 m (Allen *et al*., 1989; Tittman, 1991). Wireline logs have much greater vertical resolution than seismic profiles but little lateral resolution, so the combination of the two defines subsurface structures better than either data type can alone. Core-seismic correlations are supplemented by downhole measurements of two types. The first combines density and acoustic velocity logs to produce reflection coefficients versus depth. These can be used to produce a **synthetic seismogram** (Doveton, 1986) that provides a direct comparison between the seismic response of a drill core at various depths (metres) and two-way reflection time (seconds) of a seismic profile passing over the drill site. The second type of correlation is based on a **vertical seismic profile**. A hydrophone is lowered into a drill hole, clamped at a series of discrete depths, and the travel-times are recorded for acoustic pulses generated at the sea surface; the resultant profile provides a direct tie between depth and travel-time.

Sediment instability near the seafloor dictates that drill pipe must remain in the uppermost 40–80 m of the hole while logging, and few wireline tools provide useful measurements through metal pipe. However, two types of non-wireline techniques overcome this limitation: **logging while drilling** and **measuring while drilling** (LWD and MWD, respectively; see Allen *et al*., 1989; Bonner *et al*., 1992; Murphy, 1993). Both use specially designed logging tools that are part of the drill string, located a few centimetres to 10 m above the drill bit. Both record data while drilling, and, consequently, sediment properties are measured beginning at the seafloor in a borehole that was drilled only a few seconds to a few minutes previously.

THE EEL RIVER BASIN

Tectonism – a major control of sediment distribution and preservation

Tectonic setting of the Eel River Basin

The **Eel River Basin** (ERB) of northern coastal California is an active **forearc basin** whose history has been strongly influenced by the proximity of three tectonic plates: Pacific, Juan de Fuca and North America (Fig. 5). These plates meet today at the Mendocino Triple Junction (MTJ), with subduction of the Juan de Fuca Plate beneath North America north of the triple junction, transform motion between the Pacific and North American plates south of the triple junction, and transform motion along the Mendocino Fracture Zone (MFZ) west of the triple junction. Basement beneath the western Eel River Basin and much of its offshore extension is coastal Franciscan terrane (Fig. 6). Overall, this basement is a forearc accretionary complex composed of pre-Neogene trench sediments. Subsidence to form a forearc basin began in Miocene time, generating what is now the Eel River Basin (Fig. 7). By early Miocene, subduction rates increased and subsidence of the forearc region allowed deposition in the Eel River Basin.

The main depositional phase of the Eel River Basin is represented by the regressive Wildcat Group (Fig. 6). This succession is roughly 3000 m of upper Miocene marine mudstone at the base (Pullen Formation) grading upward to mid-Pleistocene non-marine sandstones and conglomerates at the top (Carlotta Formation). Such voluminous sediment accumulation in the forearc (Dickinson *et al*., 1979; Nilsen & Clarke, 1987) implies that the margin experienced less coupling between the downgoing plate and the overriding North American Plate than previously (Orange, 1999).

A basin-wide unconformity developed in the mid-Pleistocene, indicating a transition from regional subsidence and sediment accumulation to spatially variable deposition and erosion. This transition occurred when the Blanco Fracture Zone

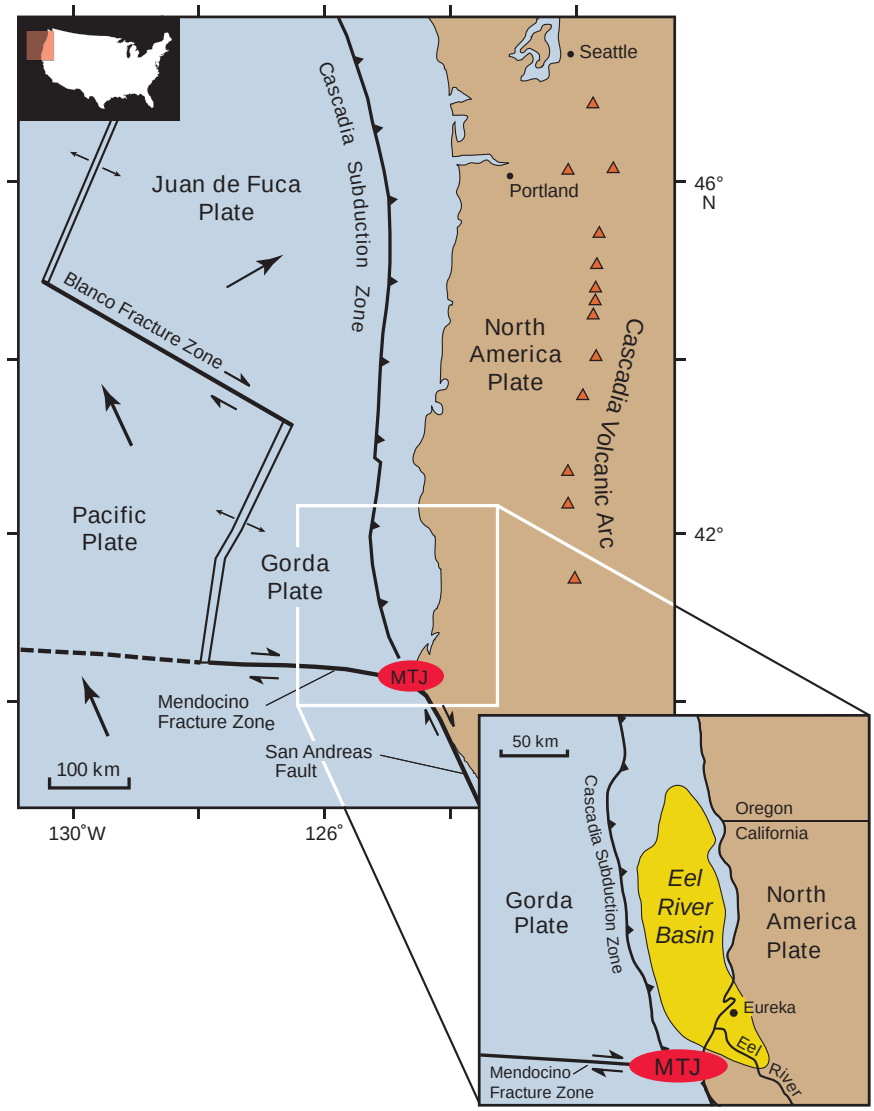

Fig. 5 Regional setting for the Eel River Basin, showing major bounding structural features: large arrows show relative plate movements; MTJ, Mendocino Triple Junction. (After Clarke, 1987; Aalto *et al.*, 1995.)

passed north of the Eel River Basin. This event at 0.7–1.0 Ma marked the change from subducting the older, colder Juan de Fuca crust to the younger, warmer, more buoyant Gorda crust (Carver, 1987). Orange (1999) suggested that the increase in coupling between the warm, young subducting slab and the overriding plate led to uplift and a change from regional deposition to regional erosion, or, at a minimum, to a change in depositional style.

The increase in plate coupling also led to an increase in offscraping of the sedimentary section from the downgoing slab (Carver, 1987). Today, the plate convergence between the Gorda and North American plates is ~3 cm yr^{-1} oriented NE–SW (Fig. 8; DeMets *et al.*, 1990). Within the southern portion of the Eel River Basin, the late Quaternary arrival of the Mendocino Triple Junction resulted in localized uplift, and a rotation of the folds and thrusts to a more WNW–ESE orientation (Clarke, 1992; Orange, 1999).

Seismic unconformities provide chronology

Fourteen unconformities defined by erosional truncation, downlapping and onlapping relationships have been identified in seismic profiles of the offshore Eel River Basin (Figs 9 & 10; Burger *et al.*, 2002). These surfaces are not to be confused with

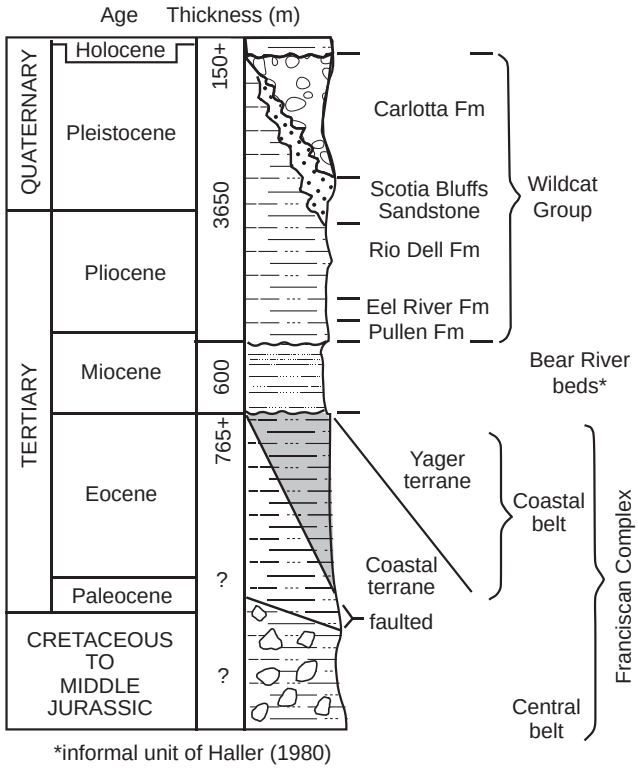

Fig. 6 Composite stratigraphic column for the Eel River Basin, constructed from outcrop studies. (From Clarke, 1992.)

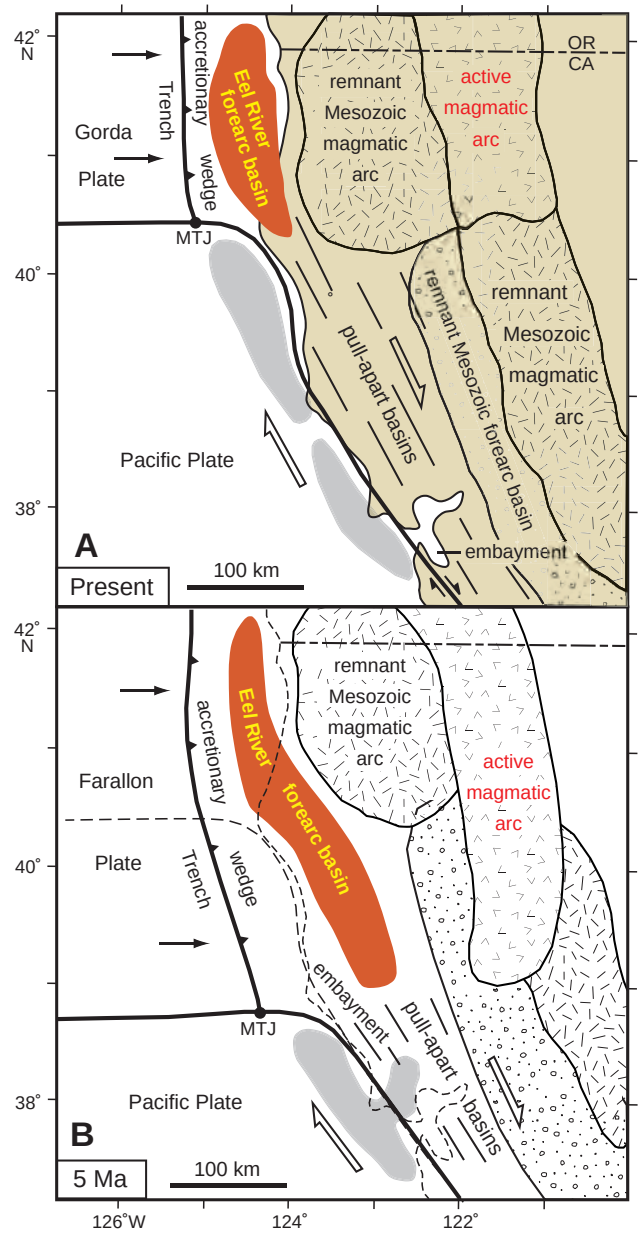

Fig. 7 Palaeotectonic maps showing the evolution of northern California during the late Neogene. Note the shortening of the Eel River Basin in response to northward Mendocino Triple Junction (MTJ) migration. The Gorda Plate is a small fragment of the former Farallon Plate. (After Nilsen & Clarke, 1987.)

the ten V-shaped, localized incised channels of presumed fluvial origin (Figs 10 & 11; Burger *et al.*, 2001). The smoother, more extensive unconformities are most clearly recognized in uplifted areas; they appear to become conformable in adjacent synclines (see Fig. 12). The most extensive, distinctive unconformities are surfaces 13, 9, 7, 5 and 1 (from youngest to oldest). Two of the most prominent unconformities, 1 and 9, have been correlated to features mapped in the onshore Eel River Basin, thereby providing age estimates for the entire package of offshore unconformities.

Surface 1 has been identified by Gulick & Meltzer (2002) as coeval with the onshore Wildcat Unconformity (Woodward-Clyde Consultants, 1980; McCrory, 1995, 1996, 2000). This constrains the seismically imaged sedimentary section offshore, equivalent to the upper ~1.5 s in synclinal areas, to be younger than ~1.0 Ma. Surface 9 has been identified by Gulick & Meltzer (2002) as coeval with the Hookton Datum onshore (McCrory, 1995, 1996). This correlation provides an age of ~500 ka to surface 9.

Burger *et al.* (2002) measured the thicknesses between all 14 surfaces on 6 seismic strike lines, averaged the results, and assigned ages (Fig. 13) based on the assumption of continuous and uniform deposition between surfaces 1 and 9, and

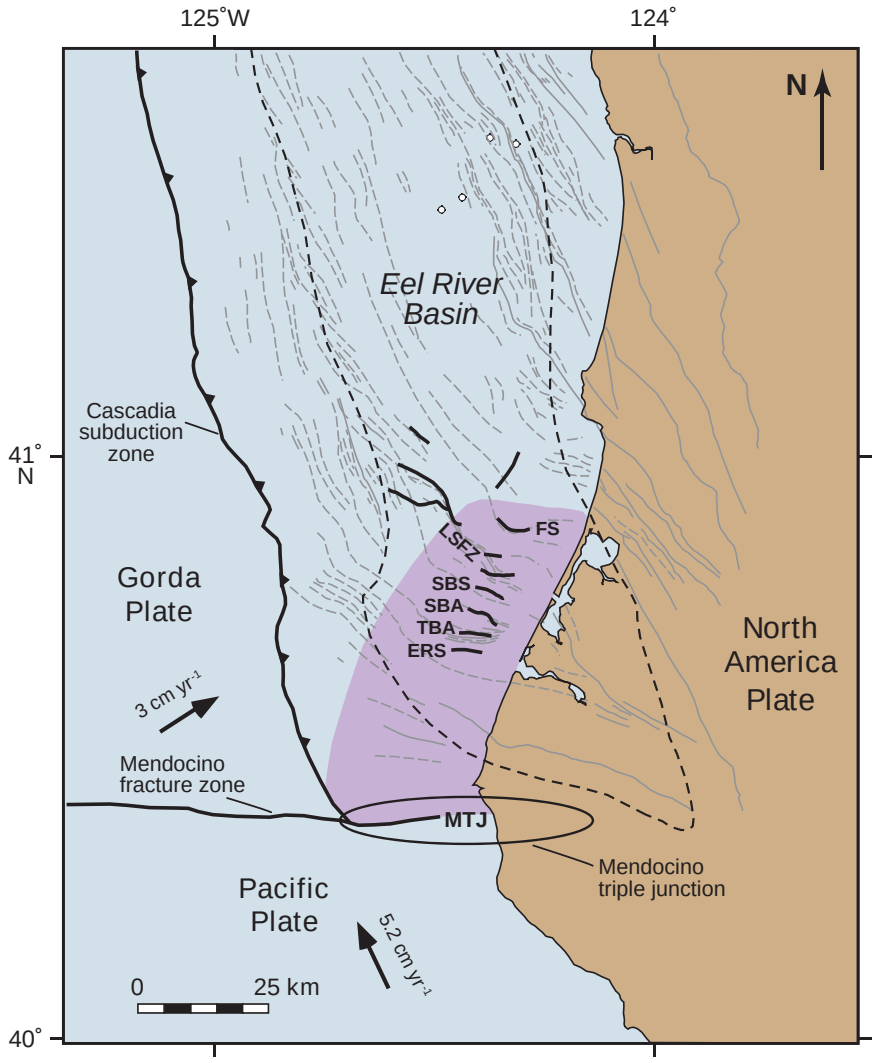

Fig. 8 Structural and tectonic setting of the Eel River Basin. Structural grain of faults (light solid lines; Clarke, 1987), anticlines and synclines (light dashed lines; Clarke, 1987) and plate motions (Gulick *et al*., 2002), influencing deformation of Eel River Basin sediments are indicated. Dark dashed line denotes extent of the Eel River Basin. Mapped structural trends are indicated by bold lines. Note the change from a general NNW–SSE orientation to NW–SE and then almost E–W orientations nearer the Mendocino Triple Junction (MTJ). Black arrows indicate modern motions (with rates) of the Gorda and eastern Pacific plates with respect to North America (adapted from Gulick *et al*., 2002). Purple area indicates estimate of the region directly impacted by the MTJ, based on inactive pre-existing folding and apparent counterclockwise rotation of these features. ERS, Eel River Syncline; TBA, Table Bluff Anticline; SBA, South Bay Anticline; SBS, South Bay Syncline; LSFZ, Little Salmon Fault Zone; FS, Freshwater Syncline. (MTJ location after McCrory, 2000; after Hoskins & Griffiths, 1971.)

similarly between 9 and the seafloor. The validity of these assumptions cannot be tested, but given that each was measured in the most conformable section of a synclinal setting on the shelf, these estimates provide useful first attempts. Burger *et al*. (2002) compared the age estimates of these surfaces to the global sea-level proxy curve derived from $\delta^{18}O$ measurements (Mederios *et al*., 2000), and concluded that glacio-eustasy was very likely an important agent in forming these surfaces.

Offshore deformation since 1 Ma

Based on seismic interpretation, several faults and fold structures are recognized beneath the shelf portion of the Eel River Basin (Fig. 14). While the amount and age of their offsets have not been determined with great accuracy, they allow basic generalizations to be made concerning the role that Gorda Plate subduction and Mendocino Triple Junction migration have played in the structural evolution of the Eel River Basin since 1 Ma.

The northward approach of the Mendocino Triple Junction impinged on the Eel River Basin beginning at ~500 ka (McCrory, 1989). Broad folds (Fig. 14) comprising the South Bay Anticline, South Bay Syncline and Little Salmon Fault Zone (SBA, SBS and LSFZ) all pre-date 1.0 Ma (surface 1, Figs 10 & 12), suggesting that Gorda Plate subduction, not Mendocino Triple Junction migration, caused this

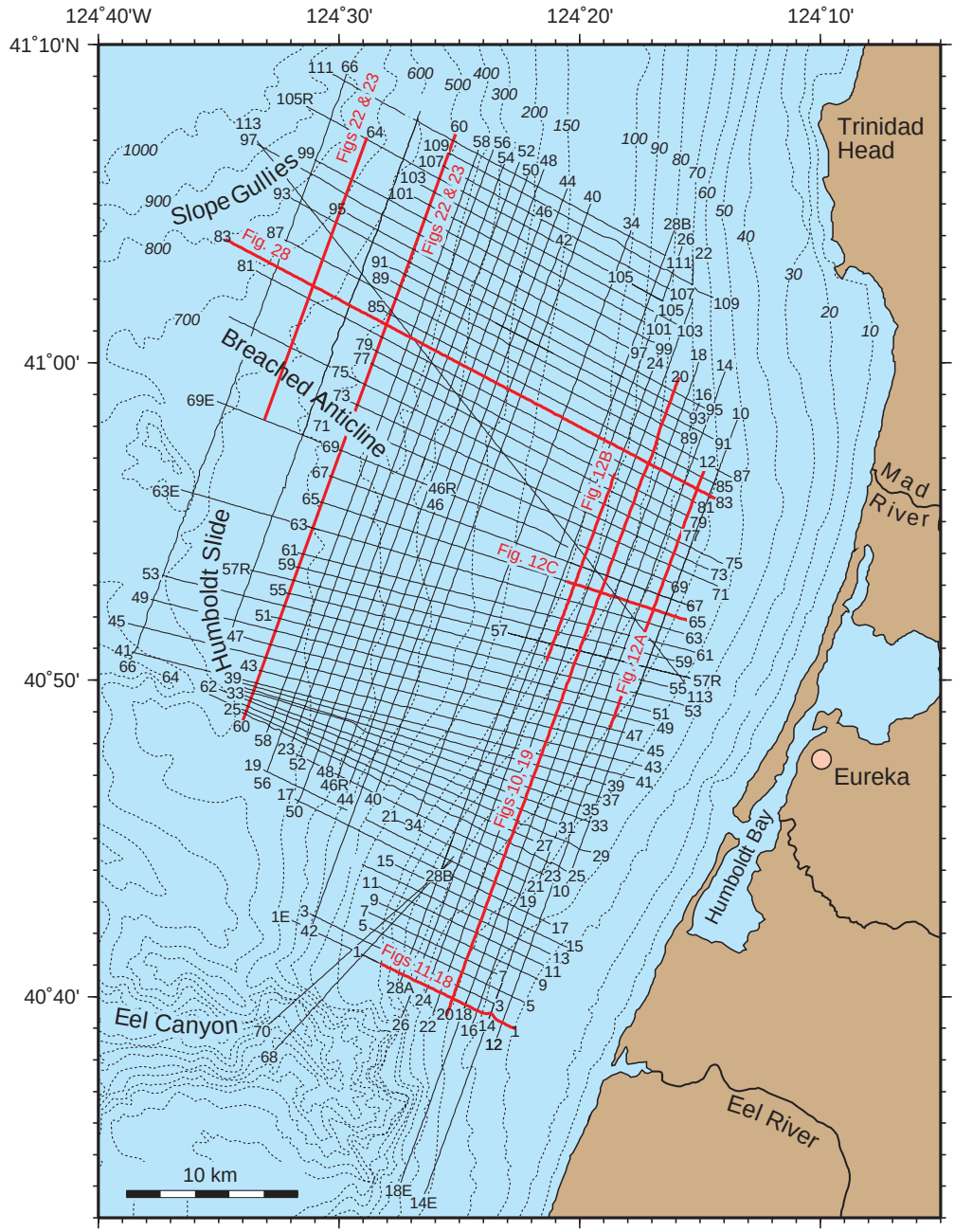

Fig. 9 Seismic grid for the Eel River Basin. Location of 48-channel high-resolution multichannel seismic profiles (numbered 1–113) collected across the basin during *R/V Wecoma* cruise W9605b, using a single 45/45 GI airgun and 600-m streamer, and then stacked 24-fold.

deformation. These older compressional features are currently oriented WNW–ESE (McCrory, 2000; Fig. 8), but when initially formed, pre-1.0-Ma features probably had a more NW–SE orientation.

Compressional folding of Eel River Basin sediments progressively ceased from south to north. Specifically, deformation of the South Bay Anticline and South Bay Syncline ended at ~1 Ma, then folding of the Little Salmon Fault Zone ended at ~690 ka, and within the Freshwater Syncline at ~600 ka (Burger *et al.*, 2002). Subduction-related folding continues today both on the shelf north

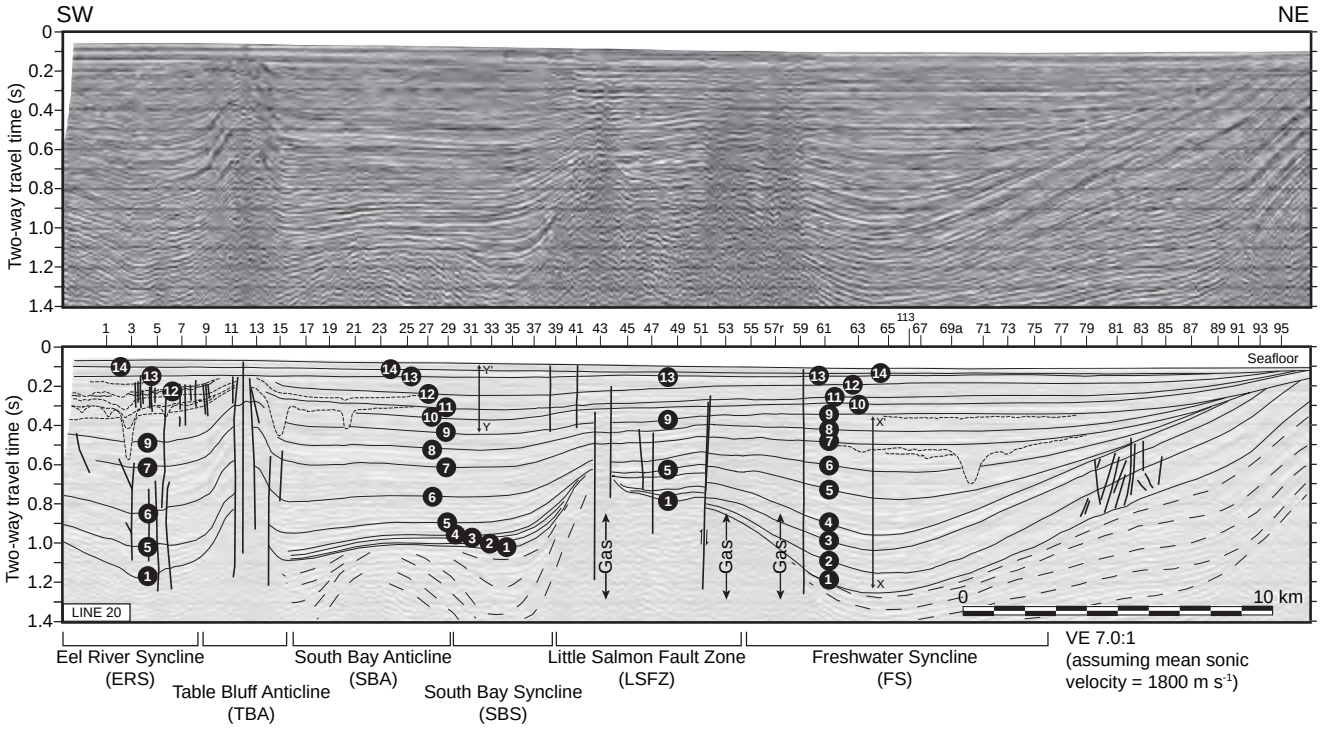

Fig. 10 Uninterpreted and interpreted versions of multichannel seismic profile 20, showing mapped faults, deformational structures and unconformities (numbered circles) in the offshore Eel River Basin. Along-strike section; see Fig. 9 for location. Near-vertical bold lines represent faults; thinner solid lines represent regional unconformities; short-dashed lines represent local incised unconformities; and long-dashed lines represent the trends of folded and truncated reflectors beneath surface 1. Vertical zones of presumed gas wipeout (Yun *et al*., 1999) are present within the Table Bluff Anticline and the Little Salmon Fault Zone. Onshore structures mapped offshore are indicated at the bottom of the interpreted profile. Locations where travel-times between surfaces were measured to estimate unconformity ages (see Fig. 9) are indicated by vertical lines labelled 'X–X'' and 'Y–Y''. Numbers across the top of the interpreted profile identify locations of crossing profiles. (From Burger *et al*., 2002.)

of Humboldt Bay (Fig. 14) and beneath the upper slope. The influence of northward motion of the Mendocino Triple Junction appears to be limited to an area ~60–70 km north of the triple junction (Fig. 8).

North–south compression is most noticeable close to the modern triple junction. Uplift indicated by a proliferation of fluvial incisions at the southern end of available seismic coverage (McLaughlin *et al*., 1994; Aalto *et al*., 1995; Gulick *et al*., 2002) occurred sometime since ~330 ka (Figs 10 & 11; Burger *et al*., 2002). A 95° orientation of the Table Bluff Anticline (TBA) within the past ~330 ka also suggests N–S compression. Counterclockwise rotation of pre-existing features, and right-lateral motion across the Table Bluff Anticline (Fig. 15), all support localized transpression (Gulick & Meltzer, 2002).

Contemporary deformation at the Mendocino Triple Junction is expressed as a zone of localized uplift, measuring 2.5–2.8 mm yr^{-1} of vertical motion (Lajoie *et al*., 1982; McCrory, 1996). This uplift affects the trend of structures along the Gorda–North American plate boundary, beginning with NE–SW deformation features in the accretionary wedge immediately north of the triple junction. These trends gradually swing toward WNW–ESE farther north, and eventually become NNW–SSE in the Eel River Basin itself (Fig. 8).

Modern tectonic activity within the Eel River Basin results in localized uplift on anticlines and subsidence on synclines. These forearc structures trend across the slope and shelf and project onshore to features such as the Russ Fault, Eel River Syncline, Table Bluff Anticline and Little Salmon Fault (RF, ERS, TBA, LSF). This alignment

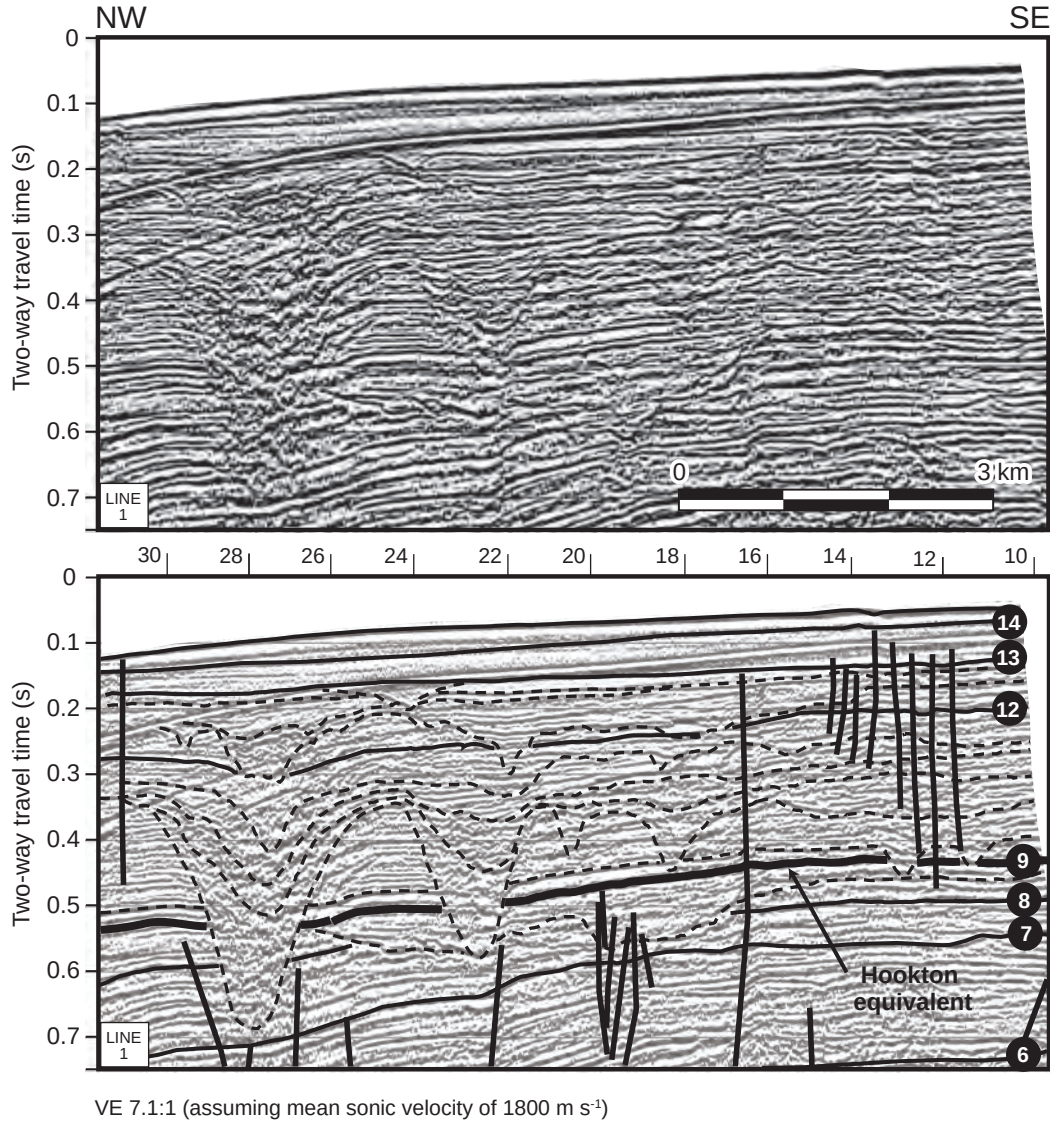

Fig. 11 Uninterpreted and interpreted portion of multichannel seismic profile 1 showing regional unconformities (solid, numbered lines). See Fig. 9 for location. Dashed lines indicate local incisions (compare with Fig. 18), which dominate the MCS grid south of the Table Bluff Anticline (see also Fig. 10). Near-vertical bold lines represent faults. The near-horizontal bold line represents surface 9, correlated to the Hookton Datum of McCrory (1995), with an estimated age of ~500 ka. Numbers at the top of the interpreted profile show locations of crossing strike profiles. (After Burger *et al*., 2002.)

and continuity suggests that the patterns, and perhaps even the rates, of deformation measured onshore can be projected offshore to provide first-order estimates of the tectonic effects on sedimentation (Orange, 1999). Onshore, modern deformation controls the topography, river drainage and configuration of wave-cut terraces. Uplift rates on the subaerial portion of the Little Salmon Fault are in the order of 2.5 mm yr^{-1}, for the Table Bluff Anticline they are 0.4–0.75 mm yr^{-1}, and for the Mad River fault zone they are 1.3–2.5 mm yr^{-1}; subsidence rates of the Freshwater Syncline are 1.4–3.3 mm yr^{-1} (see McCrory (1996) for data compilation and references). These structures are prominent despite very high erosion and denudation rates that result from the combination of climate, tectonics and exposure of relatively young sediments.

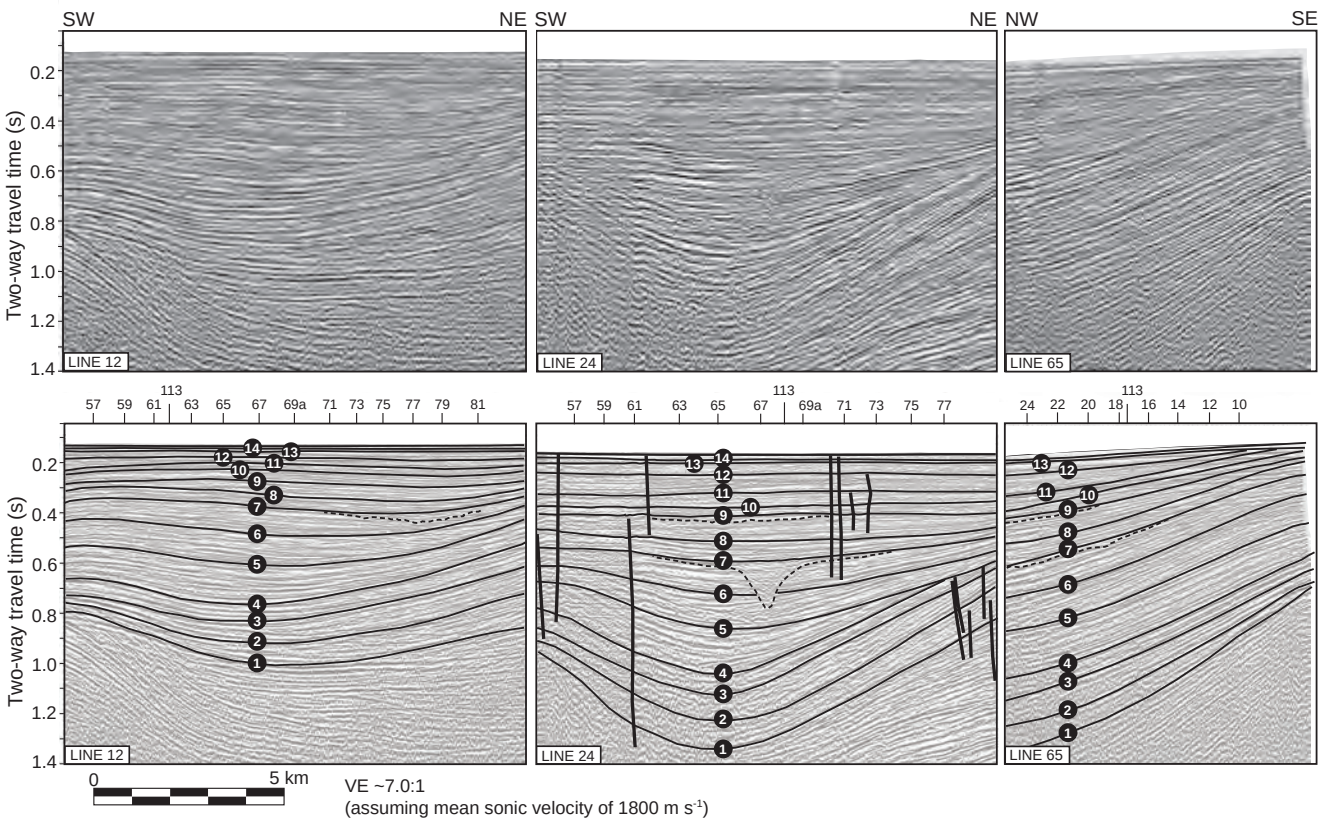

Fig. 12 Uninterpreted and interpreted portions of multichannel seismic strike profiles 12 and 24, and dip profile 65, showing the offshore expression of the Freshwater Syncline (FS). Location indicated in Fig. 9. Line 65 is oriented slightly oblique to the synclinal axis as it crosses the shelf. Bold, near-vertical lines represent faults, and numbers at the top of interpreted profiles indicate locations of crossing profiles. (From Burger *et al.*, 2002.)

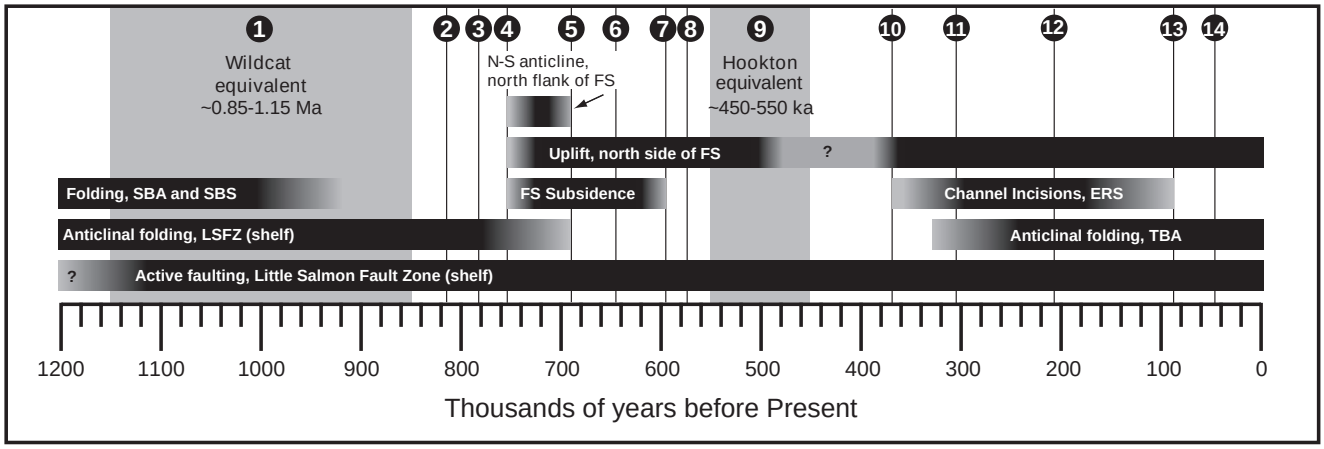

Fig. 13 Timeline summarizing the periods of deformation and channel incision on the Eel River Basin shelf. Age estimates are based on the stratigraphic arrangement of 14 seismic unconformities (numbered vertical lines), two of which are tied to the Wildcat and Hookton surfaces (~1 Ma and ~500 ka, respectively). Assumptions of uniform accumulation rates provide the ages of intervening surfaces (see Fig. 10). The structures abbreviated in this figure are listed in Fig. 10. (From Burger *et al.*, 2002.)

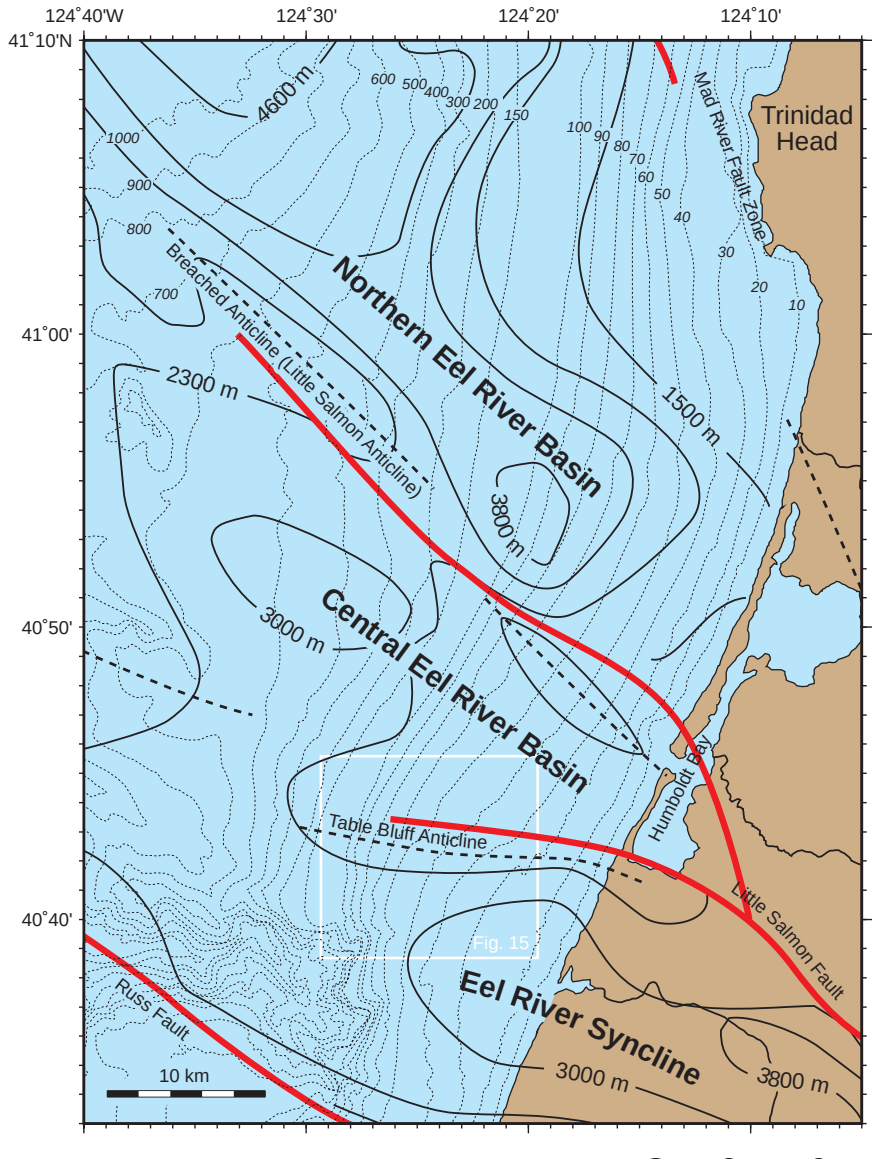

Fig. 14 Structures and sediment isopachs (solid lines) above Franciscan basement in Eel River Basin (after Crouch & Bachman, 1987). Bathymetry (italic numbers) is in metres. Three offshore sub-basins are defined by the Russ and Mad River Fault Zones, plus two antiformal trends offshore that branch from the Little Salmon Fault. Dashed lines are prominent anticlines.

Offshore stratigraphy – local variations of governing processes

The development of shelf sub-basins since 1 Ma

Isochron maps (refer to Figs 16 & 17 for all discussion in this section) show that the region of greatest sediment preservation in the Eel River Basin has gradually shifted from north to south during the past ~1.0 Myr, presumably due to structural controls and changes in the relative importance of sediment sources (Burger *et al.*, 2002). These maps also show that overall sediment accumulation rates on the shelf have decreased since ~500 ka. This latter change coincides with the northward migration of the Mendocino Triple Junction and related uplift across the southern part of the basin.

Between ~850 ka and 750 ka, an irregular depocentre oriented approximately 055° was located west of Trinidad Head and was supplied by a northern sediment source. Syndepositional uplift of the Little Salmon Fault Zone separated this depocentre from the central Eel River Basin, where little sediment accumulated during this interval (Figs 16A–D & 17A–D).

Folding of the Freshwater Syncline (FS) and relative uplift north of this feature began at ~750 ka; the associated depocentre is currently oriented

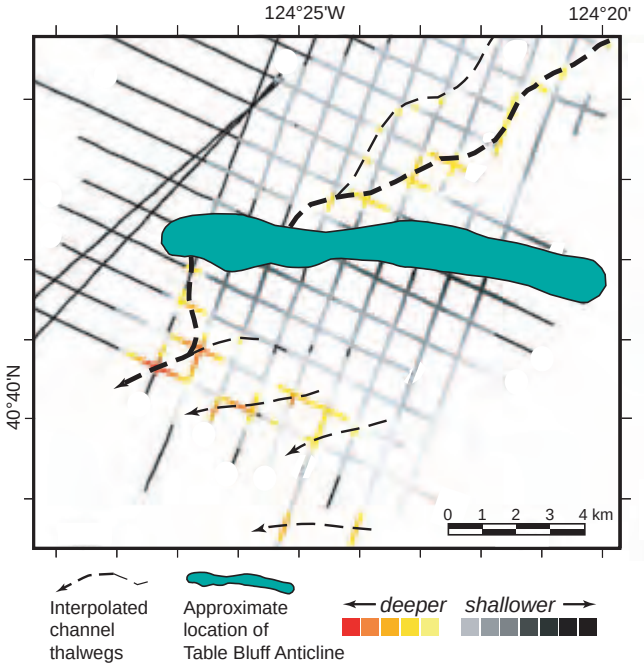

Fig. 15 Right-lateral strike-slip displacement across the Table Bluff Anticline, inferred by the offset of a buried channel (bold dashed line) on both sides of the anticline. The consistent NE–SW gradient across the anticline (relative depths of channel surface are indicated by colour along the seismic grid) strongly suggests that this was once a continuous feature, indicating that its formation pre-dates deformation of the anticline. The observed offset is ~2.0 km, indicating a slip rate of 0.6 cm yr^{-1}. (From Burger *et al.*, 2002.)

~115°, probably due to structural control by the syncline. Sediment continued to be supplied from the north. By ~690 ka, a new depocentre to the south indicates that a southern source, perhaps the ancestral Eel River, has begun to contribute sediment to the basin (Figs 16E & 17E). Less distinct partitioning of depocentres occurs after ~690 ka, when Little Salmon Fault Zone folding and uplift ended. There are depocentres beneath both northern and southern portions of the shelf from ~750 ka to ~550 ka, evidently supplied by sources from both the north and the south.

Between ~450 and 300 ka (Figs 16I–J & 17I–J), offshore sequences appear more continuous, indicating a decrease in the influence of structural deformation and resultant partitioning of sediment accumulation and preservation. Overall thicknesses per unit time also decrease, suggesting either a decrease in sediment supply after ~500 ka or an increase in sediment bypassing to the slope. Formation of the Eel Canyon after ~500 ka probably increased the amount of sediment bypassing the shelf. Relative sediment thicknesses in the north decreased after ~500 ka, and particularly after ~200 ka, indicating a decrease in sediment contribution from the postulated northern source (Figs 16L–M & 17L–M). However, minor sediment maxima west of the modern Mad River mouth after ~200 ka identify it as a sediment source, at least from then to the present.

The most recent interval considered, ~43 ka–present, reveals modern patterns of shelf sedimentation (Borgeld, 1985; Wheatcroft *et al.*, 1996; Morehead & Syvitski, 1999; Sommerfield *et al.*, this volume, pp. 157–212). A large N–S-oriented depocentre in the south (Figs 16N & 17N) is the result of input from the Eel River. A smaller depocentre to the north suggests continuing, minor input from the Mad River. Modern sediment dispersal patterns (Sommerfield *et al.*, this volume, pp. 157–212) and the dominance of the Eel River as a sediment source have been maintained for at least the last ~43 kyr.

Buried fluvial channels

Seismic profiles reveal numerous V-shaped channels, 10–250 m deep and 0.1–1.0 km wide (Figs 18–20) that incise 10 surfaces as deep as 0.5 s (~450 m) below the shelf of the Eel River Basin. These surfaces (designated with letters A–E in Fig. 18) are distinct from 14 seismic unconformities (designated with numbers; e.g. Fig. 11) also seen in profiles across the shelf (Burger *et al.*, 2002); the latter are smoother, more continuous, and more laterally extensive (Fig. 19). Many unconformities extend across the entire multichannel-seismic (MCS) grid (Fig. 9) and disappear only where they are truncated on the crests of anticlines or eroded by incisions. The origin of these regional unconformities is discussed in a later section of this paper.

An E–W trending structural high, correlative along-strike with the onshore Table Bluff Anticline (TBA; Clarke, 1987) crosses the study area. Most of the incised surfaces are concentrated south of the Table Bluff Anticline (Fig. 20); only one channel cuts into and crosses the Table Bluff Anticline, trending NE–SW. Five incised surfaces have been mapped south of the Table Bluff Anticline (Fig. 20; Burger

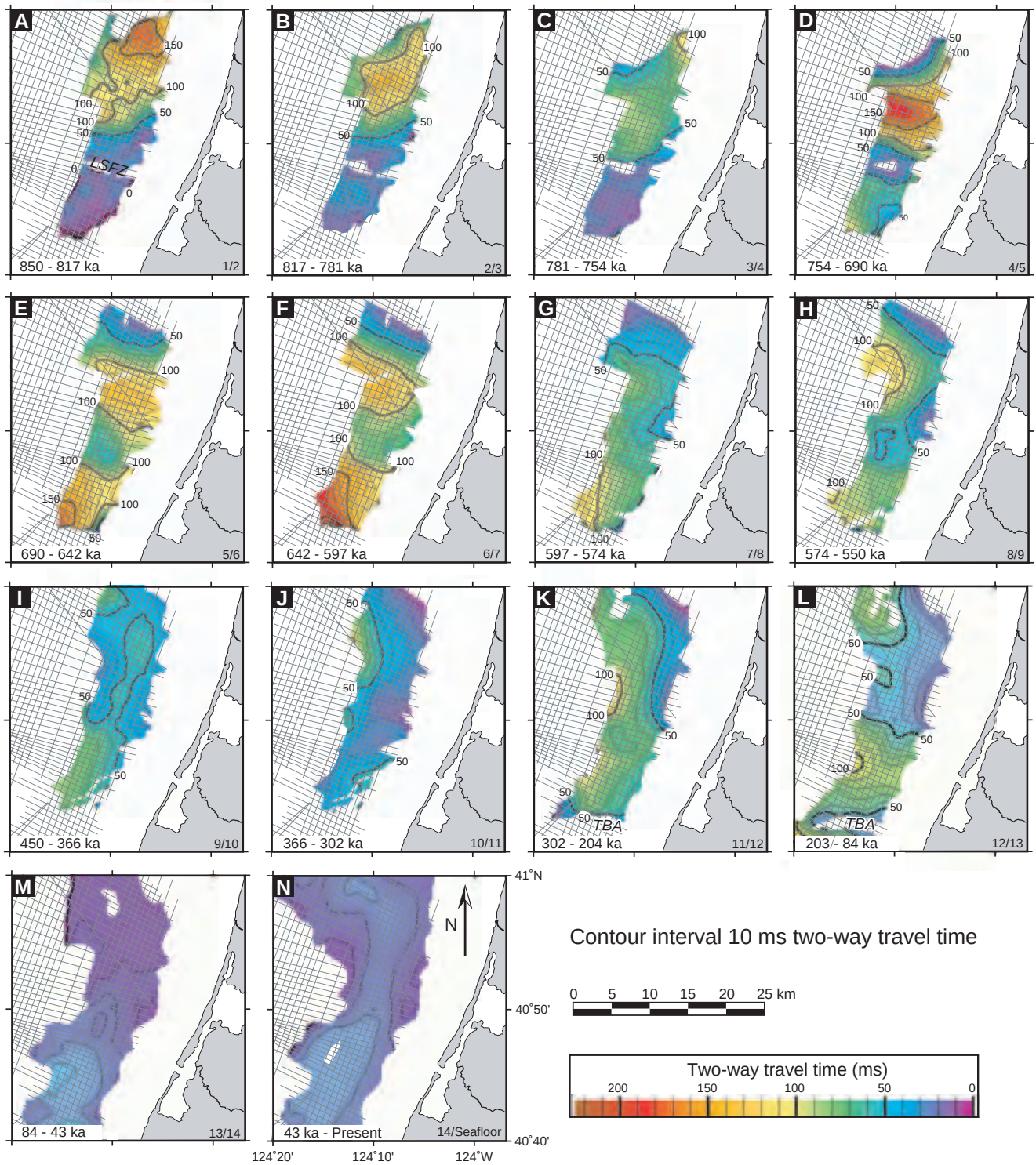

Fig. 16 Isochron maps of sequences bounded by regional seismic unconformities (including the seafloor) beneath the Eel River Basin shelf north of the Table Bluff Anticline. Ages noted on each map (bottom left) are derived from correlation to onshore stratigraphy (see text), and indicate the presumed interval of sediment accumulation for each sequence. Numbers in the lower right corner of each map identify the unconformities that define the interval shown. (From Burger *et al.*, 2002.)

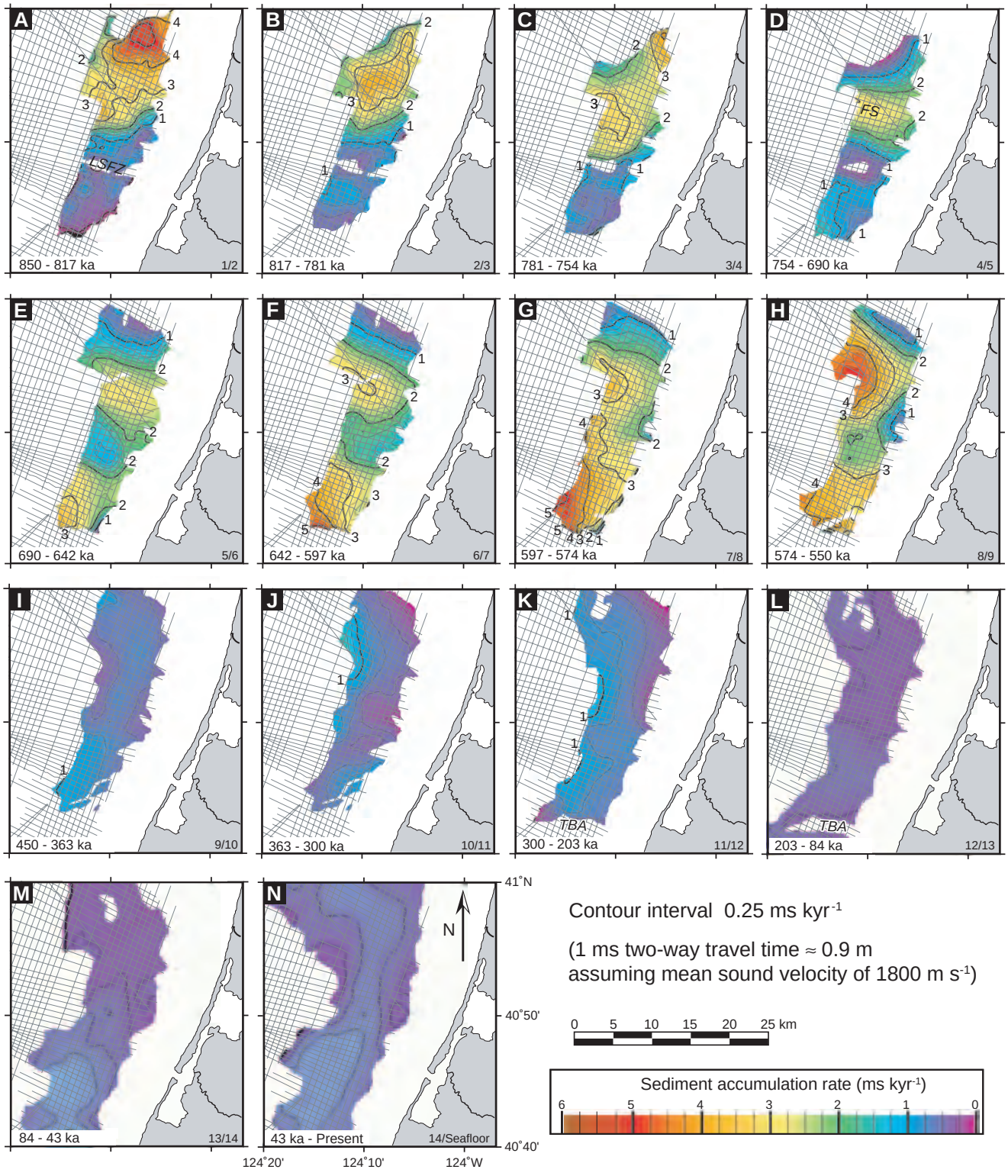

Fig. 17 Maps of sediment accumulation rate for sequences bounded by regional seismic unconformities (including the seafloor) beneath the Eel River Basin shelf north of the Table Bluff Anticline. Travel-time thicknesses from each isochron map (Fig. 16) were converted to sediment accumulation rates based on estimated time over which each sequence was deposited. Inset ages (bottom left) indicate the presumed interval of sediment accumulation for each sequence. Numbers in the lower right corner of each map identify the unconformities that define the interval shown. Note the dramatic decrease in accumulation rates across the margin after ~450 ka, presumably coincident with arrival of uplift and deformation in the southern Eel River Basin related to the Mendocino Triple Junction. (From Burger *et al.*, 2002.)

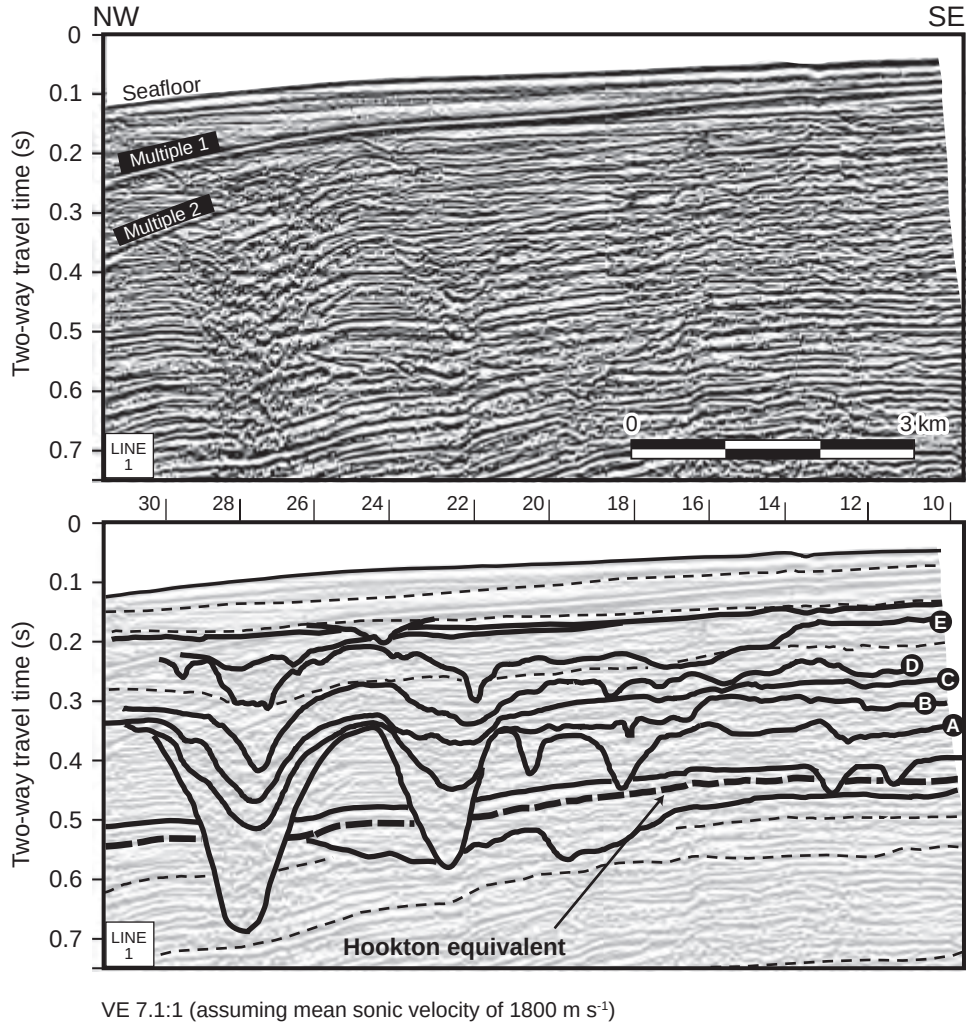

Fig. 18 Uninterpreted and interpreted versions of seismic line 1 (see Fig. 9 for location), showing superimposed/stacked incisions (lettered, solid lines). Labelled incisions are mapped in Fig. 20. Numbered, vertical lines indicate locations of crossing profiles. Thin, dashed lines (see Fig. 11) indicate regional unconformities; bold, dashed line indicates a surface correlated to the Hookton Datum of McCrory (1996). (After Burger *et al*., 2001.)

et al., 2001). All channels that cut into and define these surfaces trend south-west and deepen toward modern embayments along the north side of Eel Canyon (Fig. 21). North of the Table Bluff Anticline, incisions are observed on only two surfaces, and are prominent on only one. However, like those to the south, these incisions also display south-west orientations and they deepen seaward. The deepest incised channel (surface A, Figs 18 & 19) maintains a nearly constant gradient of ~0.4° both north-east (landward) and south-west (seaward) of the anticline (Fig. 21).

Buried Eel River Basin channels have been mapped in the shallow subsurface at water depths from ~50 m to 100 m. Their dendritic patterns (Fig. 20) are similar to latest Pleistocene–Holocene drainage features mapped by Duncan *et al*. (2000) on the New Jersey shelf that have been interpreted as either lowstand or early transgressive fluvial systems (Austin *et al*., 1996; Duncan *et al*., 2000). A fluvial origin for the Eel River Basin channels also has been proposed (Burger *et al*., 2001), based on the compelling seismic evidence of dendritic trends, low gradients, cross-shelf extent and location on the shelf where lowstand subaerial exposure is likely to have occurred.

Although Eel River Basin incised surfaces mapped using MCS profiles have not yet been dated

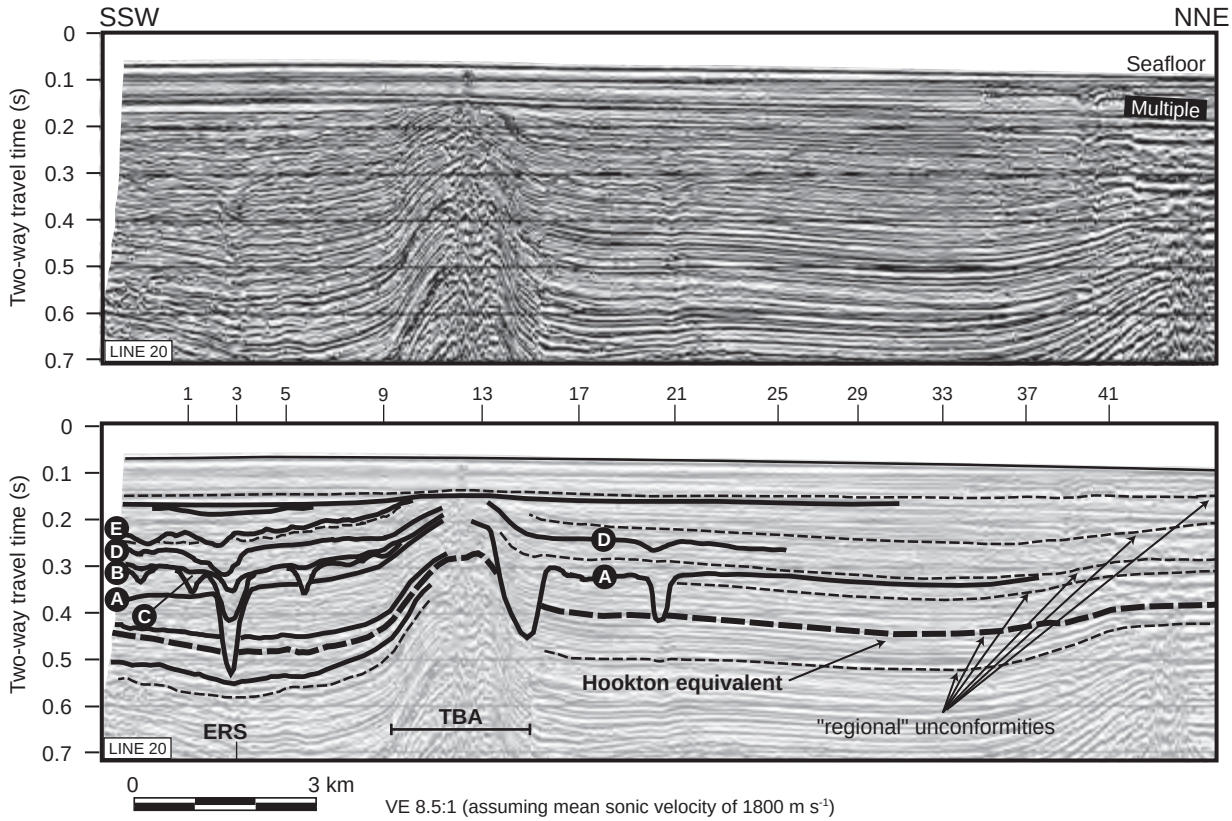

Fig. 19 Uninterpreted and interpreted versions for the southern end of seismic line 20 (see Fig. 9 for location), showing superimposed/stacked incisions. Solid, lettered lines indicate the incised surfaces mapped in Fig. 20. Numbered, vertical lines indicate locations of crossing profiles. Thin, dashed lines indicate regional unconformities that extend across most of the southern shelf; bold, dashed line correlates to the Hookton equivalent (Fig. 18). TBA, Table Bluff Anticline; ERS, Eel River Syncline. Width of TBA deformation as derived from this profile is shown in plan view for each of the shelf strike lines in Fig. 20. (After Burger *et al*., 2002.)

directly, Burger *et al*. (2001) estimated their ages by correlating a prominent unconformity recognized in the offshore seismic grid to the onshore Hookton Datum (McCrory, 1995). The latter is an angular unconformity correlated across the onshore Eel River Basin that represents a hiatus spanning 450–550 ka ± 35 kyr (McCrory, US Geological Survey, personal communication, 2001). All 10 offshore incised surfaces post-date the offshore Hookton equivalent. Consequently, if these features are the result of fluvial incision into an exposed coastal plain, they could not have originated during glacio-eustatic lowstands with 100 kyr cyclicity. It is likely that some channels were initiated by relative lowstands resulting from local tectonic uplift (Burger *et al*., 2001).

The consistently NE–SW trend for Surface A incisions on both sides of the Table Bluff Anticline suggests that the observed drainage represents a single system disrupted by uplift (Fig. 20). The continuity of Surface A (Fig. 21) further suggests that it pre-dates the anticlinal deformation. Continuity of the Hookton equivalent across the trend of the Table Bluff Anticline confirms that uplift must be younger than 500 ka. The incised surfaces are almost exclusively located south-west of the Table Bluff Anticline (Figs 18–20), so the rising Table Bluff Anticline may have been the source for those shelf-drainage systems.

The large number of incised surfaces leading to Eel Canyon indicates that this feature must have existed through numerous oscillations of relative sea level, and strongly controlled off-shelf drainage during lowstands. Based on initiation of incised unconformities at the southern end of the basin after the formation of the Hookton equivalent, it

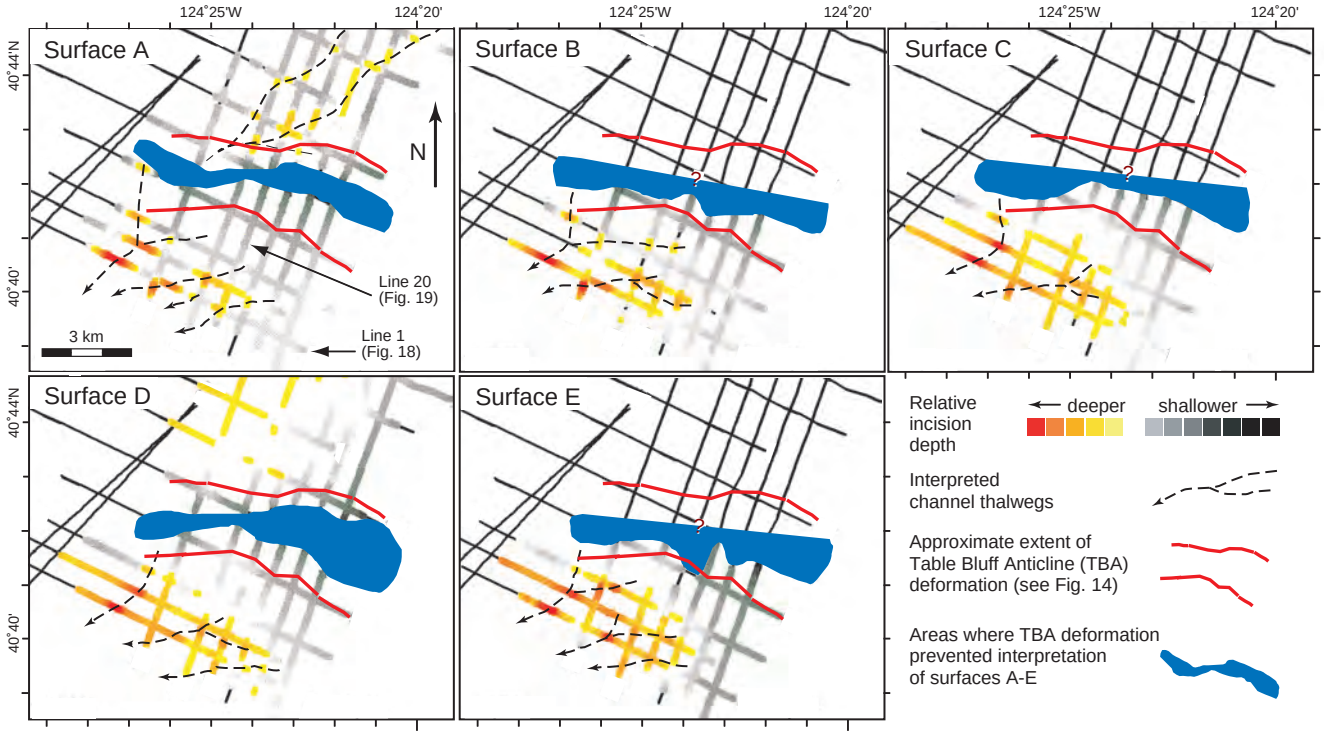

Fig. 20 Maps of the southernmost portion of the seismic grid (Fig. 9), showing the five most deeply incised surfaces (A is oldest, E is youngest; see Figs 18 & 19). Colours of interpreted portions indicate relative incision depth, according to the colour bar (right). The range of the colour scale was normalized by the seismic interpretation software to the maximum and minimum time-depth values for each surface, so the represented colour-scale range is different for each surface. Dashed lines are interpreted orientations of channel thalwegs. The red lines indicate the approximate lateral extent of Table Bluff Anticline (TBA) deformation as defined on each of the shelf strike lines. The blue solid areas indicate where surfaces could not be mapped because of TBA deformation; northern boundaries of these areas are not defined for surfaces B, C and E, because they could not be identified north of the TBA. (From Burger *et al.*, 2001.)

appears that the canyon formed soon after ~360 ka. Burger *et al*. (2002) speculated that sedimentation in the Eel River Basin shifts dramatically in response to variations in relative sea level: during high-stands, some fluvial suspended load can travel northward and seaward; during lowstands, rivers disgorge both suspended and bedload sediments much closer to the shelf edge where they are more readily captured by shelf-indenting canyons.

Processes on the Eel continental slope

The tectonically active Eel River Basin provides sharp along-margin contrasts that help to distinguish processes controlling the accumulation, preservation, and post-depositional deformation of sedimentary strata on the upper continental slope. The combination of large sediment supply from the Eel River (Brown & Ritter, 1971), late Pleistocene glacio-eustatic sea-level fluctuations (e.g. Ruddiman *et al.*, 1989) and offshore deformation (Orange, 1999; Burger *et al.*, 2001, 2002; Gulick & Meltzer, 2002; Gulick *et al.*, 2002), including frequent earthquakes (Couch *et al.*, 1974; Field & Barber, 1993), have all contributed to a lengthy history preserved in the slope stratigraphy.

The Little Salmon Fault Zone forms a prominent anticline onshore, but has little to no bathymetric expression on the shelf. Seaward of the shelf break, however, the rates of tectonic uplift exceed the rates of sediment accumulation. As a result, the Little Salmon Fault, and its associated hanging-wall anticline (Little Salmon Anticline), crop out on the upper and middle slope in a right-stepping, en échelon pattern (indicated by the **breached anticline** in earlier Figs 9 & 14). This structure forms a drainage divide on the slope, separating two different slope morphologies and their underlying sediment

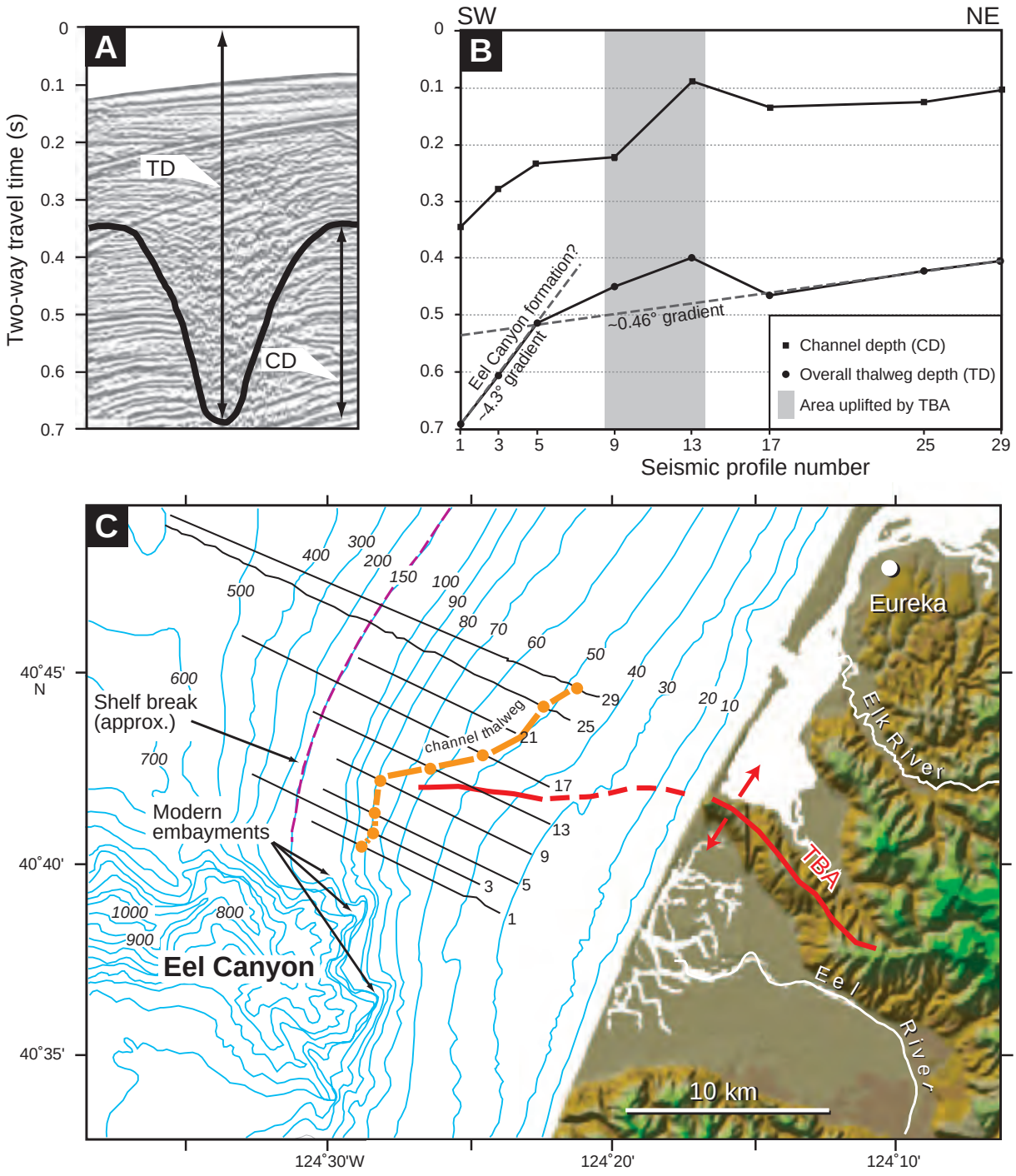

Fig. 21 Influence of Table Bluff Anticline deformation on channel development. (A) Time/depth used to indicate changes in channel gradients and incision depths across the Eel River shelf: CD, channel depth, measured from overbank to thalweg; TD, overall thalweg depth, measured from present sea level to centre of interpreted thalweg. (B) Trends of measurements from north to south for channels in surface A (Figs 18–20). Dashed lines show interpolated channel gradients (calculated using a mean sediment velocity of 1.8 km s^{-1}), suggesting a fluvial source to the north-east. Deviations are attributed to uplift caused by the Table Bluff Anticline (TBA), and deepening as a result of a transition from fluvial to canyon processes. (C) The southern end of the Eel River Basin, showing the spatial relationship between dip seismic profiles, the channel mapped in (B), the TBA (red) and the Eel Canyon. Solid orange circles on the dip profiles represent positions of the channel thalweg. Modern embayments along the flanks of the Eel Canyon are where the mapped channel may have discharged during a preceding relative lowstand. Bathymetry in metres; dashed purple line represents the shelf break, which occurs at ~150-m isobath. (From Burger *et al.*, 2001.)

packages. The slope south of the Little Salmon Anticline is discussed in detail in Lee *et al*. (this volume, pp. 213–274) with reference to the 'Humboldt Slide', and the corresponding region north of the Little Salmon Fault is discussed here.

There is no canyon north of the Little Salmon Anticline that would alter the transport of sediment to the Eel River Basin slope between times of sea-level change. As a result, slope sedimentation to the north is more uniform through time than it is south of the Little Salmon Anticline. Concordant, parallel reflectors observed in most areas of the northern upper slope suggest hemipelagic settling dominated by fine-grained sediment. Despite this comparatively uniform sedimentation, the slope north of the Little Salmon Anticline is characterized by an abundance of buried channels (Figs 22 & 23). These features incise 11 surfaces that have

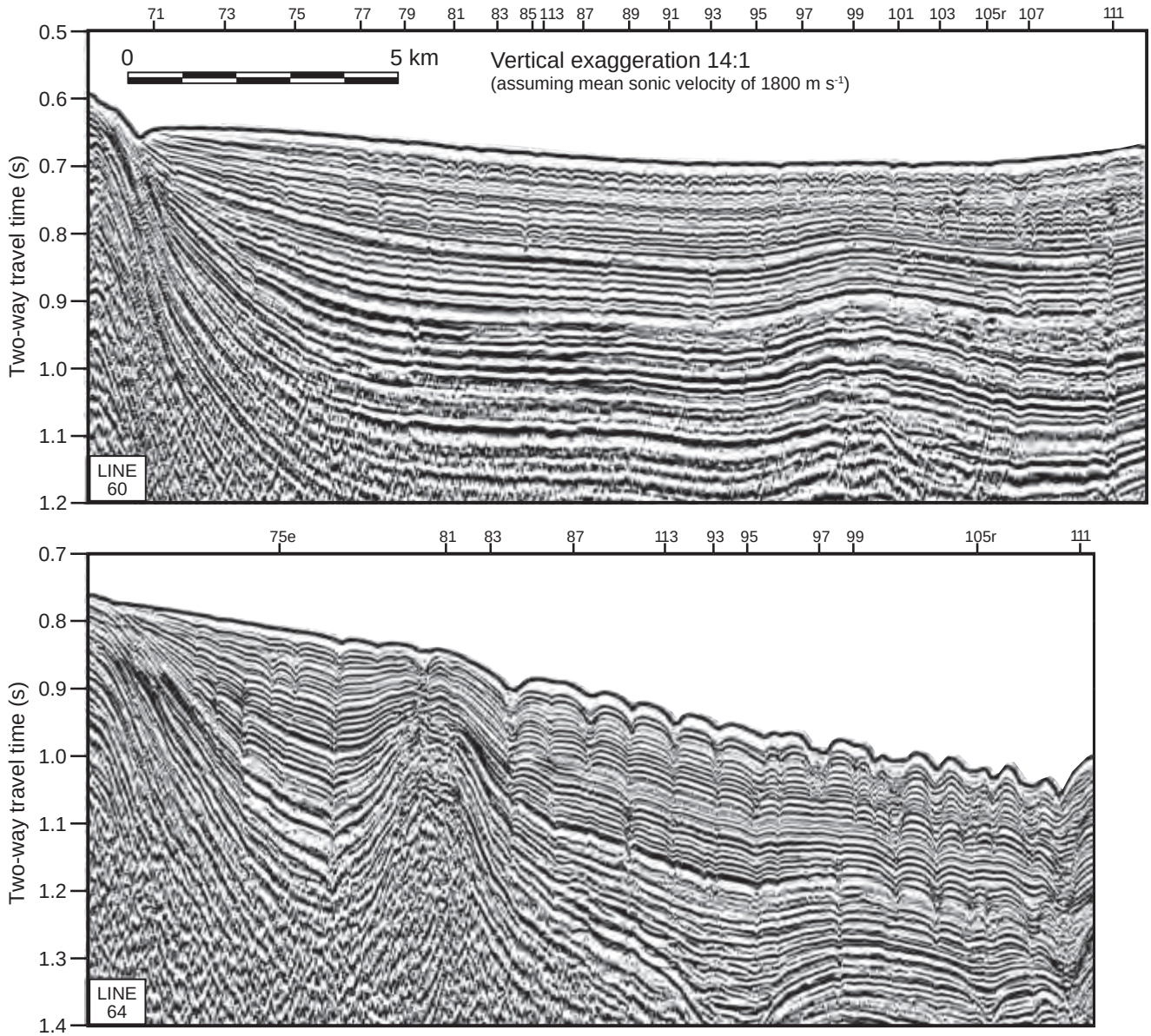

Fig. 22 Uninterpreted portions of seismic lines 60 and 64, showing the downslope evolution of slope channel geometries. Interpretation sections are shown in Fig. 23. Locations of profiles are indicated in Fig. 9. Numbered lines at top indicate locations of crossing profiles. (From Burger *et al*., 2002.)

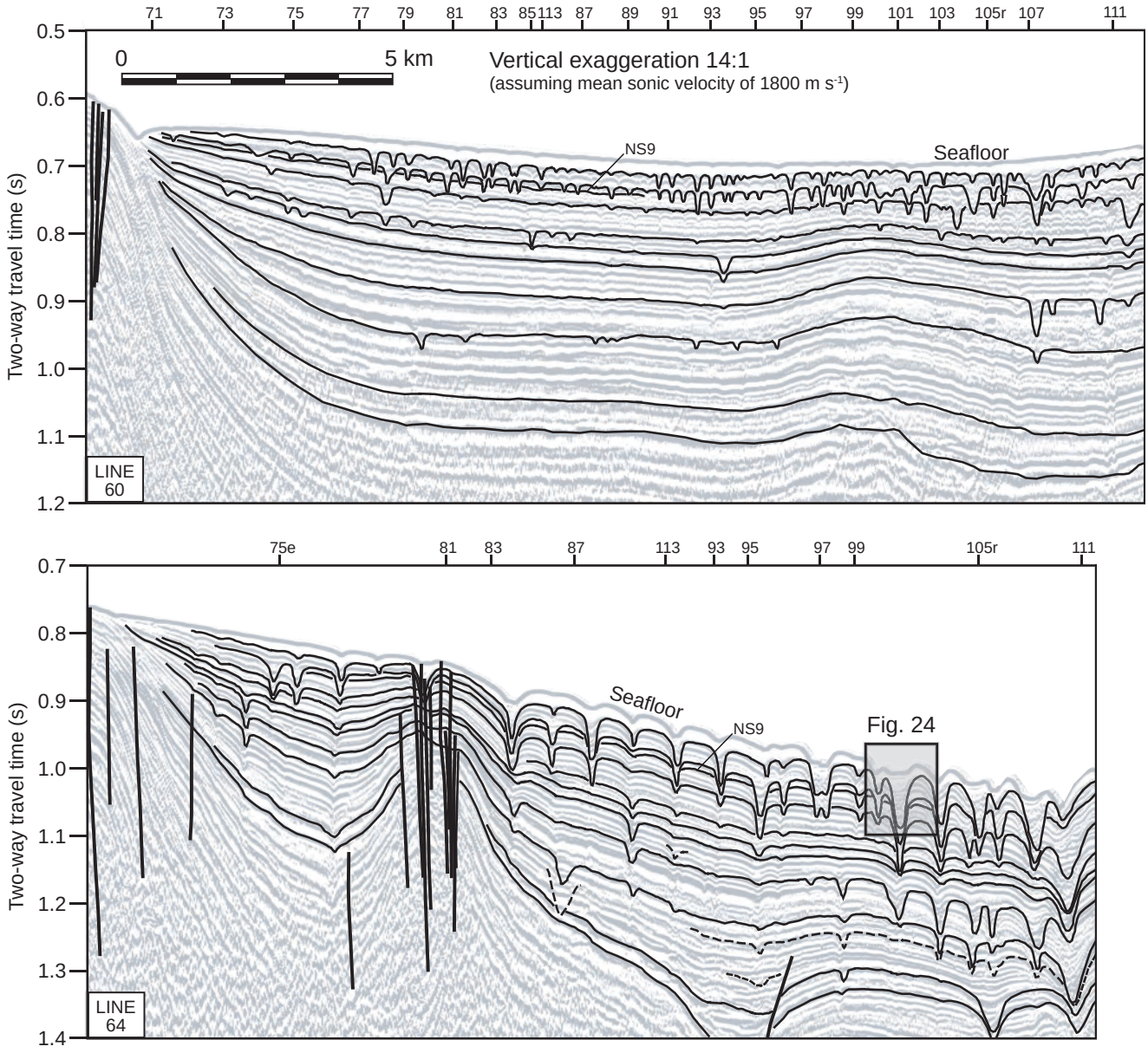

Fig. 23 Interpreted portions of seismic lines 60 and 64, showing the downslope evolution of slope channel geometries. See Fig. 22 for uninterpreted data. Near-vertical bold lines represent faults. Note the expression of larger channels on older surfaces seaward, as well as the increase in numbers of channels on younger surfaces. Channel highlighted on line 64 is shown in greater detail in Fig. 24. (From Burger *et al*., 2002.)

been traced seaward from the shelf break by Burger *et al*. (2002). The channels trend directly downslope, are 5–110 m deep, 50–1000 m wide, and are generally spaced 1–2 km apart. Older channels are more deeply incised and wider than younger channels. All are V-shaped in cross-section and commonly stacked directly above one another. The density of channels on any given surface increases seaward from the upper slope, and then decreases again as they coalesce farther downslope. Most have a distinctive sedimentary fill consisting of high-amplitude basal reflections that decrease in amplitude upwards and become more draping in character (Fig. 24). Subdued but detectable topography of most channels appears to be the nucleus for the start of the next younger channel.

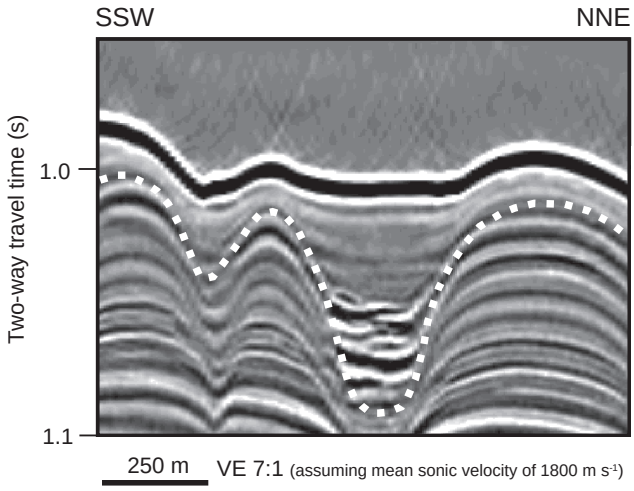

Fig. 24 Detailed image of a slope channel (white dotted line) from seismic profile 64 (see Fig. 23). Note the high-amplitude basal fill, buried by reflectors of decreasing amplitude, suggesting a fining upward progression of channel-fill sediment. (From Burger *et al*., 2002.)

Gullies ~1–3 m deep have been observed in high-resolution seismic profiles to ~65 m below the seafloor in the same upper-slope area where channels occur (Field *et al*., 1999; Spinelli & Field, 2001). These gullies are below the vertical resolution of airgun-based MCS profiling, and are generally more closely spaced (~100–1000 m) than the more deeply buried channels. However, the morphologies of the two types of features are similar and the gullies merge into the larger channels downslope, suggesting they are simply tributaries to the channels (Spinelli & Field, 2001).

Gullies are incised during regressions by downslope transport of coarse-grained sediment (Spinelli & Field, 2001). Today, they are much closer to Mad River than to Eel River. With evidence that Eel River sediments preferentially debouch into Eel Canyon during lowstands, Mad River is implicated as the source of gully-carving sediments (Fig. 25). If the deeper, larger channels are linked to the same process of formation, then it is likely that the channels are gullies that were either too large or too distal to be totally filled more often than once every 100 kyr. Pratson *et al*. (1994) have shown that mid- to lower-slope canyons off New Jersey can remain clear of sediment through several glacio-eustatic cycles, while the heads of canyons on the upper slope are repeatedly buried and re-excavated. A similar process may have occurred on the Eel slope, making the gullies shorter-lived equivalents of the downslope extensions termed 'channels'.

The density and distribution of channels have changed through time. Younger surfaces display many large channels, distributed fairly evenly across the upper slope. In contrast, older surfaces display a smaller number of large channels concentrated at the northern end of the study area (Figs 22 & 23). Gas-charged sediments that degrade the image quality of seismic profiles are less prevalent north of the Little Salmon Anticline than to the south, and consequently northern surfaces can be correlated to surfaces mapped beneath the shelf.

Gas in the sediment column

Gas is generated in the subseafloor by two mechanisms (Kvenvolden *et al*., 1993): bacterial degradation of scavenged organic matter; and chemical production of complex hydrocarbons (from organic

Fig. 25 (*opposite*) Interpreted areas of sediment transport, erosion and deposition on the upper slope of Eel River Basin during various stages of sea level. (A) Highstand: suspended sediment from the Eel River bypasses the shelf to the upper slope, depositing fine-grained sediment in the Humboldt Slide area, and hemipelagic sediment on the more distal slope north of the Little Salmon Fault Zone (LSFZ). Slope channels and gullies north of the LSFZ are inactive. Sediment also bypasses the shelf and upper slope through Eel Canyon. (B) Falling stage: increasing amounts of Eel River sediment bypass the shelf and upper slope by way of Eel Canyon. Sediment is eroded, supplying increasing amounts of fine-grained sediment to the upper slope. Sediment discharged from the Mad River deposits progressively closer to the upper slope, increasing slope sediment input north of the LSFZ. Channels north of the LSFZ reactivate along pre-existing trends, and also become bypass conduits. (C) Lowstand: most Eel River sediment bypasses the shelf and upper slope through Eel Canyon. Minimal sediment deposition is expected in the Humboldt Slide area. The Mad River extends to the shelf edge and its sediment causes erosion of slope channels seaward of its mouth. (D) Transgression: bypass of sediment through Eel Canyon decreases, and supply of eroded shelf sediment resumes in the Humboldt Slide area. However, as shelf sediment sources become more distal, slope channels north of the LSFZ begin to infill, first by relatively coarse basal lags, then by finer grained hemipelagic sediment (see Fig. 24). (From Burger *et al*., 2002.)

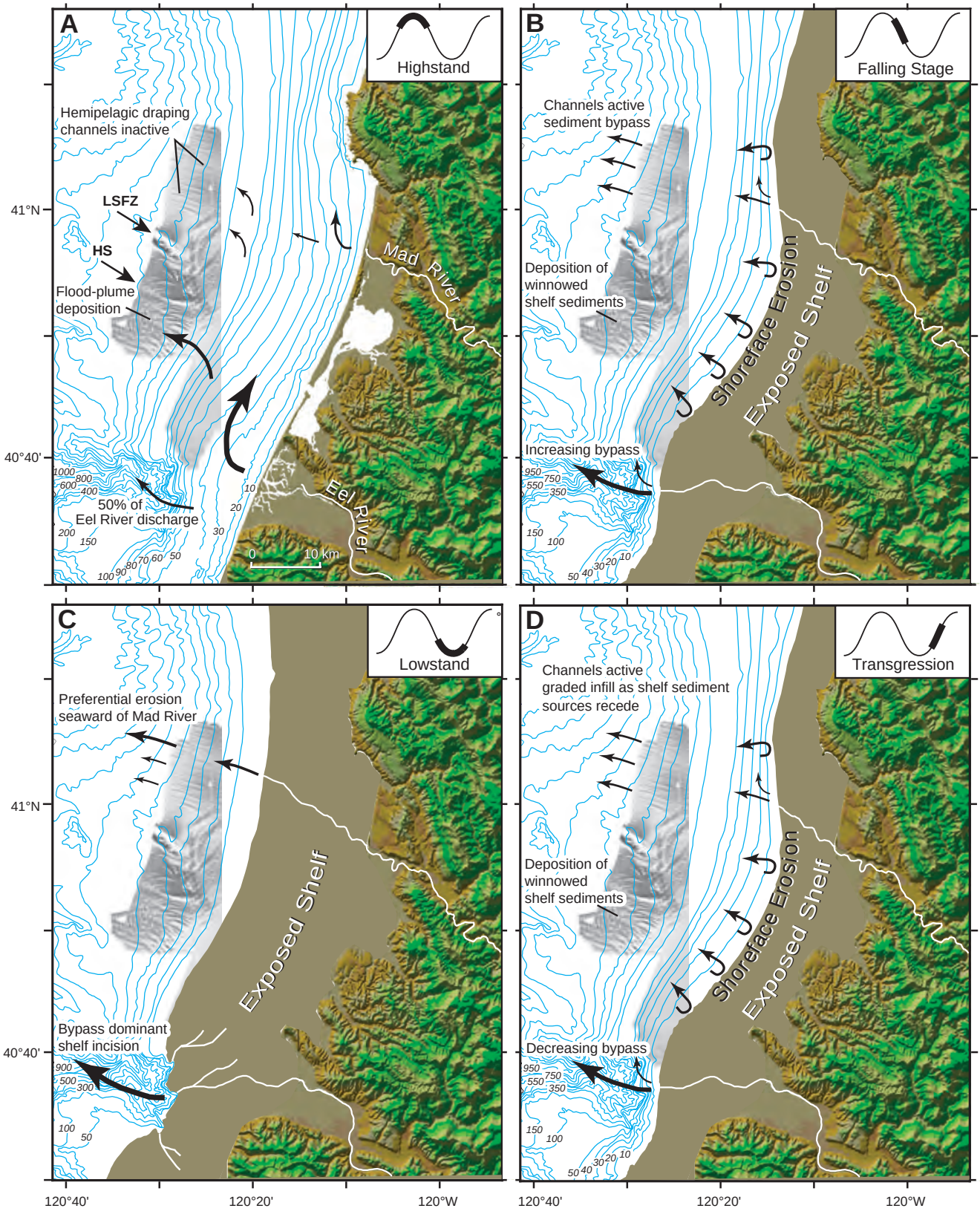
A
Highstand
Hemipelagic draping
channels inactive
LSFZ
HS
Flood-plume
deposition
50% of
Eel River discharge
Mad River
Eel River
0
10 km
B
Falling Stage
Channels active
sediment bypass
Deposition of
winnowed
shelf sediments
Shoreface Erosion
Exposed Shelf
Increasing bypass
C
Lowstand
Preferential erosion
seaward of Mad River
Exposed Shelf
Bypass dominant
shelf incision
D
Transgression
Channels active
graded infill as shelf sediment
sources recede
Deposition of
winnowed
shelf sediments
Shoreface Erosion
Exposed Shelf
Decreasing bypass
41°N
40°40'
120°40'
120°20'
120°W

matter and pre-existing oil) under favourable conditions of pressure, temperature and anoxia. The former, **biogenic**, origin predominantly generates methane; the latter, **thermogenic**, origin generates methane at early stages that under proper conditions can lead to ethane, pentane and other long-chain hydrocarbons. Biogenic gas is generated in the upper few hundred metres below the seafloor (the presumed bacterial habitat), but if sealed completely can become buried to greater depths. By contrast, thermogenic processes require conditions generally found at considerably greater depths, and any gas of this type that is detected a few hundred metres below the seafloor has very likely migrated up from deeper levels of origin.

The Eel River Basin (Fig. 26) has potential for hosting both types of gas (Lorenson *et al.*, 1998). Biogenic gas can be expected to result from the rapid burial of both organic-rich fluvial sediment and marine plankton that flourish in the nutrient-rich upwelling waters of the northern California margin (see Leithold & Blair, 2001). The tectonic

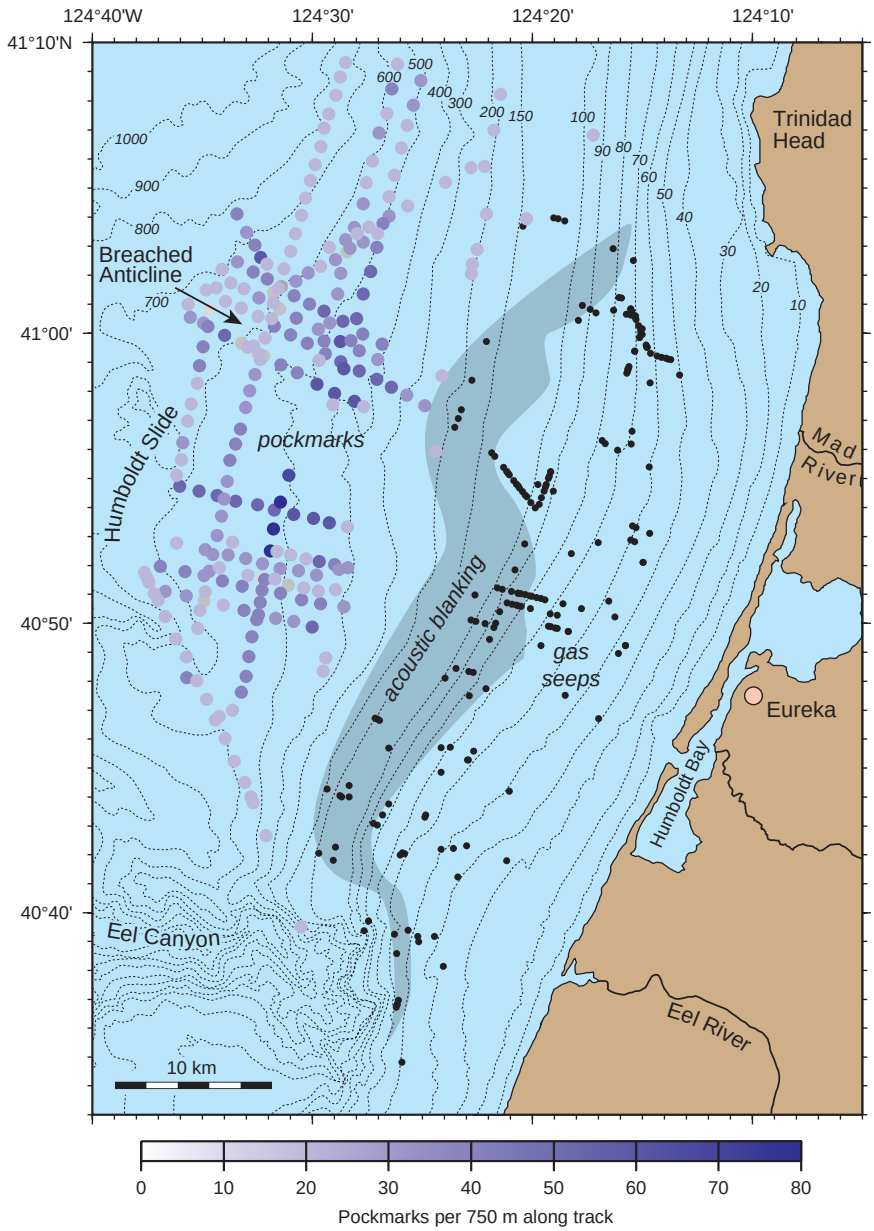

Fig. 26 Indicators of gas in the sediments of the Eel River Basin. The dark blue region along the outer shelf is an area of acoustic blanking of MCS reflections, interpreted to be due to gas in the sediments. Small black circles predominantly on the shelf are water-column plumes identified in 3.5-kHz records and assumed to be gas seeps. Larger circles on the slope are pockmarks detected with deep-towed sidescan; range of purple hues denotes number of pockmarks per 750 m along and across track (i.e. counts ranged from 1 to 80). (After Yun *et al.*, 1999.)

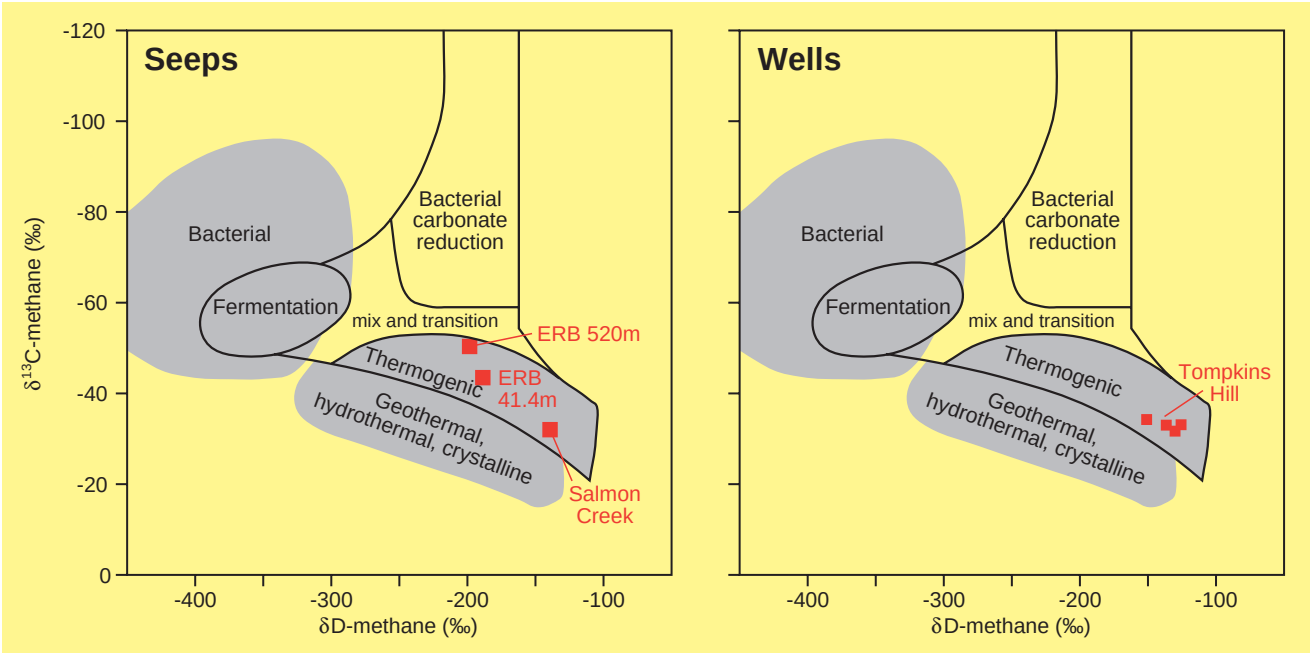

Fig. 27 Isotopic character of gas in the Eel River Basin (ERB) measured in seeps (offshore) and wells (onshore). The $\delta^{13}C$ versus deuterium in methane plot distinguishes between biogenic and thermogenic sources, and suggests that methane in the Eel River Basin is predominantly thermogenic. (From Lorenson *et al.*, 1998.)

setting of this accretionary prism provides post-depositional conditions that lead to thermogenic hydrocarbons as well (Kvenvolden & Field, 1981). Limited geochemical analyses of gas from onshore wells and from seeps both onshore and offshore have determined that thermogenic gas is the more common (Fig. 27; Lorenson *et al.*, 1998).

The abundance of gas in the offshore Eel River Basin has a significant impact on our ability to understand the long-term record of this continental margin. Gas in sufficient quantity impedes the acquisition of an acoustic image, which is usually the most informative stratigraphic approach through remote sensing. Furthermore, the evidence of gas seen venting into the water column or inferred by epifaunal chemosynthetic communities and explosive craters demonstrates that gas has influenced the development of the long-term record.

The loss of reflector strength due to gas-charged formations, **acoustic wipeout**, has proven to be insurmountable in the Eel River Basin. The towed Huntec boomer system (Field *et al.*, 1999; Spinelli & Field, 2001) found large areas of acoustically impenetrable seafloor. A single 45/45-cubic-inch GI gun was also largely unsuccessful in imaging subsurface features in a margin-parallel corridor between 80 m and 200 m water depths (Fig. 26). Amoco Corporation provided reconnaissance profiles acquired by JEBCO Geophysical using a 3380-cubic-inch airgun array that could penetrate to more than 1 km below the seafloor in adjacent regions. Despite this powerful source, the same wipeout zone was encountered on the outer shelf and upper slope. This zone generally parallels isobaths, and is only locally affected by NW–SE structural trends (Yun *et al.*, 1999).

Active gas **seeps** in the Eel River Basin have been detected by water-column reflections in 3.5-kHz records from less than 300 m of water depth (Yun *et al.*, 1999). Side-scan-sonar images show no association with seafloor topography, and MCS profiles indicate no correspondence with underlying structures. Seeps have been the target of camera and water-sampling surveys using the *ROV Ventana* (Monterey Bay Aquarium Research Institute; Orange *et al.*, 1999). Active seeps have been located by gas bubbles seen escaping from the seabed, while dormant seeps have been inferred by the presence of chemosynthetic communities

that depend on fluids and gas (Kulm & Suess, 1990). Studies of similar shallow-water seeps have revealed discontinuous venting thought to be the result of diurnal tidal effects and changes in water temperature (see Hagen & Vogt, 1999). The cause and repeat time of active gas venting in the Eel River Basin are not known.

Seabed **pockmarks** are conical depressions that are the result of recent or active fluid expulsion (Hovland & Judd, 1988). Abundant small pockmarks are observed almost exclusively on the upper continental slope (not the shelf) of the Eel River Basin (Yun *et al*., 1999) (Fig. 26). Pockmarks range from ~10 m (grid-size limit of sidescan data) to > 25 m in diameter, and are typically 3 m deep. They are randomly distributed, clustered, or aligned. Field *et al*. (1999) examined pockmarks in relationship to erosional and aggradational gullies along the slope north of the Humboldt Slide and the breached Little Salmon Anticline, and concluded that there is no compelling evidence linking these morphological features. Yun *et al*. (1999) have counted > 3500 pockmarks along roughly 1500 km of shiptrack with sidescan swath width of 500–750 m, and find that > 95% occur in water depths > 400 m. Pockmarks are most abundant on the immediate north and south sides of the breached Little Salmon Anticline, including the region of the Humboldt Slide (Lee *et al*., this volume, pp. 213–274).

Stratigraphic modelling

Matching stratigraphy to observations

Backstripping (Syvitski *et al*., this volume, pp. 459–529) has been used to simulate the Eel River Basin long-term stratigraphic development (Fig. 28), using a sea-level curve for the past 125 kyr imposed on the relatively steep dips, rapid subsidence and high sediment supply that characterize this margin. The complex, multistage sea-level fall from marine Oxygen Isotope Stage 5 (125 ka) to Stage 2 (18 ka) produces a series of progradational packages. Considerable sediment removal during both regressive and transgressive parts of the observed cycles leaves the margin interrupted by numerous erosional surfaces. The large sea-level rise since the Last Glacial Maximum has covered the entire section with a smooth marine trangressive drape. The model run used a tectonic subsidence at the shelf edge of 2.1 mm yr^{-1} which coincides with the 1.4–3.3 mm yr^{-1} rate derived onshore from the displacement of marine terraces (Orange, 1999).

A section through the Freshwater Syncline (Fig. 28) helps to resolve patterns that are consistent with the model predictions. The seismic profile shows a series of strong, slightly divergent reflectors on the shelf, topped by the relatively transparent Holocene transgressive drape. These reflectors have been highlighted in red (Fig. 28c) to correspond with the erosion surfaces in the model, although not all are necessarily unconformities. More steeply dipping reflectors, highlighted in yellow, are contained within the packages defined by these unconformities, and correspond to prograding shorefaces and other dipping interfaces. Additional surfaces seaward and landward of the dipping reflectors (highlighted maroon and green, respectively; Fig. 28c) have shallower dips subparallel to the major reflectors. Based on their position relative to the assumed shoreface, these surfaces have been correlated to marine and fluvial deposits, respectively. Although these features are at the limits of the resolution of the image, similarity between observations and predictions is encouraging.

Several discrepancies should be noted. The initially rapid progradation of the margin depicted in this model (Fig. 28A & B) is an artefact of the start-up conditions, as is the depositional minimum at the base of the slope; neither feature corresponds to observations from the actual data. The model predicts much less sediment accumulation on the slope than is observed in profiles; sediment-supply and/or slope-failure parameters of the model apparently do not match reality. Other parameters should be adjusted to maintain the correct shelf width. Another limitation is that the model does not accumulate sediment on the uppermost slope, even when the modelled amount of sediment failure is reduced significantly. This appears to be due to the erosion of the shelf edge during modelled transgression, a process that has been reported previously to explain hardgrounds on the uppermost slope (Lee *et al*., 1999). On the shelf, the model predicts that the strata below the Holocene transgressive drape should be a complex package of nearshore deposits interfingered with marine shales and a limited amount of non-marine strata

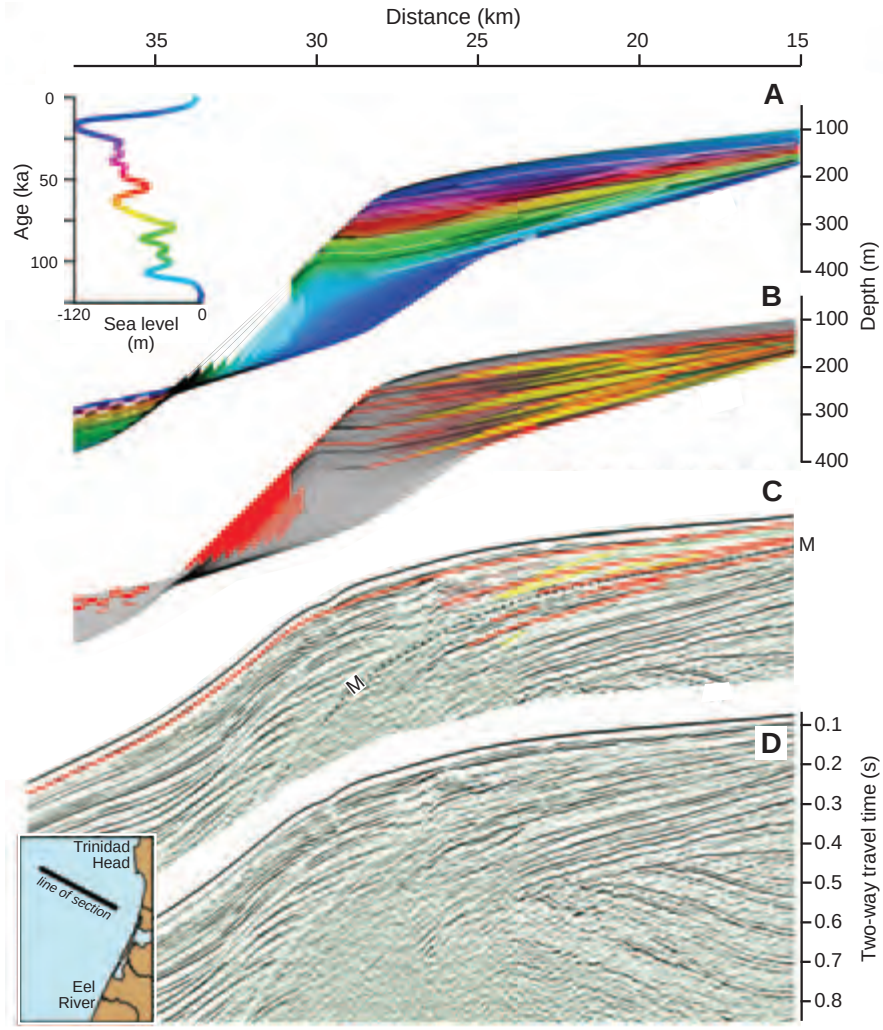

Fig. 28 Model of stratigraphic development in the Eel River Basin compared with seismic stratigraphy. Data shown are from line 83 (Fig. 9). (A) Model at top shows 5-kyr time steps keyed by colour to time and position within sea-level curve shown at left. Sea-level history since 125 ka comes from SPECMAP (Imbrie *et al.*, 1984), assuming sea level was 120 m below present at marine Oxygen Isotope Stage 2. The model fails to account for slow accumulation rates on the lower slope shown in white. (B) Model and (C) seismic profile show the same stratigraphic units, with colours indicating environments of deposition. Red and yellow lines on the profile denote erosion surfaces and prograding shorefaces (see text). (D) The uninterpreted profile plotted against two-way travel time, with a location map (inset).

(Fig. 28A & B). Below the thick transgressive drape, the strata of the Eel River margin do not reflect the seafloor bathymetry; a similar contrast between bathymetry and buried stratal geometry can be seen on the New Jersey margin as well (see below).

There are intriguing and unresolved differences in the stratigraphy between the Eel River margin (ERM) and New Jersey margin (NJM) that have been captured in the respective forward models. The New Jersey margin has extensive, well-developed prograding clinoforms; similar progradation is lacking off California. The Eel River margin exhibits considerable tectonic deformation that includes much greater subsidence than is found off New Jersey, with the result that Eel River margin sediments reveal considerably greater seaward divergence of reflectors beneath the shelf. Over the long term, the accommodation space created on the Eel River shelf is filled by sediments delivered to the margin. The balance between progradation and subsidence results in a stationary position of the shelf edge (Ulicny *et al.*, 2002). Within sea-level cycles, sediment depocentres transgress and regress across this margin, but each sequence builds to a similar position.

A model of sequence-stratigraphic development

Based on STRATAFORM observations of the Eel River Basin, a conceptual model can explain sequence development that results in syncline filling modulated by sea-level variations (Burger *et al.*, 2002). The Eel River shelf becomes progressively exposed during times of falling sea level (Fig. 29).

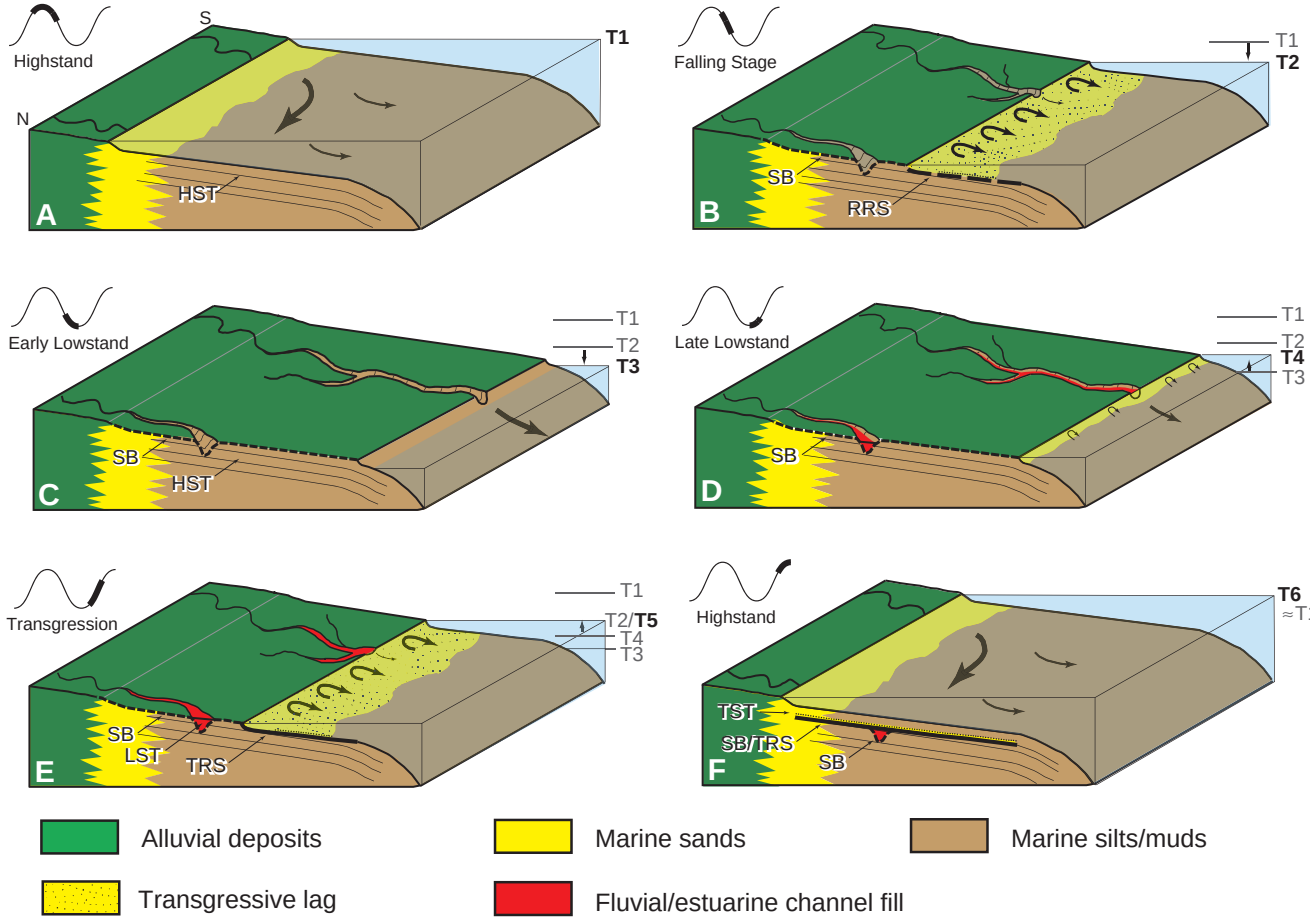

Fig. 29 Proposed sequence-stratigraphic model for the Eel shelf. (A) Highstand: alongshelf-directed, shallow-marine sediment transport and accumulation occurs, as at present. (B) Falling stage: shelf is progressively exposed, and a regressive ravinement forms by shoreface erosion as it crosses the shelf. The exposed shelf represents the lowstand sequence boundary. (C) Early lowstand: sea level approaches the former shelf edge; sediments largely bypass the shelf through fluvial channels. (D) Late lowstand: fluvial gradients decrease, initiating channel infilling seaward; shoreface erosion of the shelf resumes. (E) Transgression: shelf channels are progressively infilled seaward to landward; vigorous erosion forms a prominent transgressive ravinement as the shoreface advances across the shelf. Lowstand sediments and the sequence boundary are eroded in all but deeply incised areas. (F) Highstand: alongshelf accumulation of sediments resumes. Over most of the shelf, highstand deposits directly overlie highstand sediments from the previous sequence. SB, sequence boundary; RRS, regressive ravinement surface; TRS, transgressive ravinement surface; SB/TRS, composite surface; HST, highstand systems tract; LST, lowstand systems tract; TST, transgressive systems tract. (After Burger *et al*., 2002.)

Rivers incise a widening coastal plain and deliver sediment to a narrowing shelf (Burger *et al*., 2001). It is likely that a regressive ravinement surface forms by shoreface erosion during these periods. Numerous profiles in the southern Eel River Basin show that the Eel River often has diverted sediment from the shelf by extending close to or into the head of Eel Canyon, through which fluvial sediments continued farther seaward. Incised channels also have formed in response to uplift of the Table Bluff Anticline (Burger *et al*., 2001). Farther north, the Mad River shelf valley also has extended to the shelf edge during times of falling sea level; fluvial sediment is then funnelled directly to the slope and the Gorda Fan. Poorly preserved interfluves between shelf valleys, as well as occasionally preserved valley fill,

are the only deposits retained on the shelf during times of lowered sea level. As sea level begins to rise, fluvial gradients decrease, and incised shelf channels fill preferentially with an upward-fining sequence of fluvial sands grading into estuarine facies. Accumulation in the areas between channels very likely remains low to absent.

During transgression, the shoreface retreats across a widening shelf (Fig. 29), and erosion removes lowstand sediments in all but the most deeply incised areas and transports these materials seaward. The regressive ravinement and interfluve portions of the sequence boundary formed during the previous sea-level fall are probably completely cannibalized. Erosion then forms a transgressive ravinement, winnowing removes the fine-grained sediment, and a thin, coarse lag deposit forms as a result, immediately above the ravinement unconformity. Where the transgressive ravinement truncates the previous lowstand surface (in most areas), the surface becomes a composite sequence boundary. Highstand silts and muds from the previous sequence underlie similar sediments from the ensuing highstand, separated only by the ravinement and the thin transgressive lag. Lowstand deposits are preserved only as hummocky channel fills, between the sequence boundary and ravinement surface in deeply incised areas.

THE NEW JERSEY MARGIN

Cenozoic sedimentation on a passive margin

Observations

The New Jersey margin (NJM; Fig. 30) is a classic example of a passive margin. Rifting began in Late Triassic times (Grow & Sheridan, 1988), and seafloor spreading commenced by the Callovian (~165 Ma; Middle Jurassic; Sheridan *et al*., 1983). The subsequent tectonic history has been dominated by simple thermal subsidence, sediment loading and flexure (Watts & Steckler, 1979; Reynolds *et al*., 1991). The Jurassic section beneath the central to outer shelf is composed of thick (typically 8–12 km), shallow-water limestones and shales. A barrier-reef complex fringed the margin until the Mid-Cretaceous (Jansa, 1981). Accumulation rates were generally low during Late Cretaceous to Paleogene time, when the offshore region was predominantly a starved **carbonate ramp** (Poag, 1985). Carbonate accumulation ended in the late middle Eocene beneath today's coastal plain and shelf, and in earliest Oligocene times beneath the slope, probably in response to global and regional cooling (Miller *et al*., 1996b).

Sediment accumulation rates increased dramatically on the New Jersey margin in the late Oligocene to Miocene (Poag, 1985; Miller *et al*., 1997b). Although the cause of this increase is not known with certainty, it has been attributed to tectonics in the hinterland (Poag & Sevon, 1989). Sediments prograded across the margin throughout the Miocene and Pleistocene, and accumulated at rates high enough (~10–100 m Myr^{-1}) to provide detailed seismic resolution of stratal relationships (Poag, 1977; Schlee, 1981; Greenlee *et al*., 1988, 1992). Tectonic subsidence throughout the Cenozoic has been along the relatively well-defined, nearly linear part of the thermal subsidence curve (Steckler & Watts, 1982). There is little seismic or outcrop evidence to suggest faulting, rotation or other significant disturbances of the Cenozoic section (Poag, 1985), although some differential subsidence may have occurred between the Delmarva Peninsula and New Jersey (Owens & Gohn, 1985). This long, relatively undeformed, and rapidly deposited record has led many workers to conduct studies of continental-margin evolution using seismic, well and outcrop data (e.g. Hathaway *et al*., 1976; Poag, 1978, 1980, 1985, 1987; Kidwell, 1984, 1988; Olsson & Wise, 1987; Greenlee *et al*., 1988, 1992).

The earliest drilling along the mid-Atlantic margin comprised the Atlantic Slope Project (ASP) in 1967, conducted by a consortium of oil companies investigating the stratigraphy of the continental slope (Weed *et al*., 1974; Poag, 1978). Each site was limited to 330 m sub-bottom penetration; all were open-hole drilling from a dynamically positioned ship; no hydrocarbons were reported. The US Geological Survey (USGS) conducted similar operations on the shelf and upper slope in 1976 (the Atlantic Margin Coring Project, or AMCOR; Hathaway *et al*., 1979). Drilling was open-hole from an anchored vessel, and again was limited to 330 m sub-bottom depth.

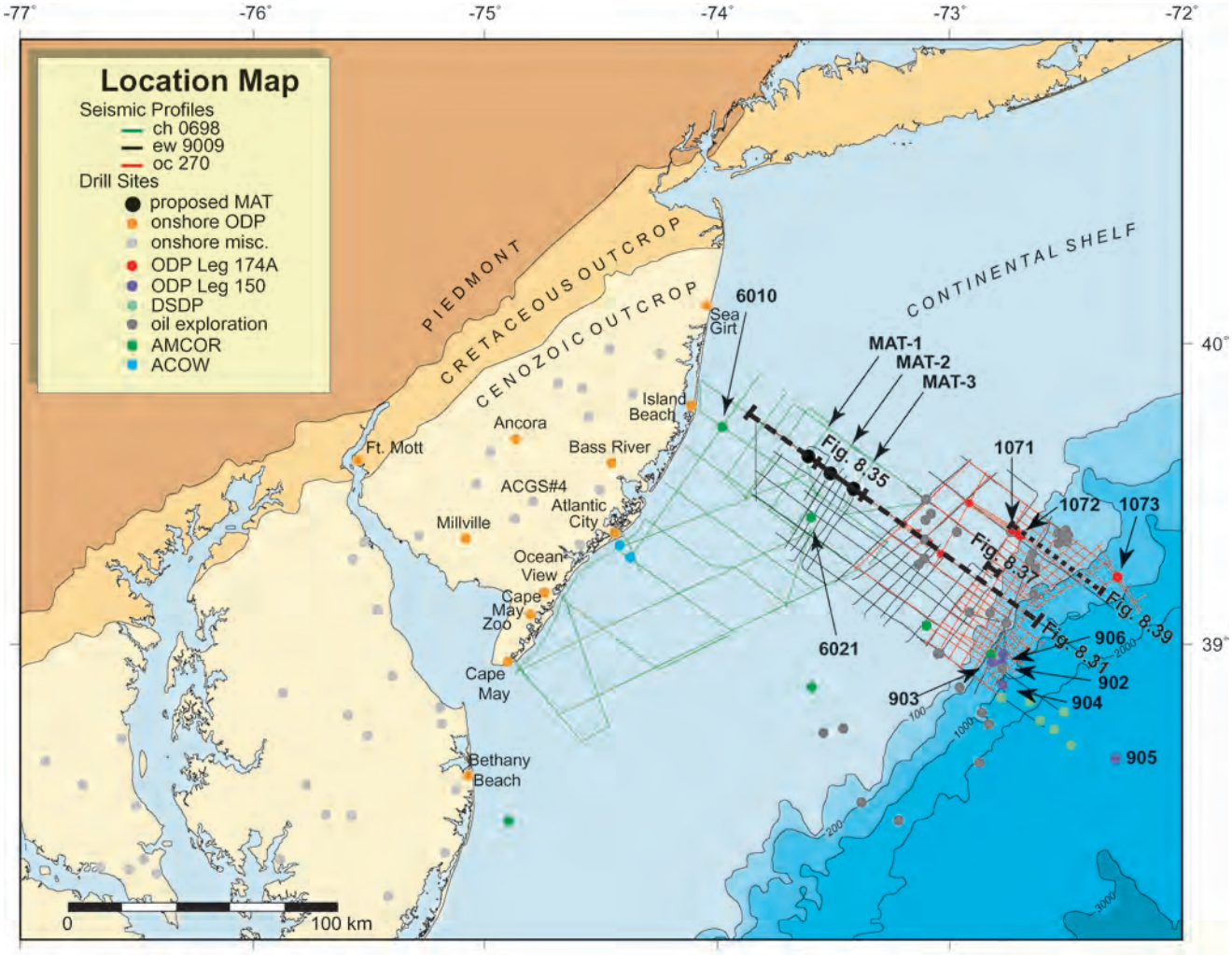

Fig. 30 Location map of New Jersey data discussed in the text. Three grids of multichannel seismic profiles (lines) collected aboard the *R/V Ewing* (Ew), *R/V Oceanus* (Oc), and *R/V Cape Hatteras* (Ch) and many wells (dots) are shown. The locations of seismic profiles shown in Figs 31, 35, 37 and 39 are shown.

Industry exploration continued along the margin in the 1970s and early 1980s (Libby-French, 1982; Prather, 1991). Roughly three dozen wells were drilled, and while some hydrocarbon shows were reported on the outer shelf, none was large enough to be commercially profitable. Some of the survey data (reconnaissance geophysics, wireline logs and petrological analyses of sidewall cores) has proven useful to researchers for baseline studies of the long-term record (e.g. Greenlee *et al.*, 1992; Fulthorpe & Austin, 1998).

Legs 93 and 95 of the Deep Sea Drilling Project (DSDP) were designed as the beginning of a margin-wide New Jersey Transect (NJT; also known as the Mid-Atlantic Transect) (Figs 30 & 31) to investigate sea-level effects on passive margins (Poag *et al.*, 1987; van Hinte *et al.*, 1987). Ocean Drilling Program (ODP) Leg 150 (Fig. 31) moved closer to land by drilling four sites (902, 903, 904 and 906) between 445 m and 1250 m water depths (Mountain *et al.*, 1994), although still on the slope and more than 140 km from shore.

A land-based drilling programme (Figs 30 & 31) was designed to complement the slope portion of the New Jersey Transect (Miller *et al.*, 1994). Three holes comprising ODP Leg 150X were cored and

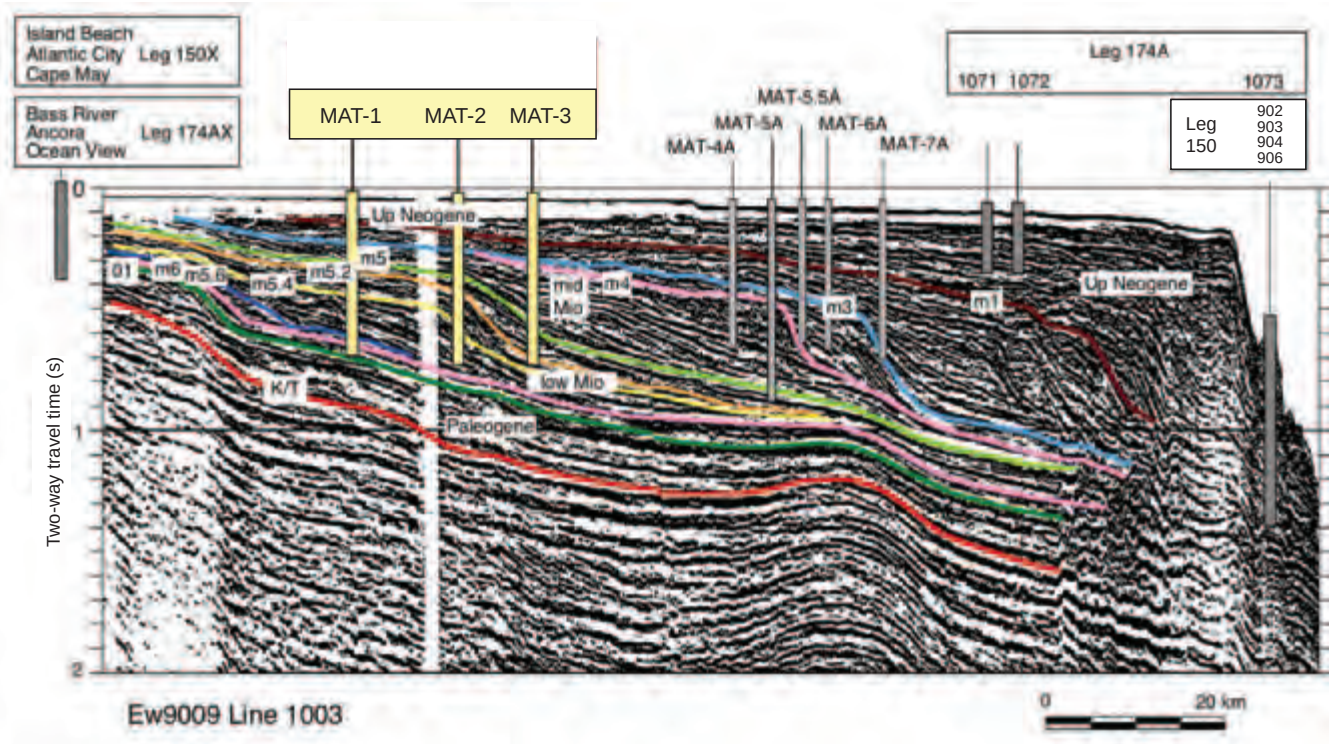

Fig. 31 Interpreted dip-oriented multichannel seismic line Ew1003. Location shown in Fig. 30. As much as 14 km of post-rift sediments lie beneath the outermost shelf, but only the upper 2 s are shown. Major sequence boundaries of post-Eocene age have been traced from the inner shelf to the slope, where they were sampled by ODP Leg 150 (general site locations shown in this profile). Sandy sediments prevented comparable penetration and recovery on the outer shelf during ODP Leg 174 (general site locations shown). Several sites have successfully recovered samples and logged across the equivalent surfaces beneath the coastal plain (Miller *et al*., 1994, among others). Sites designed to recover lower and middle Miocene clinoform strata have been proposed as ODP MAT sites (also shown). (After Miller & Mountain, 1994.)

logged along the outer edge of the coastal plain (Island Beach, Atlantic City and Cape May; Miller *et al*., 1997b) to a maximum depth of 457 m and oldest strata of Maastrichtian age. Subsequent drilling by ODP Leg 174AX (Bass River, Ancora, NJ) reached Cenomanian strata at 596 m (Miller *et al*., 1998b, 1999). These efforts focused on understanding sea-level changes during the Paleogene and Cretaceous, when global climate appears to have been too warm to support large polar ice caps.

A high-resolution multichannel-seismic grid was collected (Oc270; Austin *et al*., 1996) across the outer shelf and slope prior to more offshore drilling. With improved technology (shallow and short offset GI gun/streamer geometry, 12.5-m shot spacing) these data significantly increased the number of resolvable sequences. Subsequently, ODP Leg 174A (Austin *et al*., 1998) attempted to drill into middle to late Miocene clinoform packages on the outer continental margin (Fig. 31). A total of 12 holes at three sites were occupied on the shelf and slope, recovering roughly 1 km of core that ranged in age from late Eocene through to Pleistocene. Slope drilling (Site 1073) recovered a thick Pleistocene section and condensed Pliocene to upper Eocene section with excellent biostratigraphic resolution.

Onshore facies – stacked highstands

Repetitive transgressive–regressive cycles have long been recognized in the New Jersey Coastal Plain (Owens & Sohl, 1969; Owens & Gohn, 1985). The idealized transgressive sequence consists of glauconite sand at the base overlain by a regressive

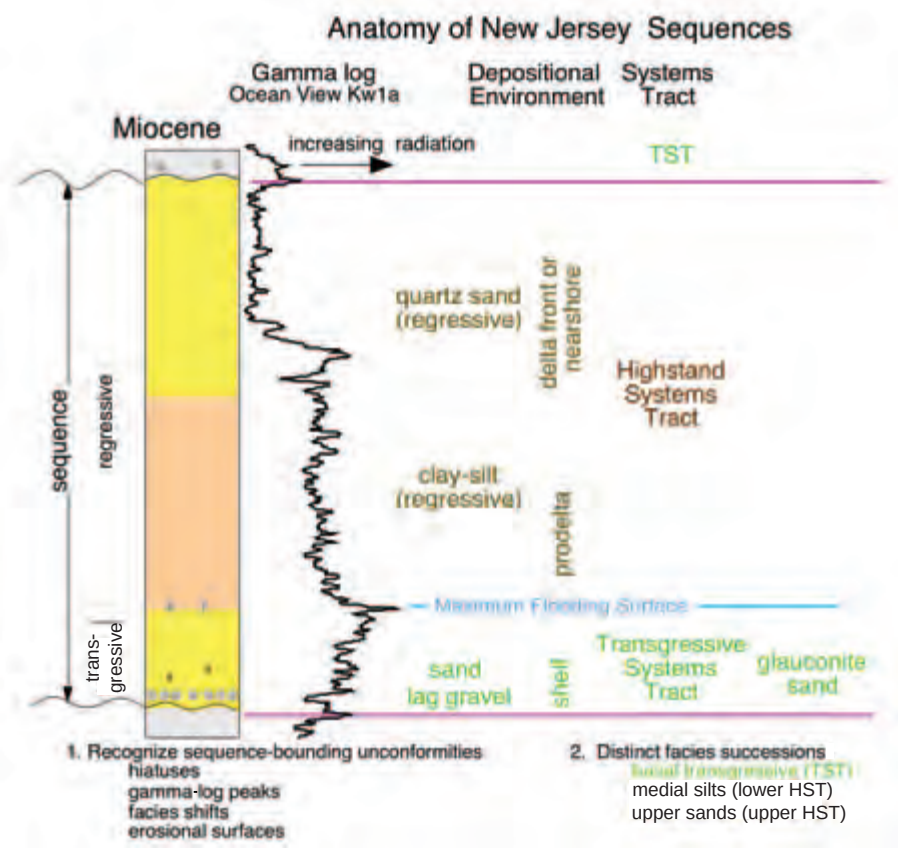

Fig. 32 Characteristics of a typical unconformably bounded sequence in Miocene sediments of the New Jersey Coastal Plain. (After Miller *et al*., 1997a.)

succession of silt coarsening upwards to quartz sand (Fig. 32) (Owens & Sohl, 1969). The basal glauconite sand (the **condensed section** of Loutit *et al*., 1988) is equivalent to the upper **transgressive systems tract** (TST) of Posamentier *et al*. (1988), the overlying silt is equivalent to the lower **highstand systems tract** (HST), and the quartz sand corresponds to the upper HST (Sugarman *et al*., 1993). These patterns result in distinct gamma-ray-log signatures, with high gamma-ray values at the base and low values at the top. Lowstand systems tracts (LSTs) are rarely preserved in the coastal plain and the TSTs are generally thin.

Thinly developed TSTs mean that the maximum flooding surface (MFS) is often difficult to distinguish from an unconformity in the New Jersey Coastal Plain, and both surfaces are typically associated with shell beds. In general, MFSs are recognized by lithofacies successions and benthic foraminiferal changes. The MFS in Miocene sequences of the New Jersey Coastal Plain is usually marked by an upward change from clayey sand to silt.

Studies of New Jersey's onshore sediments, prior to the recognition of these transgressive–regressive cycles, were hampered by a lack of adequate study material due to deeply weathered outcrops and discontinuous coring in wells. Boreholes from ODP Legs 150X and 174A (Fig. 31) led to dramatically improved understanding of regional patterns by providing continuously cored sections with > 85% recovery that enabled facies and age determination in sediments as old as mid-Cretaceous (Miller *et al*., 1994, 1996a).

Unconformities in core samples from ODP boreholes in the New Jersey Coastal Plain are identified by physical evidence (irregular contacts, reworking, bioturbation, and major facies changes) and well-log characteristics (gamma-ray peaks), and are generally associated with time gaps detected by biostratigraphic and/or chemostratigraphic (Sr-isotopic) breaks. These surfaces are interpreted as sequence boundaries, denoting a rapid fall in **base level**. Hiatuses that are not associated with obvious stratal surfaces or evidence of erosion/non-deposition are interpreted as paraconformities.

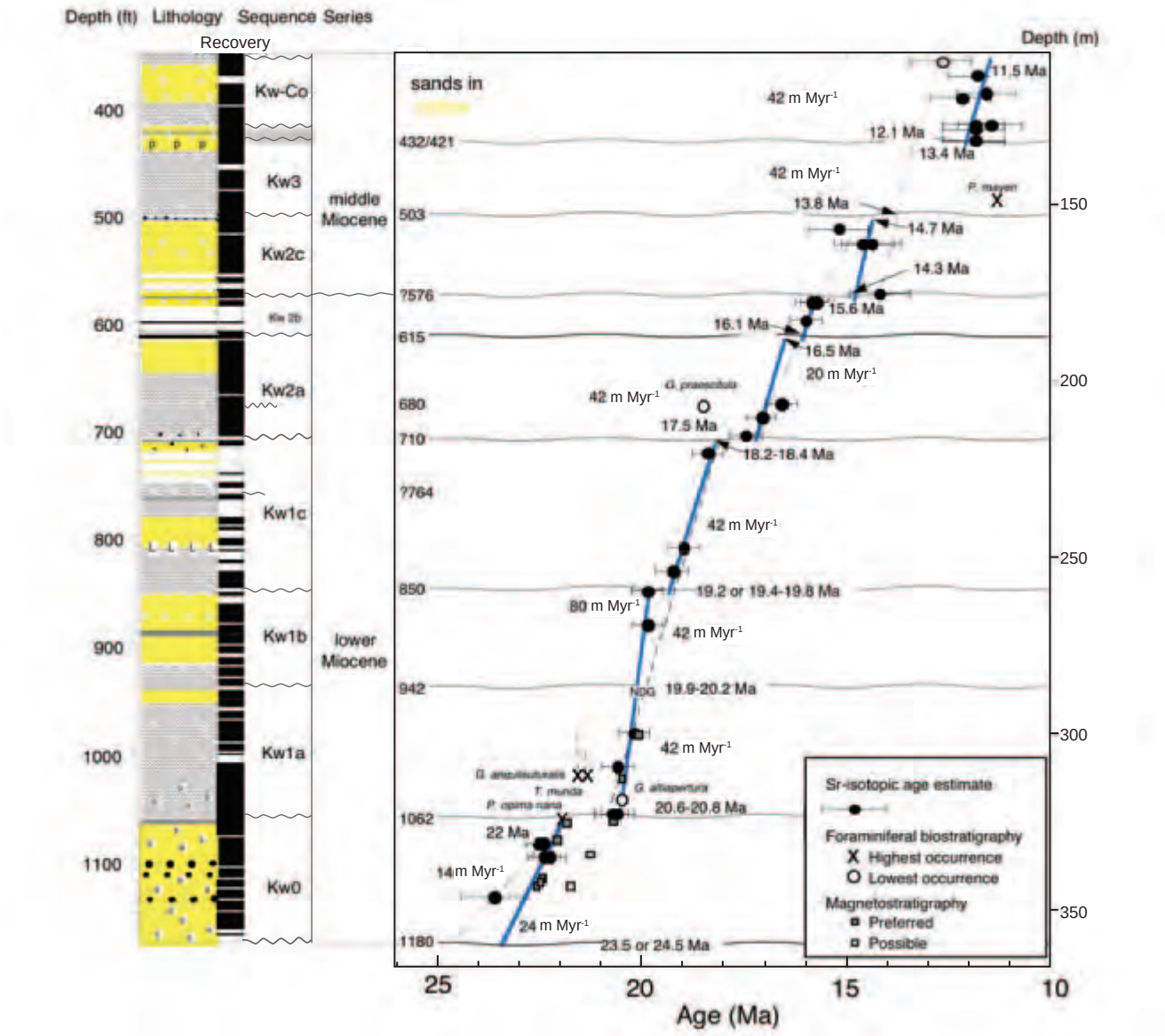

Fig. 33 Age–depth plot of a part of the Miocene section at the Cape May well (Miller *et al*., 1996b), showing the integration of ages derived from Sr isotopes, magnetic-field reversals and biostratigraphic zonations in determining a geochronology. (After Miller *et al*., 1997a.)

While hiatuses generally correlate between drill holes, downdip sections are typically more complete than updip correlatives.

The dates of Miocene sequences on the New Jersey Coastal Plain rely primarily on Sr-isotopic ages (Miller *et al*., 1997a; Sugarman *et al*., 1997), with a time resolution of ±0.3–0.6 Myr for the earlier part and ±0.9–1.2 Myr for the later part. The chronology of onshore Miocene sequences has been derived from age–depth diagrams in which sediment accumulation rates are linearly interpolated between age estimates (Fig. 33). Sequence boundaries are generally associated with hiatuses that occur throughout the coastal plain, and accompanying physical stratigraphy indicating a fall in base level. Specific facies successions vary from the Cretaceous to Miocene in response to differences in palaeodepth, provenance, preservation and deltaic influences (Owens & Gohn, 1985). In general, Miocene sequences follow the generalized pattern of all onshore sequences, and comprise three major lithofacies:

1 thin, shelly, occasionally glauconitic quartz sands of the TST, deposited in neritic (30–100 m palaeodepth) environments;
2 silty clays of the lower HST, deposited in shallower prodelta environments;
3 upper quartz sands of the upper HST, deposited in nearshore (< 30 m) and delta-front environments.

The TST is thin or absent, so the silty clays and thick sands often stack together as a series of coarsening-upward couplets (Sugarman & Miller, 1997).

Facies patterns within Miocene coastal-plain sequences Kw1a and Kw1b (Fig. 33) reveal variations in both the strike and dip directions that are due to interfingering between marine, transitional marine and deltaic environments (Fig. 34). Sequences tend to thin updip, although they occasionally thicken along strike. Highstand systems tracts generally become progressively coarser and shallower updip (e.g. the Kw1b between Cape May and Atlantic City), although the Kw1b HST at Atlantic City is finer than at Cape May because of the juxtaposition of prodelta-delta front versus neritic-nearshore environments (Fig. 34). Based on these observations, it appears that the depocentre shifted from near Island Beach during Kw1a to near ACGS#4 (Fig. 30) during Kw1b. Small-scale parasequences (shoaling-upward cycles bounded by flooding surfaces; Van Waggoner *et al*., 1988) can be detected within several sequences (e.g. within the Kw1b sequence, at Atlantic City, Island Beach and ACGS#4; within Kw1a at Island Beach; Fig. 34).

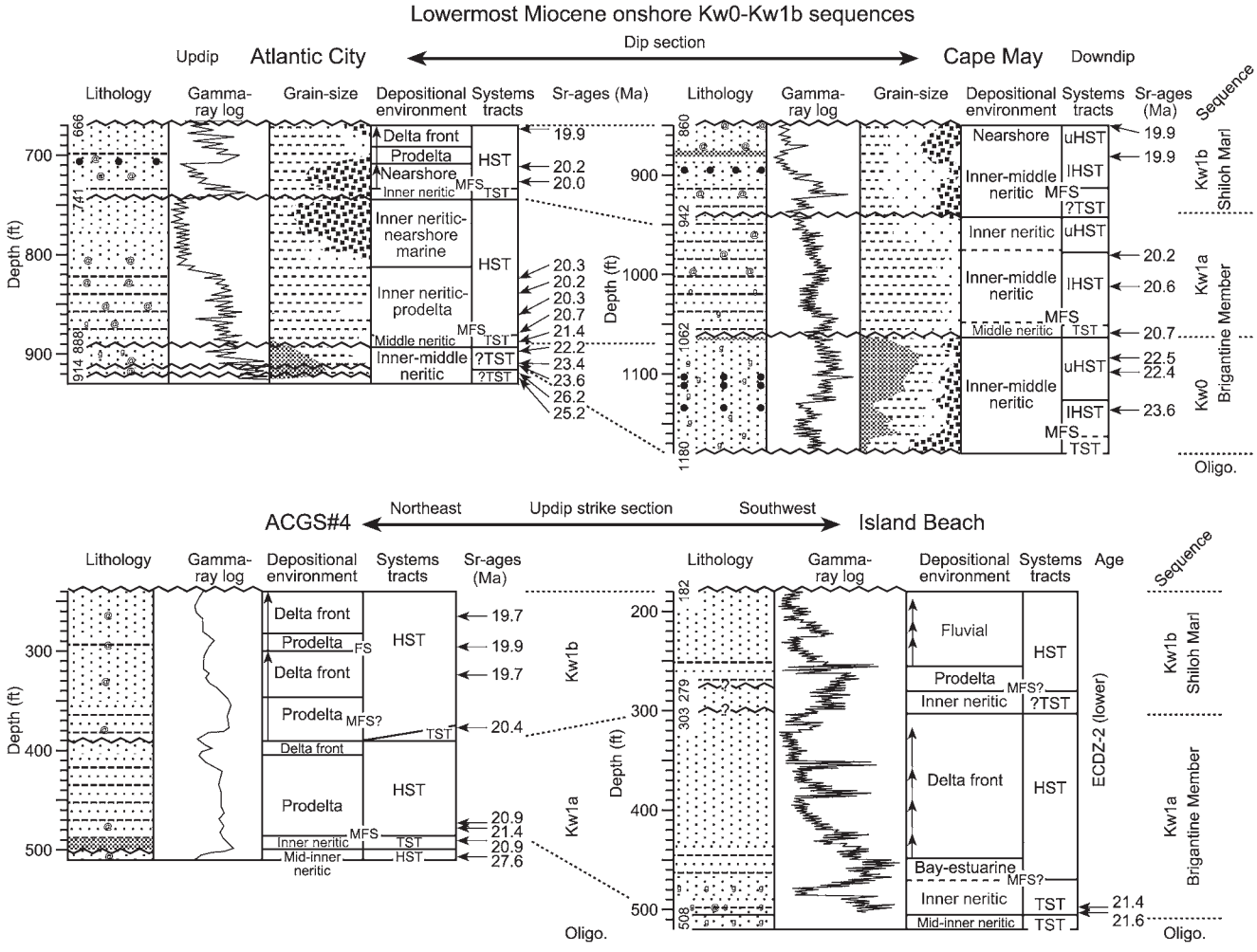

Fig. 34 Comparison of along-strike and down-dip variations of lower Miocene facies in the New Jersey Coastal Plain (see text). (From Miller *et al*., 1998a.)

Inner-shelf geometries – multiple sediment sources

Using seismic data collected by oil companies, Greenlee & Moore (1988) and Greenlee *et al*. (1988) showed prograding Miocene units beneath the inner and middle shelf. Poag & Sevon (1989) and Poag & Ward (1993) determined first-order patterns in Miocene accumulation. They mapped ancestral Susquehanna/Delaware and Hudson River drainage systems showing south-eastward trends across the margin, and they prepared isopach maps that portrayed a wide but relatively uniform early Miocene margin. Greenlee *et al*. (1992) consolidated seismic data collected to that point and identified eight sequences in well-preserved clinoforms beneath the present inner to middle shelf, thought to span Oligocene through late Miocene age.

The onshore boreholes of ODP Leg 150X were drilled with knowledge of these lower Miocene clinoforms (Miller *et al*., 1994), but the link of facies to stratal geometry still depended upon a correlation across a 30-km gap separating the closest well and the most landward seismic control. High-resolution MCS profiles collected in 1998 (ch0698, Fig. 30; Monteverde *et al*., 2000) partially filled this gap and defined candidate sequence boundaries (Fig. 35) on the basis of onlap, downlap, toplap and erosional truncation (Mitchum *et al*., 1977a,b; Vail, 1987; Posamentier & Vail, 1988). Small incised valleys (10–15 m deep; up to 6 km wide) were detected on each sequence boundary landward of the clinoform rollover points. These unconformably bounded packages were recognized on dip lines where clinoform geometries were best defined. Eleven proposed bounding surfaces have since been identified, outlining 10 different sequences (Fig. 36; Monteverde *et al*., 2000).

There is considerable along-strike variability to these surfaces. Sequences generally thin away from the dip profiles on which they are most easily recognized (Fig. 36), as boundary reflectors are frequently truncated by and/or concatenated

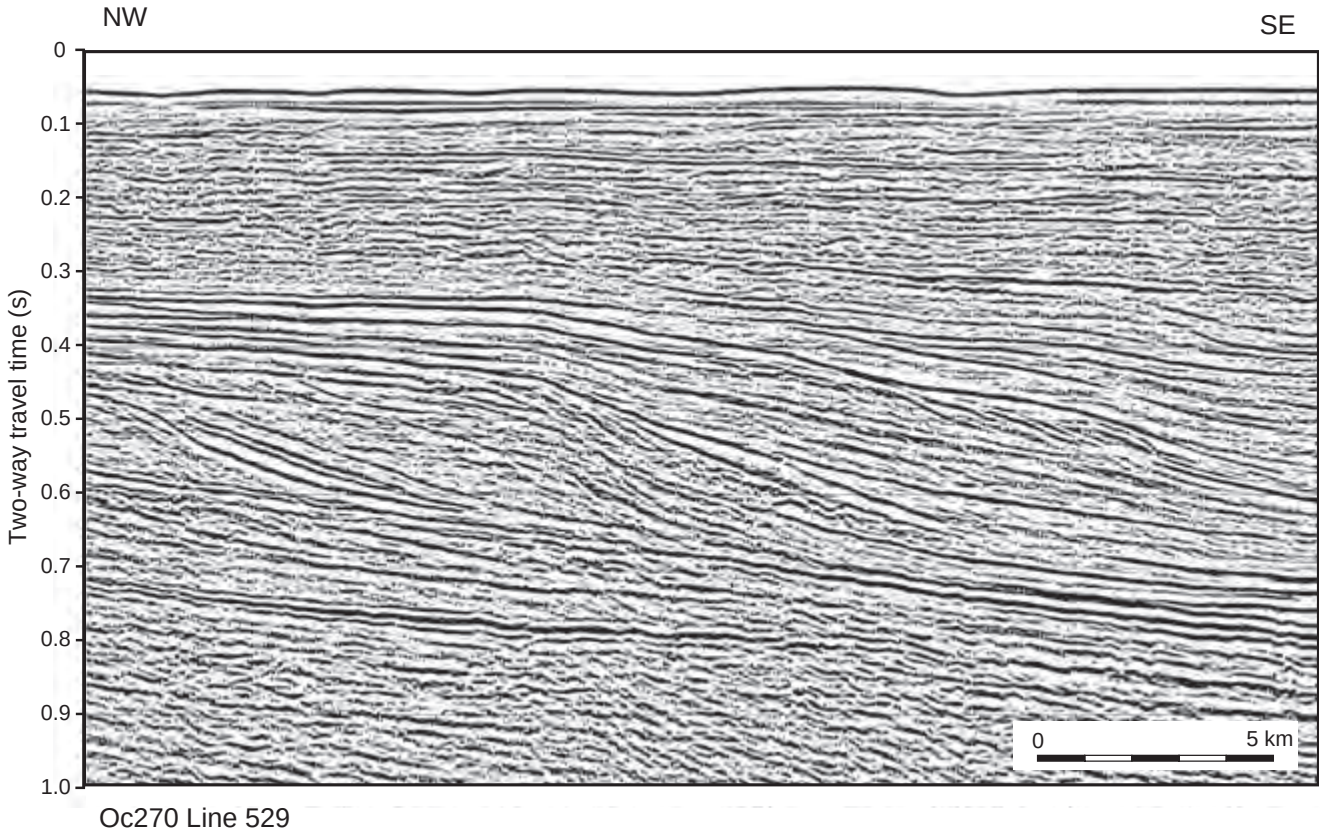

Fig. 35 Multichannel seismic profile (Oc270 line 529) along a dip line showing well-defined early and middle Miocene clinoform geometries beneath the New Jersey middle shelf. Location shown in Fig. 30.

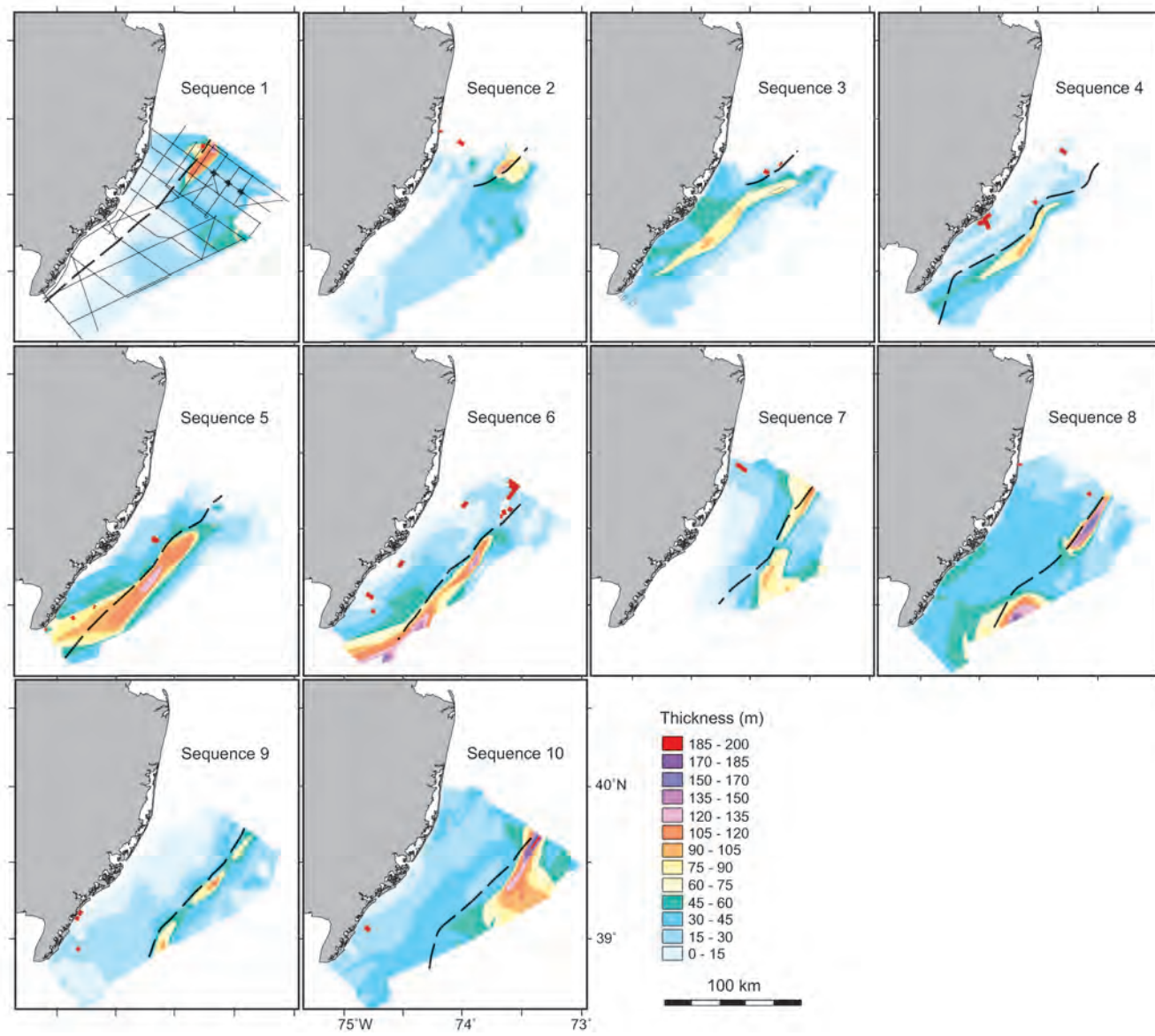

Fig. 36 Isopach maps of ten lower Miocene sequences identified in Ch0698 profiles along the New Jersey inner shelf. Seismic grid shown in Fig. 30. Sequence 1 is the oldest; sequence 10 is the youngest. Note the shift in depocentres from north to south and back to north, while there is a seaward shift in thickness patterns. The dashed line marks the clinoform rollover point at the top of each sequence. The red areas mark probable incised shelf valleys. See text for details.

with over/underlying reflectors in both updip and downdip directions. No single dip line displays all 11 sequence clinoform rollover points.

The arrangement of reflectors within sequences from the northern half of the seismic grid contrasts with those from the southern half. Northern sequences generally are thicker (Fig. 36) and contain more clearly defined internal geometries. Well-imaged lowstand deposits at the seaward toes of clinoforms are found within most northern sequences. A single shelf-edge delta of limited areal extent rests on a sequence boundary, suggesting development under lowstand conditions. Highstand deposits defined by downlapping reflector truncations prograde seaward, and are thicker and more extensive than transgressive sediments. Onlap

is rare away from the preceding rollover due to the very low seaward dip of palaeoshelf sediments landward of each clinoform rollover. Erosional truncation and incised valleys occur on each sequence boundary, and can closely approach the location of the previous clinoform rollover. Erosion and incision predominate along the north-west edge of the seismic grid. Sequences have prograded much less in the northern half of the grid.

By contrast, southern sequences have advanced farther seaward. Sequences are generally thinner and internal geometries are less well defined than those to the north. Lowstand fans and wedges (Posamentier & Vail, 1988) are not detected in the south. Instead, reflectors paralleling the downdip section of the previous sequence boundaries generally onlap steep sigmoidal clinoform foresets. Similar geometries have been attributed to an early transgressive phase by Posamentier & Allen (1993, 1999). These geometries develop under conditions of high wave energy/low tidal energy that bevel clinoform tops during relative sea-level rise, transporting the eroded sediment seaward of the clinoform rollover. This reflector geometry continues along strike into the northern grid, where it grades into more 'typical' sequence successions of lowstand, transgressive and highstand truncations. As in the northern half of the grid, highstand deposits in the south are much thicker than transgressive sediments. Updip sections are generally thin in both northern and southern regions. Incised valleys are less common in the south than in the north, and enter the seismic grid from the west-southwest.

Along-margin variations in both accommodation space and fluvial sediment supply contributed to these north–south contrasts in sequence development. Greater accommodation space in the north, apparently the result of increased subsidence, led to thicker sequences that did not prograde as far seaward as those in the south. Variable sediment supply is apparent as well. As discussed above, incised valleys are evident along the tops of individual clinoforms, suggesting rivers became entrenched during regressions, and very likely deposited their sediments into a relatively small number of deltaic lobes or wedges. Isopach maps support this speculation. Individual depocentres are relatively margin-parallel bodies with slightly arcuate seaward edges that change geographical location through time (Fig. 36).

Isopachs and the changing location of clinoform rollover points mapped across the grid for each of the 10 early Miocene sequences provide a measure of progradation, and yield insight into margin history. Sediment accumulation began in the north (Sequence 1), supplied by rivers entering the seismic grid from the north-west. Very thin distal accumulation occurred in the south during this time. The next sequence (2) again concentrated accumulation in the northern region. Beginning with Sequence 3, an additional southern sediment source became clear, and by Sequence 4 the thickest accumulation occurred in the central to southern region. The following four cycles (Sequences 5–8) reveal two distinct depocentres that moved progressively seaward with time. Deposition from the southern source either waned or moved seaward of the seismic grid by Sequence 9, and the final lower Miocene sequence (10) formed a linear, margin-parallel centre in the northern region. Onshore borehole data indicate that deltaic sedimentation dominated this interval of shelf progradation (Miller *et al.*, 1997b).

Clinoforms and incised valleys

Clinoforms are observed in ancient continental-margin sediments at a wide range of scales and ages (Vail *et al.*, 1977; Posamentier *et al.*, 1988; Bartek, 1991), but despite this ubiquity the water depths at which they form are unknown and widely debated. One viewpoint claims the gently dipping topsets of clinoforms in any setting are typically exposed during relative falls of sea level ('Type I' events, Van Waggoner *et al.*, 1988), causing the shoreline to move seaward of the rollover point. At these times, base level falls below the top of the clinoform and rivers cut into exposed strata. The contrary view claims the shoreline never passes seaward of the rollover, and the clinoform top is rarely, if ever, exposed to fluvial processes (Cathro *et al.*, 2003).

Incisions into the topsets of six mid-to-late Miocene clinoforms have been reported in profiles along the New Jersey outer shelf (Fig. 37; Fulthorpe *et al.*, 1999). These features are generally 5–12 m deep (at the limit of vertical resolution of these data), with some as deep as 20 m. Widths vary from 50 m (roughly the limit of horizontal detection) to a typical value of 100–400 m. Roughly parallel

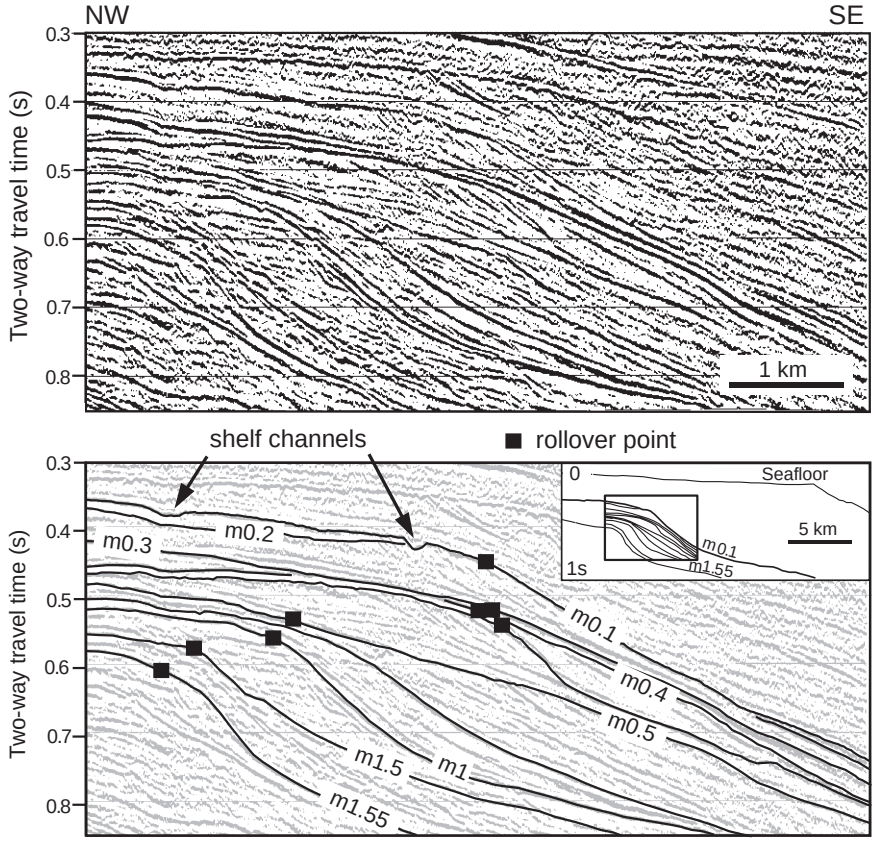

Fig. 37 Uninterpreted and interpreted seismic profile (Oc270 line 35) roughly 10 km from the modern shelf break, showing prograding mid-to-late Miocene clinoforms. See inset and Fig. 30 for location. Black squares mark the rollover points for each highlighted clinoform. Two channels landward of the existing shelf break are incised 8–13 m into the m0.1 palaeoshelf, with apparent widths of 200 m and 430 m. (From Fulthorpe *et al.*, 1999.)

channels appear to be clustered into drainage systems 10–15 km across. Incisions extend seaward of the clinoform rollover on four of 12 mid-to-late Miocene unconformities (Fulthorpe *et al.*, 2000). All are small compared with those of the modern margin (Fig. 38), and consequently most mid-to-late Miocene clinoform foresets are smooth, suggesting that sediment transported downslope was predominantly by non-channelized processes.

The size, grouping, apparent meandering and lack of discernible internal structure suggest that the incisions into clinoform topsets have been formed by rivers that flowed seaward across a gently dipping coastal plain during times of sea-level lowstand (Fulthorpe *et al.*, 1999). All are much smaller and simpler than the composite river systems that appear to have formed the Hudson Shelf Valley or other large depressions crossing modern continental shelves (e.g. Twichell *et al.*, 1977; Knebel *et al.*, 1979). Their interpretation as drainage systems is strongly supported by the recovery of lagoonal facies at ODP Site 1071 (Austin *et al.*, 1998), 3 km

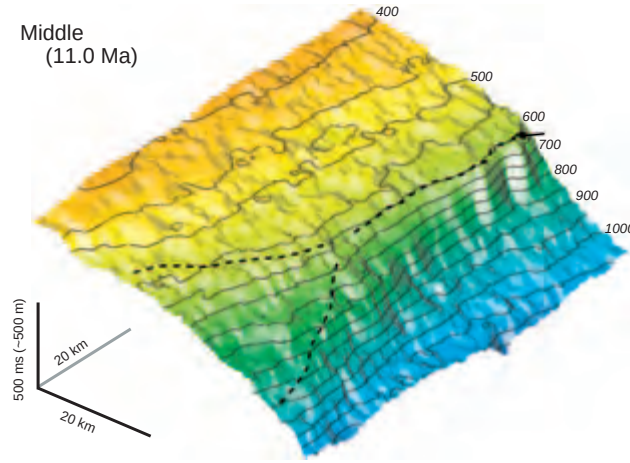

Fig. 38 Isometric view of late Miocene sequence boundary m0.2 beneath the New Jersey outer shelf. Dashed line identifies the break in gradient commonly referred to as the clinoform rollover point; note there are two such abrupt changes in gradient to the south. Evidence for minor incisions into the clinoform foreset is discussed in the text. (From Fulthorpe & Austin, 1998.)

landward of the m0.5 rollover (Fig. 37), and suggests that shorelines may occasionally reach nearly as far seaward as clinoform rollovers. However, the shallow depths of all Miocene incisions and the lack of continuity onto the dipping clinoform foresets strongly suggest that base level never falls more than a few metres below the elevation of the rollover. Early-to-middle Miocene sea-level variations have been estimated from backstripping onshore wells, and fall in the range of 20–30 m (Kominz *et al*., 1998; Miller *et al*., 1998a). If magnitudes of sea-level change were roughly the same in the late Miocene, the rollovers under discussion most probably developed in water depths of a few tens of metres at most.

Pleistocene sequences

The Quaternary record on the New Jersey margin is characterized by:

1 a low-relief hinterland that has provided only a modest amount of sediment;
2 sediment reworking across a wide, shallow-gradient shelf;
3 thermal and flexural subsidence that has had little impact on accommodation space (except for the loading effects of intermittent ice sheets).

As a result, the Quaternary section is thin (a few tens of metres) and stacked in complex patterns across the inner two-thirds of the shelf (Knebel & Spiker, 1977; Knebel *et al*., 1979; Swift *et al*., 1980; Ashley *et al*., 1991; Carey *et al*., 1998; Sheridan *et al*., 2000; Uchupi *et al*., 2001; Schwab *et al*., 2002). By contrast, large volumes of sediment reached the outer shelf and slope during the mid- to late-Pleistocene (post-750 ka), extending the continental margin several tens of kilometres past the pre-Quaternary shelf edge.

The Hudson Apron is a region of the continental slope largely free of canyons and composed of Hudson Canyon spillover sediment carried southwest by prevailing currents. High-resolution seismic profiles show that it contains four Quaternary sequences: Yellow, Green, Blue and Purple (Figs 30 & 39). The bounding surfaces between each, beginning with the base of Yellow, are p4, p3, p2 and p1, respectively (Fig. 39). These unconformities on the shelf exhibit erosional truncation or toplap. Traced to the slope, these bounding surfaces become more nearly, and in some cases, totally conformable. There is no evidence of marine onlap against these slope unconformities, in contrast to a commonly held model of deposition that buries a sequence boundary after an interval of bypass or erosion (e.g. Vail *et al*., 1977).

The base of each Quaternary sequence (i.e. surfaces p4, p3, p2 and p1; Fig. 39) exhibits a seaward increase in gradient from gentle (~1:60) to more steeply dipping (~1:20), and the inflection point is referred to as the palaeoshelf break. This buried

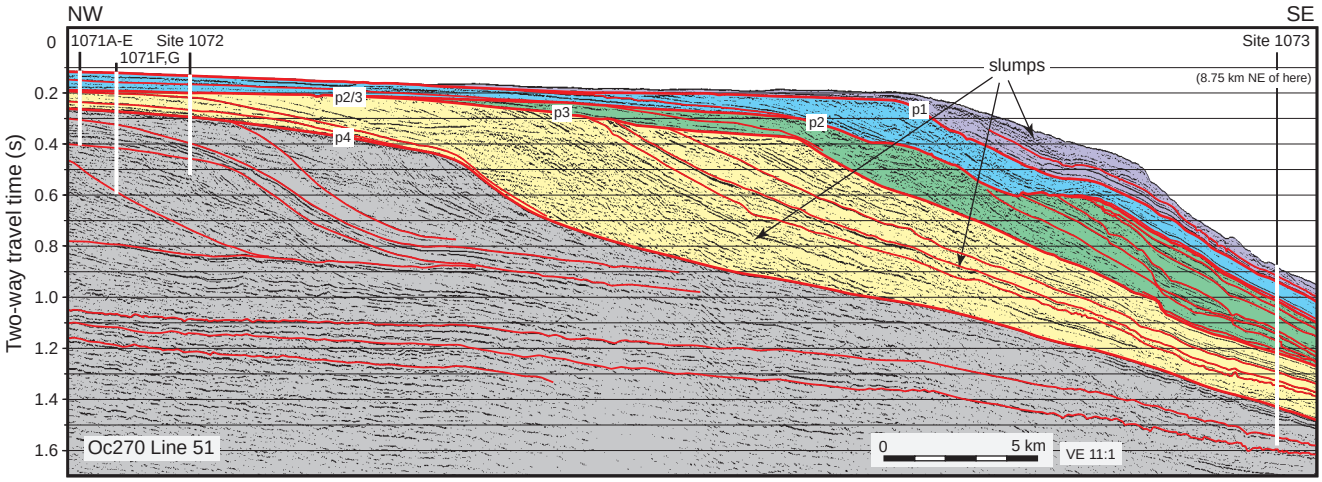

Fig. 39 Seismic profile (from Oc270 line 51) through ODP Sites 1071, 1072 and extending to the continental slope 8.75 km south-west of Site 1073. Pleistocene sequences named Yellow, Green, Blue and Purple are bracketed by sequence boundaries p4, p3, p2 and p1, respectively. See Fig. 30 for location.

physiographical feature at p4 time is 15–18 km landward of the modern shelf break, and each sequence above Yellow steps progressively seaward of the one beneath it. Reflectors within each sequence downlap onto the underlying palaeoshelf and, except for those in sequence Yellow, are conformable with the underlying palaeoslope. The youngest reflectors in each sequence terminate with angular discordance at the overlying palaeoshelf; it is not clear in most cases if this is evidence of sediment bypass and shelf toplap, or actual erosional truncation. By contrast, reflectors at the top of each Quaternary sequence on the palaeoslope are predominantly conformable with the overlying sequence boundary. Many intrasequence reflectors can be traced with ease from the palaeoshelf to the palaeoslope; exceptions occur in apparent slump deposits that are 10–50 m thick, extending continuously from the top of each palaeoslope to the limit of the survey grid at the middle of the modern slope (~1400 m water depth).

Outer-shelf and slope sequences

Three sites were drilled during ODP Leg 174A on the New Jersey margin (Figs 30 & 39); two were on the outer shelf in 88-m and 98-m water depths (Sites 1071 and 1072, respectively), and the other (Site 1073) was on the upper slope at 639 m (Austin *et al*., 1998). Key objectives were to establish reliable correlations between prominent seismic reflectors and the cored sequence, and evaluate the influence of sea-level change on the observed stratigraphic succession. Unconsolidated sand-rich units, however, were particularly difficult to recover and caused severe drilling-related and hole-stability problems. To tie the complete sequence to seismic reflections, the velocity and density logs as well as a check-shot survey proved to be essential. Figure 40 shows a time–depth comparison using both the sonic-log and check-shot data recorded in Hole 1073A. The difference between the sonic and check-shot profiles is related to frequency differences between the measurements and the presence, or absence, of stratigraphic reflectors in the immediate vicinity of the drill hole.

Where incomplete core recovery during ODP Leg 174A resulted in uncertain relationships between the sedimentary record and reflectors, geophysical data have been used to fill the gaps in the record (Fig. 41; Delius *et al*., 2001). The reflectivity coefficient series R have also been calculated from the sonic and density logs at Site 1072, enabling a more confident match between acoustic reflectors and known lithological boundaries (Fig. 41). Key reflectors were found to correspond to erosional surfaces and/or to unrecovered sand-rich units that commonly occurred at sequence boundaries. This example demonstrates that correlation between core, log and seismic data can be essential, and at these locations, in particular, resulted in an improved seismic interpretation of the drilled sequences.

1 *Yellow sequence (p4–p3)*. Four notable aspects of margin-building sedimentation occurred during sequence Yellow (Fig. 42D). First, early Pleistocene sediments comprising the base of this sequence prograded several tens of kilometres seaward with no detectable aggradation. Second, at the scale that can be resolved with existing seismic data (~5 m vertical), strata across the palaeoshelf break and on the upper palaeoslope were deposited conformably; there is no evidence of slope bypass and subsequent onlap against p4 or any reflectors within the Yellow sequence (Fig. 39). Third, the palaeoshelf break occurs parallel to and 15–18 km landward of the modern shelf break, at roughly the 110-m isobath. No slope canyons of Yellow age cut into this palaeoshelf break, although several canyons developed exclusively on the slope in the south-west area of study. Fourth, distorted and discontinuous reflectors interpreted as displaced slump sediments comprise ~20% of the Yellow sequence on the Hudson Apron, and can be traced as discrete units from the top of the palaeoslope seaward to the limit of the survey grid. Slumps appear to become more common up-section. However, slope failure occurred in the south-western part of the survey grid sometime after 750 ka; this region has remained a locus of gravity-induced failure since that time, and may have been the nucleus for Hendrickson and other nearby canyons.

2 *Green sequence (p3–p2)*. The Green sequence is identified by the same criteria as the other Quaternary units, yet it was partially eroded during emplacement of the overlying p2 sequence boundary, and now exists only beneath the outermost shelf and slope (Fig. 39). Reflectors at the top of the Yellow sequence dip gently seaward, suggesting sediment bypass along the p3 surface; there is no compelling reason to conclude that widespread erosion coincides with the p3

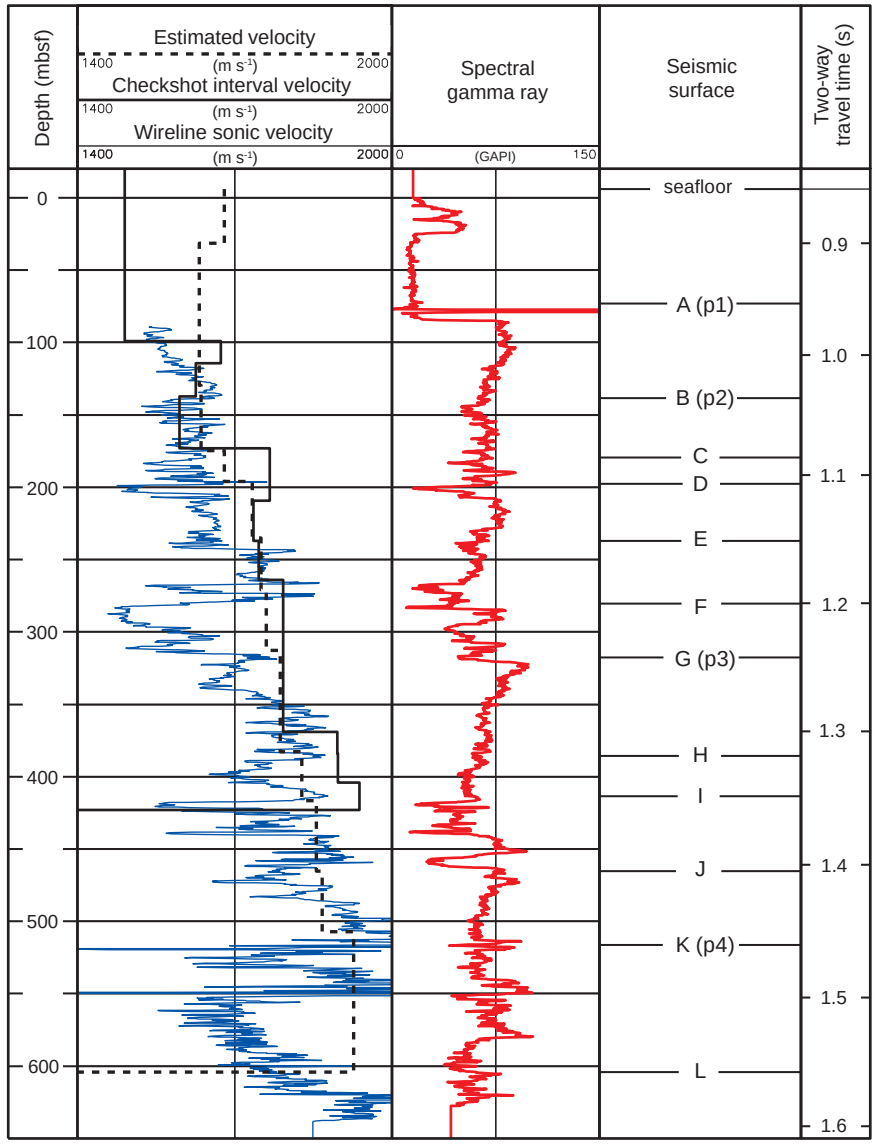

Fig. 40 Velocity-depth plot in ODP Hole 1073A showing wireline sonic velocity (blue) and interval velocities (bold, solid line to 425 m below seafloor, mbsf) calculated from the check-shot survey. Velocity estimates based on previous drilling (dashed line) and the spectral gamma-ray log (red) are also shown. Various seismic reflectors A through L identified on seismic lines are positioned at corresponding depths and the associated two-way travel-time. (From Austin *et al.*, 1998.)

sequence boundary. Strata within the Green sequence accumulated on the p3 surface during steady progradation/downlap across the gently dipping (1:130; 0.4°) palaeoshelf. Thicknesses of palaeoshelf strata (Fig. 42C) now vary from 60–70 m in the northern part of the study area to 10–20 m in the southern part. Basal reflectors on the uppermost palaeoslope, by contrast, are chaotic, suggesting slumping and debris-flow processes (and a gradient of 1:25; 2.3°). Indeed, most of the reflectors within the Green sequence immediately seaward of the palaeoshelf break have a similar chaotic character that gives way downslope to acoustically laminated, well-preserved stratification. The thickest accumulation (~230 m) is found on the palaeoslope. The palaeoshelf break at p3 time was incised by a slope canyon inherited from the underlying Yellow sequence in the south-western corner of the study area.

3 *Blue sequence (p2–p1)*. Erosion at sequence boundary p2 totally removed the Green sequence landward of the modern 125-m isobath; consequently, in this region the Blue sequence rests directly on Yellow (Fig. 39). Elsewhere, the reflectors at the top of Green provide additional evidence of erosion. In contrast to the other three Quaternary sequences, Blue did not build seaward over an abrupt palaeoshelf break; instead, the p2 surface changes very gradually from a shelf gradient of ~1:150 to a slope value

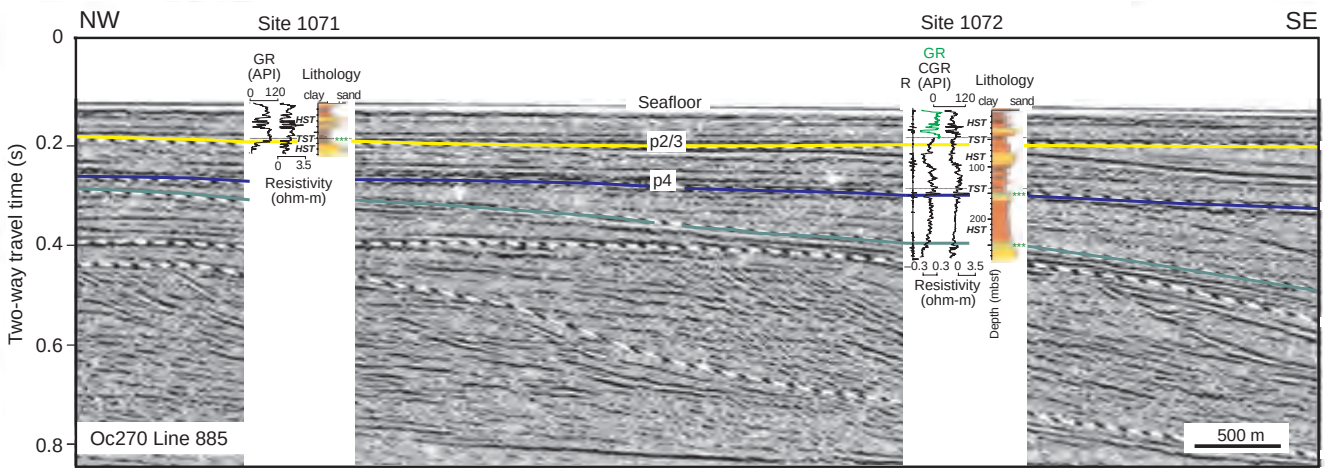

Fig. 41 Composite section showing resistivity and natural gamma-ray logs, synthetic log-lithofacies profiles, and Oc270 seismic line 885 at Sites 1071 and 1072. The reflectivity coefficient series, R, calculated from sonic and density logs allows seismic reflectors to be correlated between sites, revealing erosional surfaces and sand-rich units that were not recovered by coring. (After Austin *et al.*, 1998.)

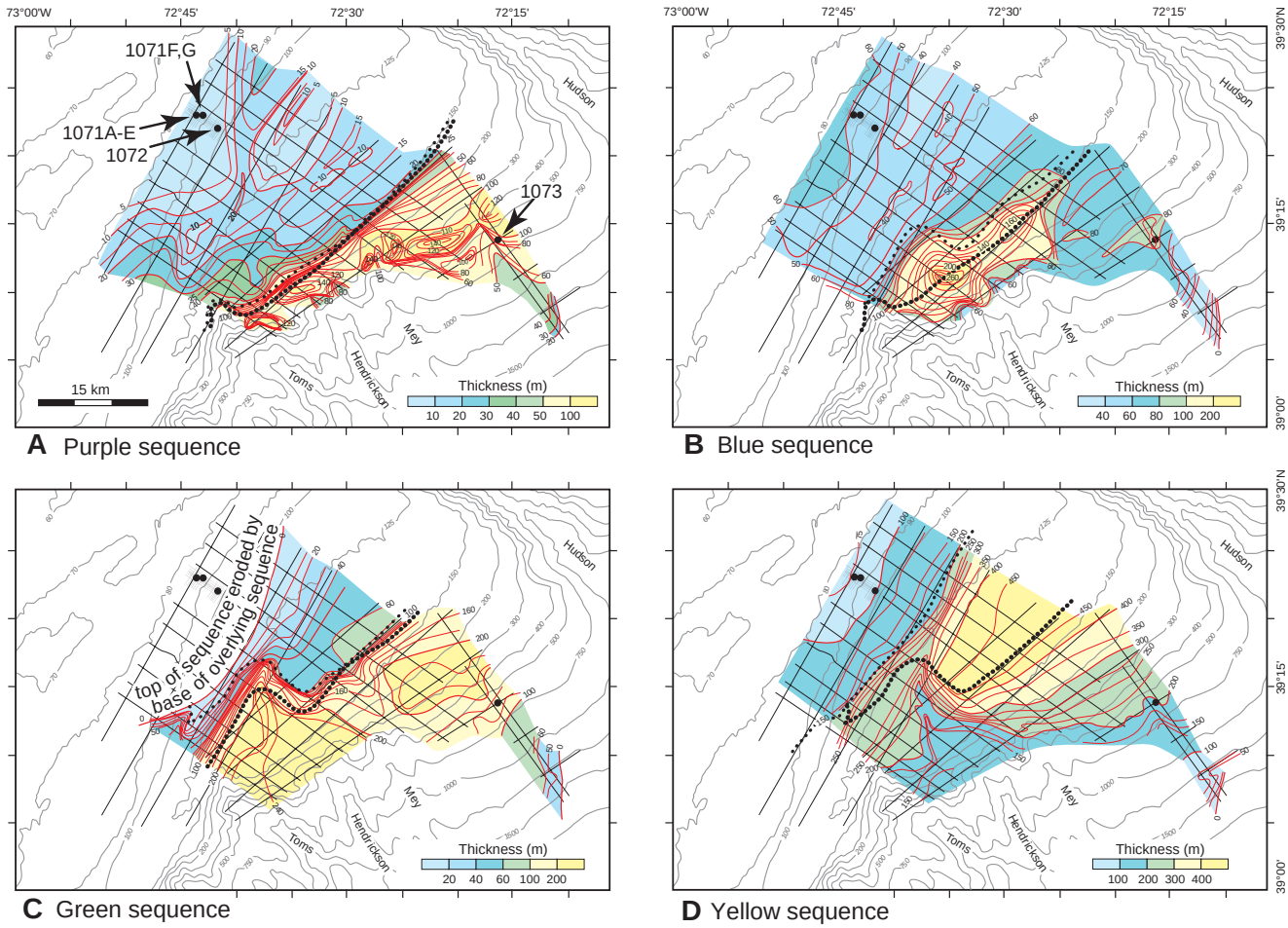

Fig. 42 Thickness of Pleistocene sequences Purple, Blue, Green and Yellow on the outer shelf and upper slope of New Jersey. The light dotted line marks the palaeoshelf break at the base of each sequence; the bold dotted line marks the palaeoshelf break at the top of each sequence. Modern bathymetry (curved grey lines and numerals) is in metres; major slope canyons are labelled; Oc270 profiles used to develop each map are displayed as thin black lines. (After Mountain *et al.*, 2001.)

of 1:20 (0.4° to 2.9°). As with underlying sequences, the only evidence of slope canyons cutting into this shelf break are in the south-west corner of the study area, most probably part of the Toms Canyon system that dominates the modern topography. Roughly 80–100 m of strata (Fig. 42B) prograded across the palaeoshelf in the northern half of the study area; build-up was ~60 m in the southern half. The thickest accumulation (~260 m) is now found immediately seaward of the palaeoshelf break. As in the other Quaternary sequences, chaotic reflections suggest that Blue strata at the top of the palaeoslope were dominated by mass wasting processes, while farther downslope the correlative units are acoustically stratified and draping.

4 *Purple sequence (p1–seafloor)*. Strong angular discordance between basal boundary p1 and underlying strata indicate erosion on the outermost palaeoshelf between sequences Blue and Purple (Fig. 39). The p1 surface dividing these units seaward of the 90-m isobath coincides exactly with reflector 'R', first mapped by Milliman *et al*. (1990) and interpreted as the contact between sediments of the Last Glacial Maximum and the subsequent transgression. Davies *et al*. (1992) and Duncan *et al*. (2000) have traced this surface landward and correlated it with the mid-shelf reflector R described by Knebel & Spiker (1979). The palaeoshelf and palaeoslope gradients of p1 are similar to those of older units, and a clear palaeoshelf break is located no more than 2 km landward of the modern shelf break. As in each of the older sequences, chaotic reflectors are gradually replaced by acoustically stratified, draping units in the seaward, downslope direction. Purple is the thinnest of the four Quaternary sequences (Fig. 42A); shelf accumulations are roughly 20 m in the northern part of the study area, and 35–40 m in the southern part. This is opposite to the trend in the other three Pleistocene sequences, and may reflect infilling around the head of Toms Canyon more than any other asymmetry in sediment supply. The thickest Purple accumulation is immediately seaward of the palaeoshelf break, but inexplicably the isopachs do not follow a trend that parallels the palaeoshelf break.

The link to eustasy

Sea level exerts a major influence on the stratal geometry of clinoforms, although the success of linking times and magnitudes of sea-level change to facies distribution continues to be debated (Christie-Blick, 1991; Miall, 1991; Reynolds *et al*., 1991; Karner & Driscoll, 1997). One supporting argument holds that if sea level falls faster than the subsidence rate beneath a clinoform rollover, the entire clinoform top will become exposed to subaerial erosion, and a prominent unconformity, or 'Type I' sequence boundary, will develop as a result (Posamentier & Vail, 1988). This event constitutes a lowering of base level, meaning the elevation that divides erosion (above) from deposition (below) falls below the top of the clinoform. Hence, marine deposition will be restricted to locations seaward of the rollover. When sea level rises, this model predicts that depocentres will move progressively landward to a location where the rates of sea-level rise, basement subsidence, sediment compaction and sediment accumulation have reached a balance. This will coincide with a time of minimal sedimentation seaward of the clinoform rollover and result in a condensed section at that location (Loutit *et al*., 1988). Critics of this model note the lack of solid geological confirmation for the link between truly global sea-level change and the facies distribution predicted within a clinoform structure. For many, the uncertainty of the magnitude and timing for past sea-level changes has made it nearly impossible to identify the exact control these changes have had on the stratigraphic record.

At ODP Site 1073 on the New Jersey upper slope, > 500 m of late Pleistocene sediment were continuously cored with 98% recovery (Austin *et al*., 1998). Global sea-level variations are well defined for this time in the geological record, and the stratigraphy can be compared against an independently established eustatic history to determine controls on stratal geometry. However, Site 1073 is at 639-m water depth on the continental slope, and this is not the setting in which the standard model of clinoform evolution was developed. The majority of sequence-stratigraphic studies have been based on clinoforms found on continental shelves or epieric seas. In these locations, even the sediments that bypass clinoform rollovers during times of rapidly falling sea-level are largely retained on the shelf, where water depths are < 150 m and seafloor gradients are 1:100. The New Jersey Pleistocene clinoforms, by contrast, developed at the edge of the existing continental shelf; the rollovers for these features were also the shelf–slope transition, and the clinoform foresets were > 150 m in height.

With a gradient of roughly 1:40, these foresets continued down to more than 2000-m water depths, before levelling to a grade of less than 1:100 on the continental rise. The interplay between sea-level change, sediment bypass and sediment build-up might follow different histories, depending on whether the clinoform is perched on a shelf or at the edge of one.

Subsidence at Site 1073 was affected by the adjacent Laurentide ice sheet during the late Pleistocene. The ice front extended across northern New Jersey, Staten and Long Island as recently as ~20 ka, roughly 150 km north-west of Site 1073 (Teller, 1987; Stanford *et al*., 2001). Modern tide gauges backed by models of crustal response to presumed ice load show that New York harbour is currently sinking at roughly 2 mm yr^{-1} due to relaxation of the peripheral bulge that surrounded the former ice sheet (Tushingham & Peltier, 1991; Gornitz *et al*., 2001). This serves as a warning to researchers that the impact of sea-level change on sequence architecture in this region requires an especially careful assessment of subsidence.

An oxygen isotopic record was constructed from 500 m of Pleistocene sediment recovered at Site 1073 (Fig. 43). The $\delta^{18}O$ record was correlated to the SPECMAP composite curve (Imbrie *et al*., 1984) to provide a detailed age model extending back to 770 ka (McHugh & Olson, 2002). This correlation was accomplished by visual curve matching constrained in three independent ways. First, datums based on radiocarbon dates, biostratigraphy and magnetostratigraphy anchored several depths to specific ages. Second, planktonic forams were identified as glacial and interglacial assemblages, providing additional confidence in matching peaks and troughs of the measured and composite $\delta^{18}O$ records. Third, surfaces comprising four Pleistocene sequence boundaries were traced to Site 1073, and their depths were correlated to cores with a reliability of roughly ±10 m (Austin *et al*., 1998; Mountain *et al*., 2001). The authors assumed that the sedimentation changes expressed at sequence boundaries on the shelf would have a discernable impact on the facies successions at Site 1073, and, in the absence of other information, this helped to choose the depths matching breaks in the $\delta^{18}O$ to SPECMAP correlation.

Sixteen Pleistocene glacial and interglacial fluctuations of global ice volume were identified at Site 1073 on the basis of measured $\delta^{18}O$ variations (Figs 43 & 44): Oxygen Isotope Stages 1 (partial), 2–4, 5 (partial) and 8–18. Stage 6 was a time of major erosion across the shelf and slope (Sheridan *et al*., 2000), and the resulting unconformity on the upper slope is manifest in profiles by an erosional surface at 79.5 m and in the core samples by the absence of Stages 6 and 7. This hiatus was the only clearly identifiable break in the $\delta^{18}O$ record of Site 1073, despite the compelling evidence of sharp changes in sedimentation, and possible erosion at each of the four correlatives to sequence boundaries p1–p4 traced from the shelf (see Austin *et al*., 1998). By contrast, the correlations of p2 (145 m) and p3 (325 m; dividing sequences Blue from Green, and Green from Yellow, respectively; see Fig. 39) coincide with the Oxygen Isotope Stage (OIS) 8–9 and 11–12 transitions, respectively. While time may be missing across these two surfaces, this cannot be verified at the resolution of the available $\delta^{18}O$ proxy. The base of the Pleistocene section at Site 1073 (524 mbsf; ~770 ka) rests unconformably on probable Pliocene/Miocene sediments, and corresponds to boundary p4 and the base of sequence Yellow.

These correlations show that sediments deposited in glacial OIS 8 comprise the entire 65-m Blue sequence, supporting the argument that bypass concentrates sediment accumulation seaward of the clinoform rollover during eustatic lowstands. In contrast, the 80 m of sequence Green correspond to OIS 9–11, and the 200 m of sequence Yellow extend without apparent interruption from OIS 12–18. Clearly, there is no consistent, one-to-one correspondence between glacio-eustatic oscillations and the formation of sequence boundaries as they have been identified. Furthermore, sequence boundaries do not even appear to coincide with a consistent stage of glacio-eustasy: p3 matches the transition from glacial to interglacial (OIS 12–11), while p2 does just the opposite (OIS 9–8). Much of the explanation for these observations is probably linked to the location of Site 1073 on the upper continental slope.

There are numerous facies variations (with no detectable hiatuses) confined entirely to individual sequences at Site 1073. These variations suggest oscillations of proximal/distal sediment sources, and may track eustatic changes (McHugh & Olson, 2002). However, the more fundamental structure

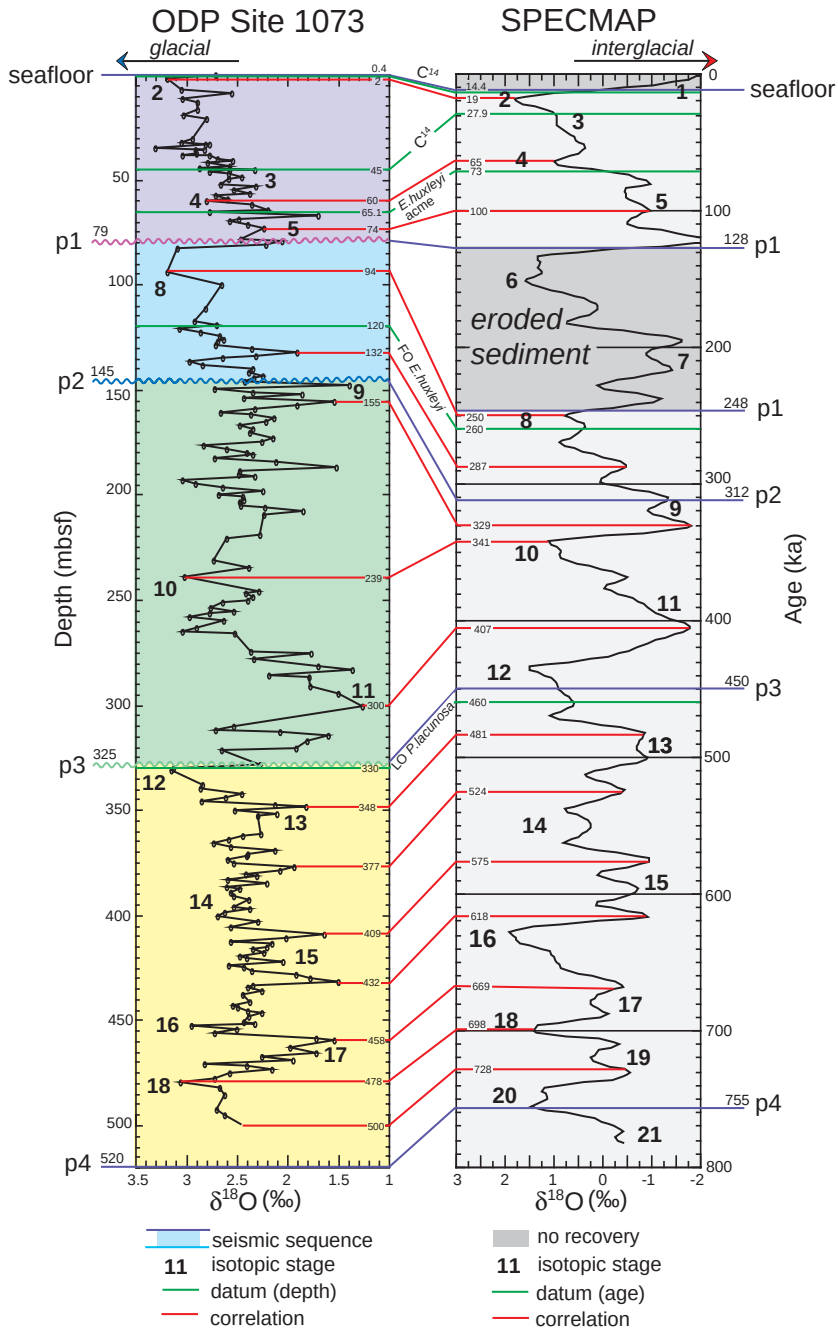

Fig. 43 Measured values of $\delta^{18}O$ at ODP Site 1073 plotted against depth (mbsf, metres below seafloor), compared with the global composite SPECMAP $\delta^{18}O$ curve plotted against age (Imbrie *et al.*, 1984). Green lines mark correlations based on biostratigraphic index fossils; red correlations connect visually matched features of the $\delta^{18}O$ data. Marine Oxygen Isotopic Stages 1 through to 18 are shown, with the exception of Stages 7, 6 and part of 5, which are assumed to have been removed by erosion. The Yellow, Green, Blue and Purple intervals (Fig. 39) at left mark the intervals at Site 1073 bracketed by sequence boundaries p4, p3, p2, p1 and the seafloor, respectively. (After McHugh & Olsson, 2002.)

of stratal architecture is unambiguously defined by the four sequences Yellow, Green, Blue and Purple (Fig. 39). Furthermore, sediment accumulation rates within the three youngest sequences follow an identical pattern, increasing upwards by as much as an order of magnitude (Fig. 44). It remains to be determined just what process is responsible for this pattern, but it does not appear to be global sea level. The loading/unloading of the craton during advance and retreat of the Laurentide ice sheet, and its consequences on the drainage of rivers and glacial lakes along the adjacent margin, is surely a factor. The timing and magnitude of these effects are not yet known with sufficient precision to evaluate rigorously the impact on Pleistocene sedimentation along the New Jersey shelf and slope.

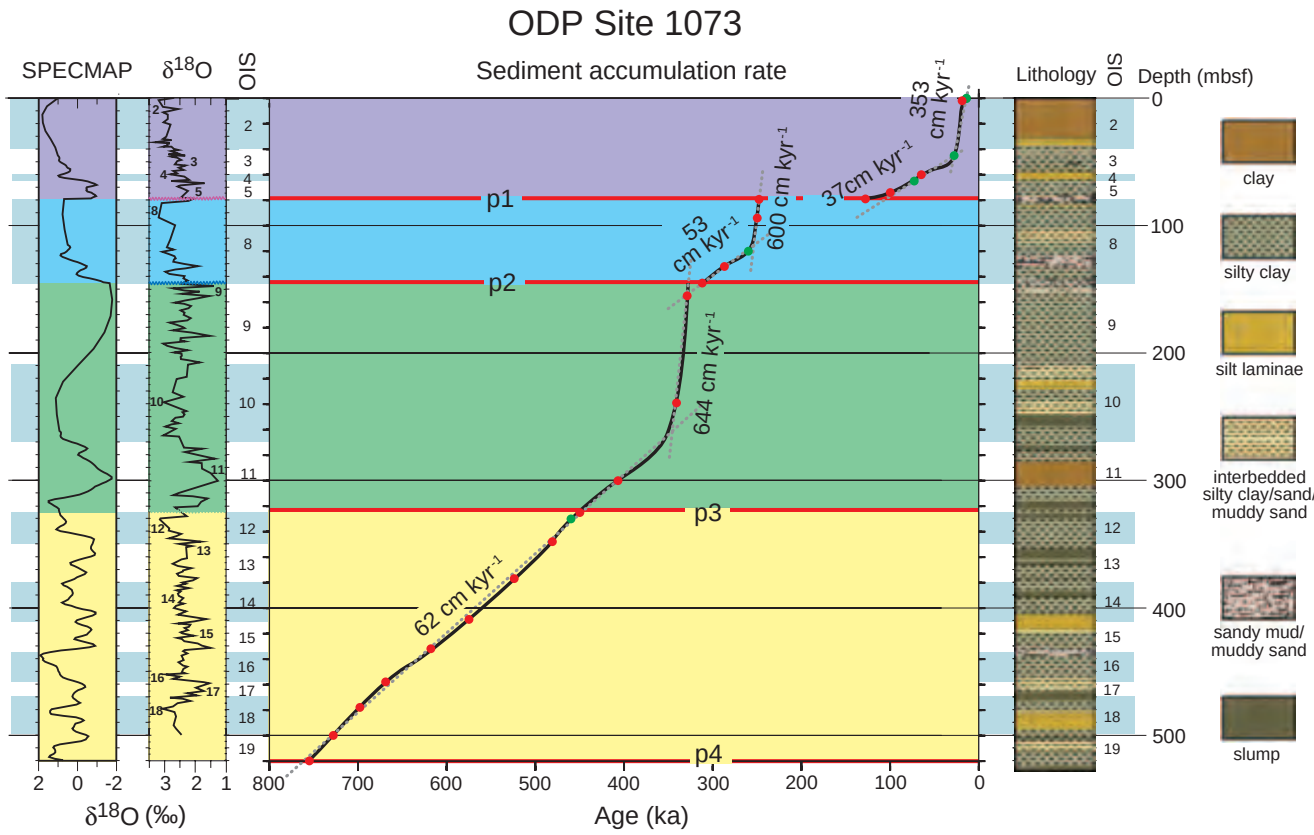

Fig. 44 Age versus depth of Pleistocene sediments at ODP Site 1073 and derived sediment accumulation rates. Ages were obtained by correlation of measured $\delta^{18}O$ values to those of the SPECMAP curve. The SPECMAP curve is plotted versus depth, assuming the age model derived from the correlation shown in Fig. 43. Marine Oxygen Isotope Stages (OIS) 1–19 are labelled, with glacial times highlighted in light blue. Generalized lithofacies are shown at the right. The Yellow, Green, Blue and Purple intervals mark the depths at Site 1073 bracketed by sequence boundaries p4, p3, p2, p1 and the seafloor, respectively. (After Mountain *et al.*, 2001; McHugh & Olsson, 2002.)

The last eustatic cycle and its preserved record

The New Jersey margin is a compelling natural laboratory for understanding the formation and evolution of the seafloor, and for investigating the relationship of shallowly buried subsurface stratigraphy to changing base levels. A range of high-frequency seismic techniques (e.g. sidescan sonar, multibeam bathymetry and backscatter, seismic reflection) and shallow-sampling tools (e.g. grab sampling; push, piston and rotary coring) has been used innovatively to examine the most recent stratigraphic record on the New Jersey shelf and uppermost slope.

Characterizing the seafloor

Surveys of sidescan backscatter and multibeam bathymetry extended from water depths of ~20 m to the edge of the shelf (Fig. 45; Goff *et al.*, 1999). These data augmented soundings from the National Ocean Survey, and the resultant maps have been used over the past decade to interpret details of seafloor morphology (e.g. sand ridges and dunes, ribbon morphology, iceberg scours) and to relate them to the underlying preserved stratigraphy. The bathymetric data proved that the modern seafloor on this margin bears little resemblance to the geology of the underlying 15–20 m of sedimentary section. Goff *et al.* (1999) showed that swales (floored by sand ribbons) located between clusters of largely relict sand ridges on the middle shelf are erosional in nature, responding to modern south-westward bottom currents. Sinuous furrows on the outer shelf ~100–400 m wide, kilometres long and ~1–4 m deep were identified as iceberg scours preserved in semi-lithified clays of the southern Hudson Apron (Fig. 45). Duncan & Goff

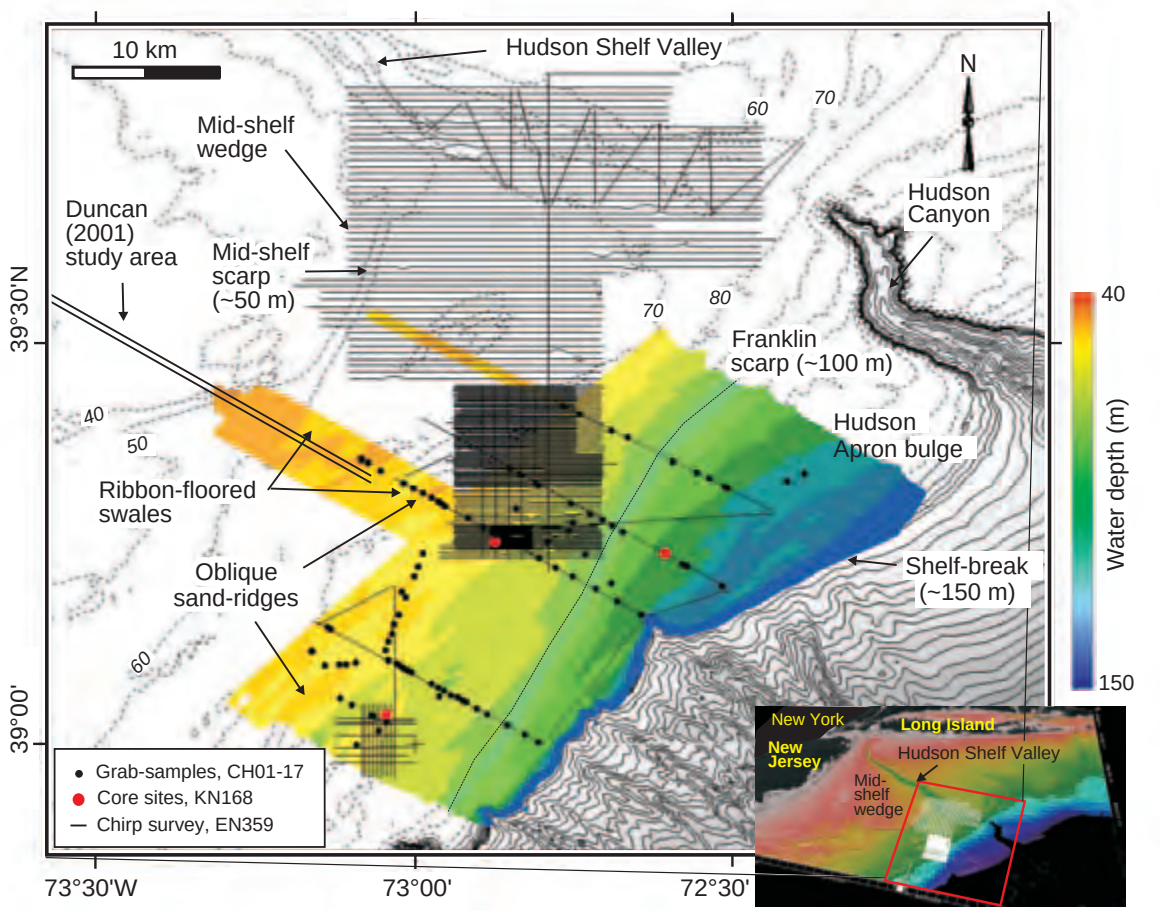

Fig. 45 Locations of deep-towed, Chirp seismic-reflection profiles collected aboard *R/V Endeavor* (cruise EN359), superimposed on multibeam (colour contoured; Goff *et al*., 1999) and NOAA bathymetry (dashed lines contoured in metres) of the New Jersey middle and outer continental shelf. Inset locates the study area within a three-dimensional rendering of the Mid-Atlantic Bight. Locations of grab samples (CH01–17) are identified.

(2001) mapped these keel marks and interpreted two discrete phases of iceberg rafting, which they related to Laurentide meltwater events at 17 ka and 25 ka.

Goff *et al*. (2000) attempted to correlate backscatter intensities with grain-size distribution, based upon ~300 grab samples. They identified a prominent linear correlation of backscatter intensity and grain size; coarser grain sizes generally equated to higher backscatter. There was a disproportionate effect on backscatter from the coarsest fraction, in particular shell hash, which proved abundant within older sediments in deeper water. Larger grain sizes also tended to occur on the seaward slopes of dunes oriented transverse to flow. Mid-shelf ridges were generally winnowed of fine-grained material, and muds within swales confirmed their erosional nature. Goff *et al*. (2004) built upon these earlier results, integrating the bathymetry and grab-sample data with geotechnical measurements. Grain-size distributions were found to be multimodal. In the absence of shell hash and gravel, backscatter correlated with seismic velocity and the percentage of fine sediments. Mean sand-size and the percentage of fine sediments were the primary controls on compressional-wave velocity of seafloor sediments.

Goff *et al*. (2005) have explored evidence for recent seafloor erosion on the New Jersey shelf, using all available data from the outer shelf (Fig. 45). Timing of erosion is constrained by seafloor truncation of stratigraphic horizons that can be dated. Erosional depths are everywhere ~3 m to > 10 m, and ribbons characterized by alternating areas of high and low backscatter mark eroded shelf strata. High backscatter is associated with shell hash and

with concentrations of well-rounded gravels and cobbles, both considered erosional lag deposits. The reworking of the seafloor during transgression is characterized first by sand-ridge evolution to water depths of ~40 m, then by erosional modification caused by selective wave and bottom-current resuspension of sediments at greater water depths.

Tying stratigraphy to latest Pleistocene–Holocene eustatic base-level changes

The shallow subsurface of the New Jersey shelf represents the composite stratigraphic record of the last regression and transgression (Milliman *et al*., 1990; Davies *et al*., 1992; Lagoe *et al*., 1997; Buck *et al*., 1999; Duncan *et al*., 2000). The concept of a single lowstand erosion surface, formed during shelf exposure accompanying the Last Glacial Maximum, has been replaced by a new paradigm involving a complicated surficial stratigraphy evolving continuously throughout the latest eustatic cycle.

Davies *et al*. (1992) imaged a shallowly buried set of incisions beneath the outer shelf. These data illustrated conclusively that the outer shelf represents a complex stratigraphic section completely unrelated to the modern seafloor (Austin, 1996). Duncan *et al*. (2000) mapped three regional seismic stratigraphic horizons on the middle and outer shelf.

1 'R', forming the base of an outer-shelf wedge and earlier identified as the Last Glacial Maximum erosion surface (Milliman *et al*., 1990), was reinterpreted as the product of multiple erosional episodes during the previous regression. Piston coring had previously confirmed that sediments below 'R' are > 45 kyr old (Davies & Austin, 1997).
2 The 'Channels' horizon, initially interpreted as evidence for fluvial drainage by Davies *et al*. (1992), was recognized as a widespread surface representing dendritic patterns of fluvial erosion formed during shelf exposure at or near the Last Glacial Maximum. Analyses of a piston core within one of these incisions confirmed that its sedimentary fill records fluctuating marginal-marine and mid-shelf depositional environments during the Holocene transgression, which flooded these fluvial systems ~12.5 ka (Buck *et al*., 1999).
3 'T', previously unrecognized, was interpreted as a flooding surface or ravinement within the transgressive systems tract.

Mapping of multiple dendritic, drowned fluvial drainage systems has since been refined and amplified. Nordfjord *et al*. (2005), armed with these maps (Fig. 46), have used quantitative geomorphological analysis to estimate palaeohydrological parameters linking observed channel morphologies to the hydrodynamic setting in which the channels were incised. Large ratios of width to depth, along with low sinuosities and slopes, suggested modern braided streams – but no such braiding was apparent. These buried systems are likely to be immature, having never reached equilibrium prior to drowning by the Holocene transgression. Furthermore, palaeoflow estimates for these fluvial systems were too high for non-tidal creeks, given the low hydraulic gradients typical of such a coastal-plain setting. Therefore, flows that carved these drainages must have been initially high, consistent with the occurrence of meltwater pulses crossing a coastal plain after the Last Glacial Maximum (Nordfjord *et al*., 2005).

To the south-west, Fulthorpe & Austin (2004) identified and mapped a prominent seismic facies boundary 0–20 m below the seafloor (Fig. 47). This boundary, separating seismically transparent sediments from an underlying stratified facies, defined two populations of apparent incisions trending north-east and east-northeast. Stratified blocks within the transparent facies, lying occasionally within incisions with steep flanks, indicated that the transparent facies was formed by catastrophic disruption of the underlying stratified material (Fig. 48). These incisions may have formed from meltwater discharges associated with the multiple breaching of glacial-lake dams to the north ~19–12 ka (Uchupi *et al*., 2001), lending support to the hypothesis that local forcing can produce regionally significant erosional unconformities on periglacial shelves even in the absence of base-level changes.

Tracking sediment movement across the margin

The regionally significant 'R' horizon (Fig. 48) matches the p1 reflector that defines the base of the Purple sequence mapped with MCS data along the outermost shelf (Figs 42–44). As discussed further earlier, p1/R correlates to 79 mbsf at ODP Site 1073 where Oxygen Isotope Stages 6 and 7 are missing (McHugh & Olson, 2002). This age range points

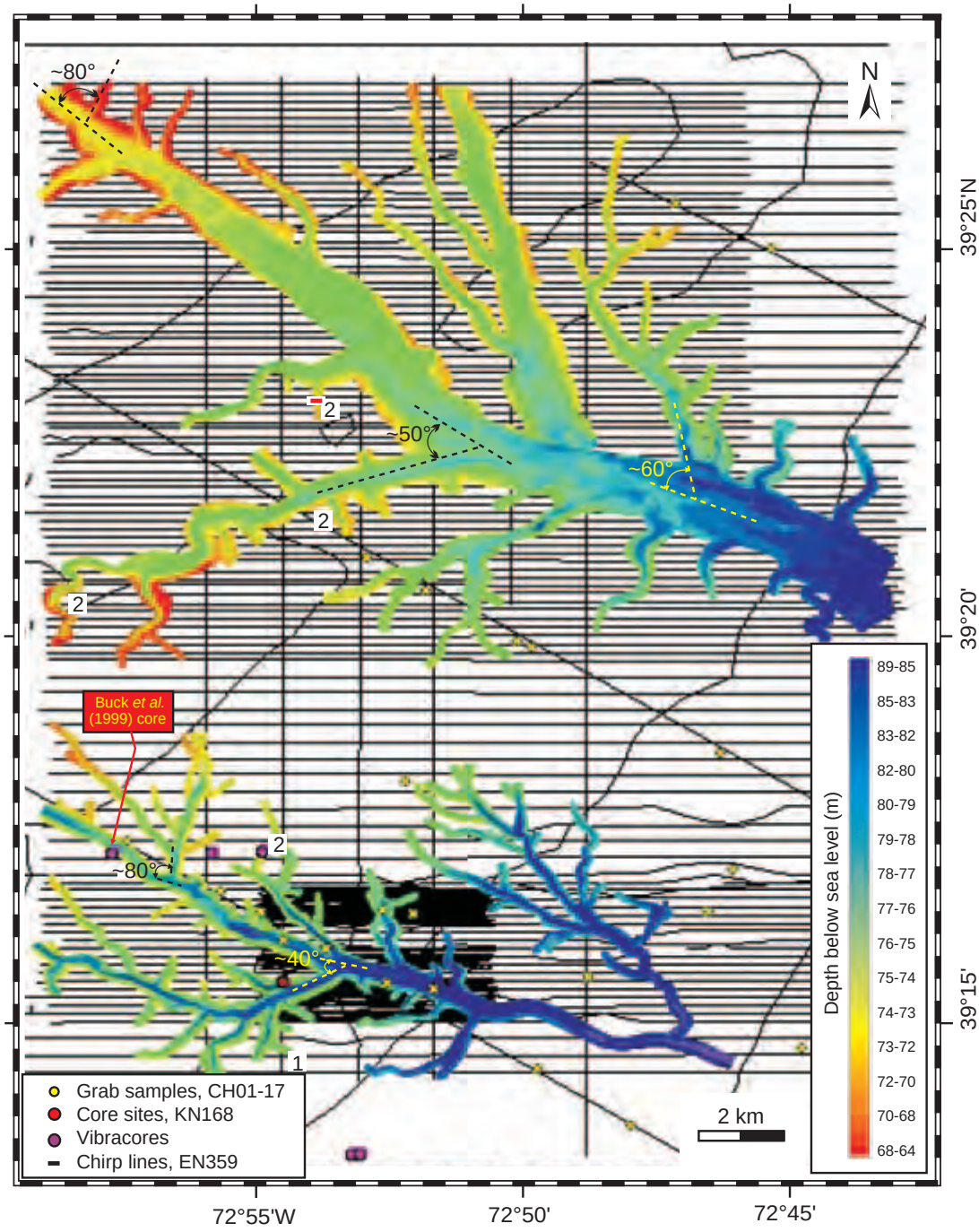

Fig. 46 Interpolated, shallowly buried fluvial drainage systems mapped beneath the New Jersey outer continental shelf. These drainage systems exhibit dendritic patterns. Depths are in metres below ambient sea level. Location of the Buck *et al*. (1999) vibracore is also shown.

toward glacially induced sea-level lowstand as the cause of the hiatus, and suggests that where this surface has been mapped landward to the middle shelf (Knebel *et al*., 1977; Milliman *et al*., 1990; Davies & Austin, 1997; Duncan *et al*., 2000) it may represent a longer interval of missing record.

Subtle topographic changes during the regression marked by the p1/R surface may have

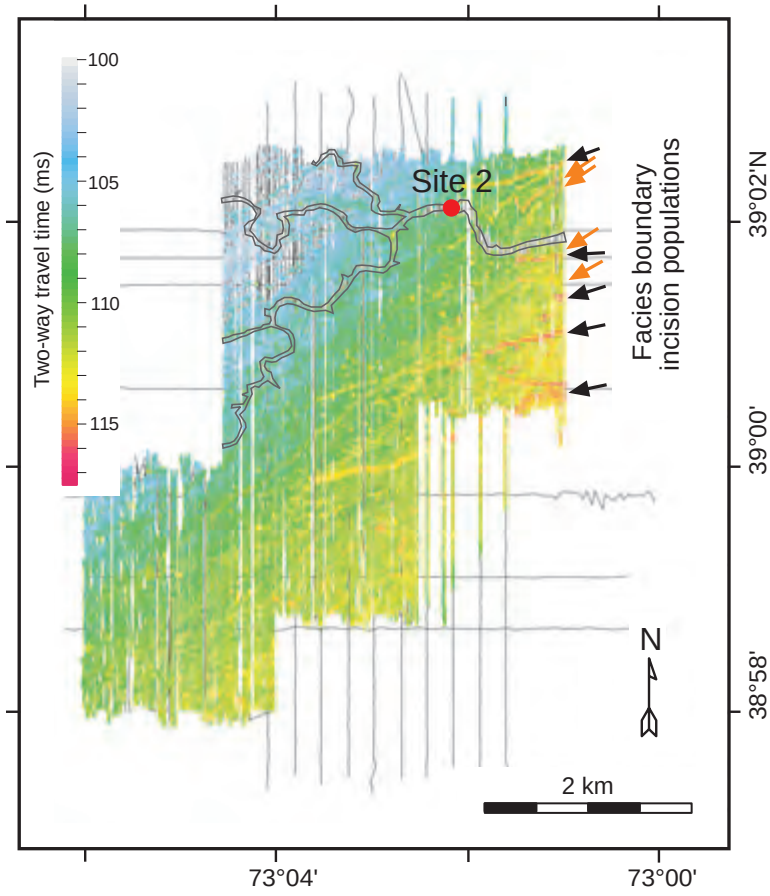

Fig. 47 Map of seismic facies boundary made by interpreting densely distributed Chirp profiles. Facies boundary irregularities align to form two populations of apparent incisions: one trending north-east (orange arrows), and the second with a more easterly trend (black arrows). The facies boundary dips south-east across most of the mapped area, except in the south-east, where it onlaps horizon 'R'. Incisions in both populations meander less than the overlying channel system (in grey), which is perhaps coeval with the 'channels' horizon mapped to the north-east (Nordfjord *et al.*, 2005). These incisions may all be caused by periodic floods crossing the shelf from breached glacial lakes to the north. Depths are in milliseconds, two-way travel-time. (From Fulthorpe & Austin, 2004.)

modulated cross-shelf sedimentation, building the shelf outward as distinct, toplapping wedges above 'R'; in places, these wedges look much like delta fronts (Gulick *et al.*, 2005). They may be important regression markers in clastic-dominated outer-shelf settings along passive margins. Furthermore, seismic-facies data indicated that these wedges represent interbedded lithologies, and in places are sandy, suggesting progressive winnowing of shelf sediments seaward to the shelf-break. Fulthorpe *et al.* (1999) have postulated a similar cross-shelf sediment-transport mechanism for the New Jersey margin during Miocene lowstands; i.e. a line-source delivery of fluvial sediments by small rivers to the outer shelf. From there, both channelized and non-channelized downslope transport processes have moved sediments into deeper water. The presence or absence of canyon incisions on the New Jersey slope has been dictated not only by fluctuations in base level, but by local conditions, including rates of sediment supply, grain-size distribution and possible slope collapses related to fluid escape (Fulthorpe *et al.*, 2000).

New Jersey submarine canyons

Studies of submarine canyons and their role in continental-margin evolution are based on seismic-reflection data, cores, outcrops and, to a lesser degree, high-resolution bathymetric data. The morphology of modern submarine canyons and theories for their formation are thoroughly discussed in Pratson *et al.* (this volume, pp. 339–380). In this paper, submarine canyons are considered in the context of the stratigraphic record that fills them.

In studying the character of Miocene canyons now buried within the New Jersey slope (Fig. 49), Mountain (1987) interpreted V-shaped canyons to have been cut by turbidity currents and U-shaped canyons to have been carved by mass wasting (see also Twichell & Roberts, 1982; Farre *et al.*, 1983). Buried canyons are typically ~50–100 m deep and

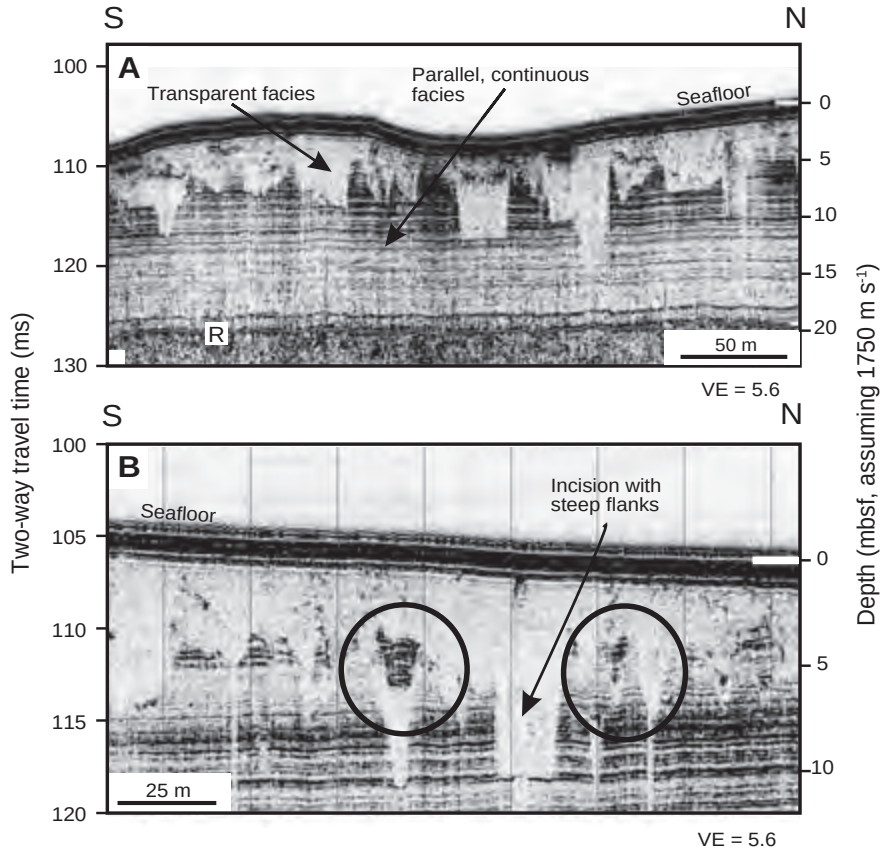

Fig. 48 Seismic facies above horizon 'R'. (A) Relationship between seismically transparent (above) and parallel, continuous/stratified facies (below) within the mapped area and above horizon 'R'. Seismically transparent facies, incised by meandering channels near the seafloor, is up to ~20 m thick. Irregular boundary between these facies resembles steep-sided (commonly 50°–90°) incisions, which truncate underlying reflections. (B) Stratified blocks (circled) occur within the transparent material and within incisions defined by the facies boundary. The presence of these blocks suggests that the parallel, continuous/stratified facies has been catastrophically eroded and then quickly redeposited in topographic lows, along with the remainder of the transparent-facies material. Labels: mbsf, metres below seafloor, VE, vertical exaggeration. (From Fulthorpe & Austin, 2004.)

1–2 km wide (Fig. 50; Mountain, 1987; Miller *et al*., 1987b; Pratson *et al*., 1994; Mountain *et al*., 1996). In addition, STRATAFORM studies off New Jersey and in Eel River Basin have identified many smaller, buried gullies in the vicinity of canyons. These features are typically 1–10 m deep, 100–200 m wide, and are directed downslope (Field *et al*., 1999; Fulthorpe *et al*., 2000; Spinelli & Field, 2001). Buried gullies tend to be V-shaped, and many may have been tributaries leading into nearby buried canyons (Pratson *et al*., this volume, pp. 339–380).

The paths of buried canyons and gullies are difficult to trace between seismic lines in typical two-dimensional surveys. Modern gullies are similar in dimension, and they coalesce with increasing regularity downslope to produce a tributary-style drainage pattern. For example, 11 gullies along the New Jersey upper slope merge into just four gullies on the lower slope (Pratson *et al*., 1994). The buried gullies may have a similar distribution, but the profile coverage is too sparse to determine this. To date, available data suggest that gullies may abruptly start and stop on the slope with few intersections (Fulthorpe *et al*., 2000; Spinelli & Field, 2001).

The drainage pattern of buried canyons also appears to be linear and largely directed downslope, though a few may meander (von der Borch *et al*., 1985) or have sharp turns due to faults and other structures (Kelling & Stanley, 1970; Song *et al*., 2000). Furthermore, they may branch off into tributaries near the palaeoshelf break (Martin & Emery, 1967; McGregor, 1981). Buried canyons have been found on the New Jersey upper slope where they primarily occur between modern canyons (Mountain, 1987; Pratson *et al*., 1994; Mountain *et al*., 1996; Fulthorpe *et al*., 2000). Farther downslope, all the buried canyons merge into and have been re-excavated by a modern canyon (Pratson *et al*., 1994). This re-use of the buried canyons appears to be due to their diminishing depth of burial downslope.

Sediments that fill buried canyons are a mixture of mass-wasting debris, turbidites and hemipelagic drape. Although these deposits are commonly interbedded with one another, sedimentological studies of buried canyons have detected a common

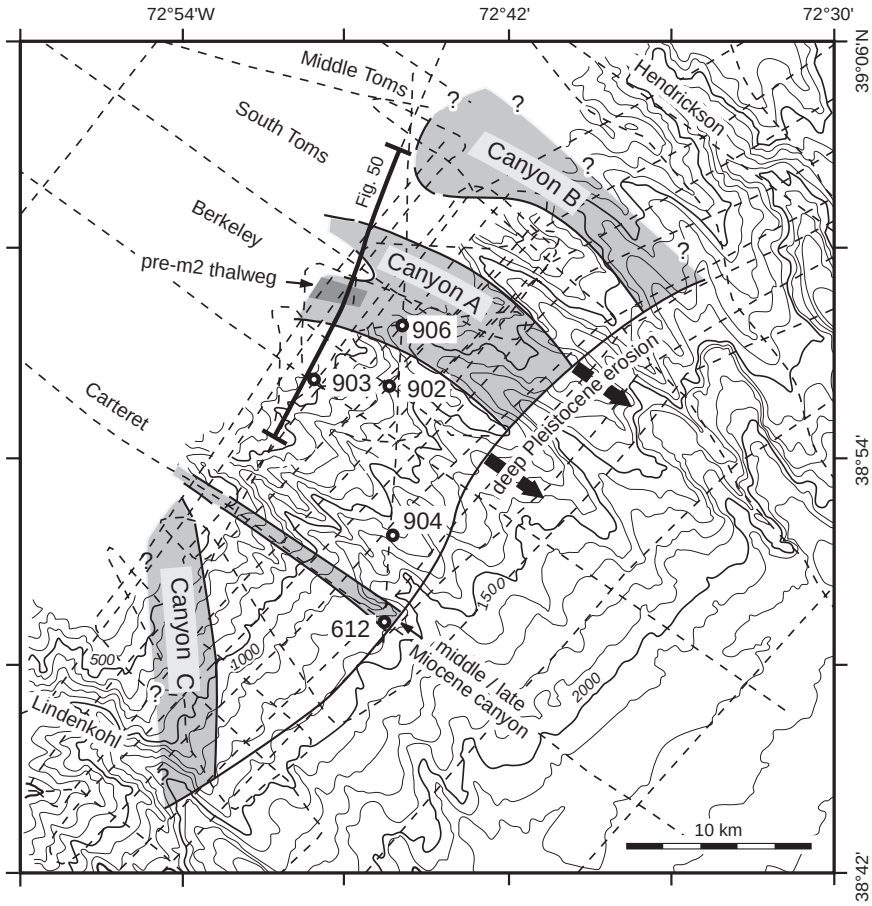

Fig. 49 Locations of drill sites (ODP Leg 150; DSDP Leg 95) and seismic profiles (Ew9009 MCS; ODP Leg 150) used to locate three middle Miocene canyons (grey shaded areas labelled A, B and C) and one younger canyon, all now buried on the New Jersey upper slope. Bathymetry is based on SeaBeam (Pratson *et al*., 1994). Modern canyons are labelled. (After Mountain *et al*., 1996.)

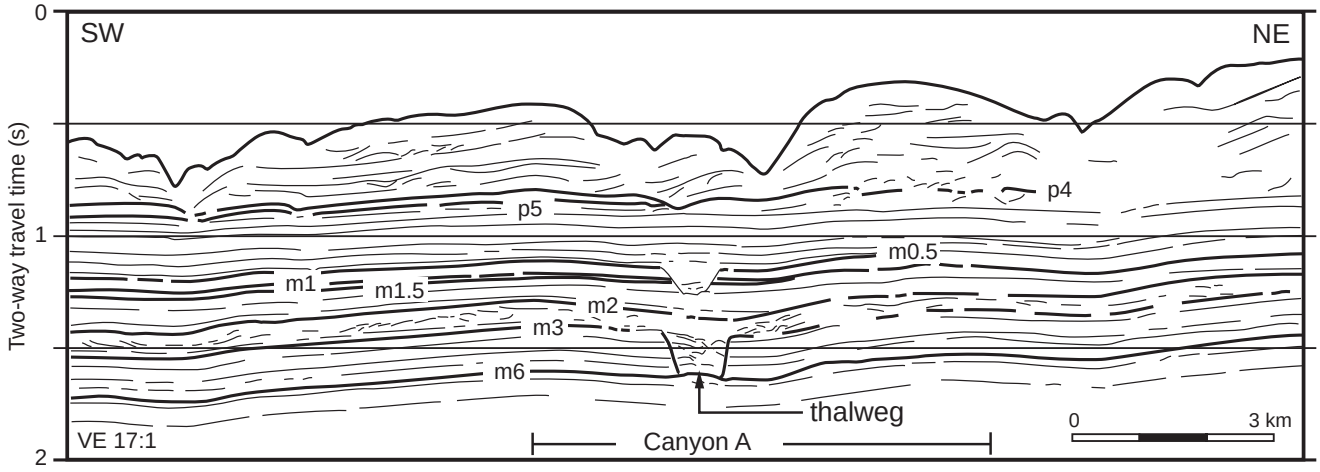

Fig. 50 Line drawing interpretation of seismic profile Ew9009 MCS line 1026 along the New Jersey slope. Several sequence boundaries are traced from the shelf, as noted. At this location (Fig. 49) Canyon A is completely filled below reflector m2. (After Mountain *et al*., 1996.)

sequence to canyon fill (Stanley & Kelling, 1978; May *et al*., 1983; Goodwin & Prior, 1989; Bruhn & Walker, 1995; Mountain *et al*., 1996; Wonham *et al*., 2000). The lowermost units tend to consist of coarse-grained sediments that are a combination of lag deposits and mass flows derived from either debris flows or turbidity currents (Fig. 51). These typically decline in frequency upwards, where finer-

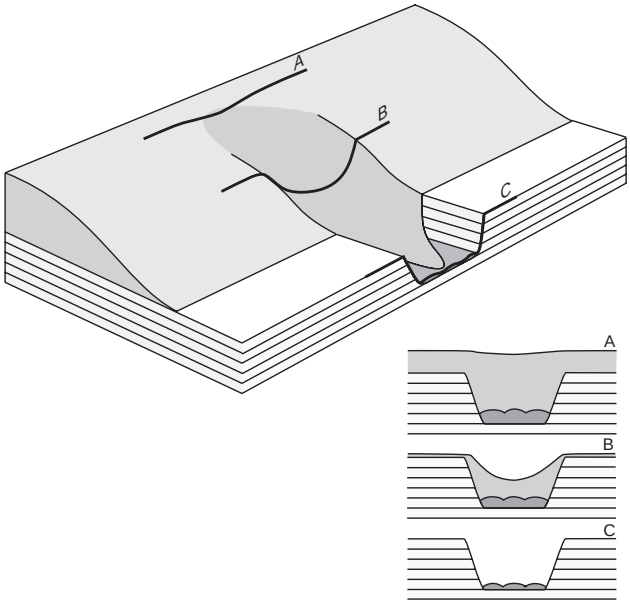

Fig. 51 An isometric view of the New Jersey slope as it may have looked at the time of reflector m2, crossed by hypothetical profiles A, B and C. Drilling at ODP Site 906 showed that the oldest deposits on the canyon floor are debris from the widening and headward erosion of the original slump scar, and are overlain by shallow-water turbidites which demonstrate that the canyon connected with a source of shelf sands. The major volume of infilling sediment is laminated claystone between these sands and reflector m2. (From Mountain *et al*., 1996.)

grained turbidites become more common. The turbidites are likely to have been deposited by decelerating turbidity currents, and are often capped by hemipelagic units, suggesting periods of even more gradual filling. ODP Site 906 (Mountain *et al*., 1994) drilled directly through the thalweg of a mid-Miocene slope canyon and determined this three-part succession with clarity. The basal fill is composed predominantly of a conglomerate formed by semi-indurated mid-Miocene slope sediments. These demonstrate that this canyon widened through wall collapse, and some or all of the initial debris was not removed from the canyon floor. Shallow-water turbidite sands rest with angular unconformity on this conglomerate at Site 906, and provide the majority of the fill. These sands thin seaward, and at the 1500-m isobath no fill is observed. Hemipelagic slope sediments overlie the turbidite sands.

According to Posamentier *et al*. (1988), canyon filling should occur during periods of relative sea-level rise. This conclusion is supported by observations of other margins (Ruch *et al*., 1993), and by recent laboratory experiments simulating strata formation during changes in base level (Wood *et al*., 1993; Heller *et al*., 2001). However, many submarine canyons around the world that were active during the Last Glacial Maximum have remained exposed and unfilled during the subsequent eustatic rise.

Sediment failure and headward erosion can be important precursors to shelf-break sands finding a ready conduit to the deep sea. Sea-level fall is very likely to be a secondary process in the formation of slope canyons. The data at Site 906 has narrowed the critical events to the following (all dates have a standard error of ±0.5 Myr): initial slope failure occurred at 13.5 Ma; continued mass wasting widened and lengthened the canyon, and a source of shallow-water sands began spilling into the canyon at roughly 13.0 Ma. This phase was replaced by a fill of laminated silts very likely as a result of transgression of the shelf. By 12.4 Ma, the history of this canyon was complete. This and presumably other New Jersey canyons were buried on the upper slope before burial on the lower slope; as a result, canyon piracy was more common in the latter setting. Consequently, the stratigraphic record of lower slope canyons can be especially complex.

Sedimentation in open-slope regions (i.e. between canyons) is more uniform and continuous, and occurs as:

1 settling of fine-grained hemipelagic sediment carried off-shelf in dispersed plumes;
2 overflow of turbidity currents from neighbouring canyons;
3 transportation along-slope by prevailing bottom currents.

As canyon thalwegs deepen by erosion, canyon interfluves build, with the net result that canyon morphology becomes more accentuated.

Stratigraphic modelling

Reconstructing the margin

The New Jersey margin developed its present-day character of stacked clinoforms beginning in Oligocene times. Since then, siliciclastic clinoforms

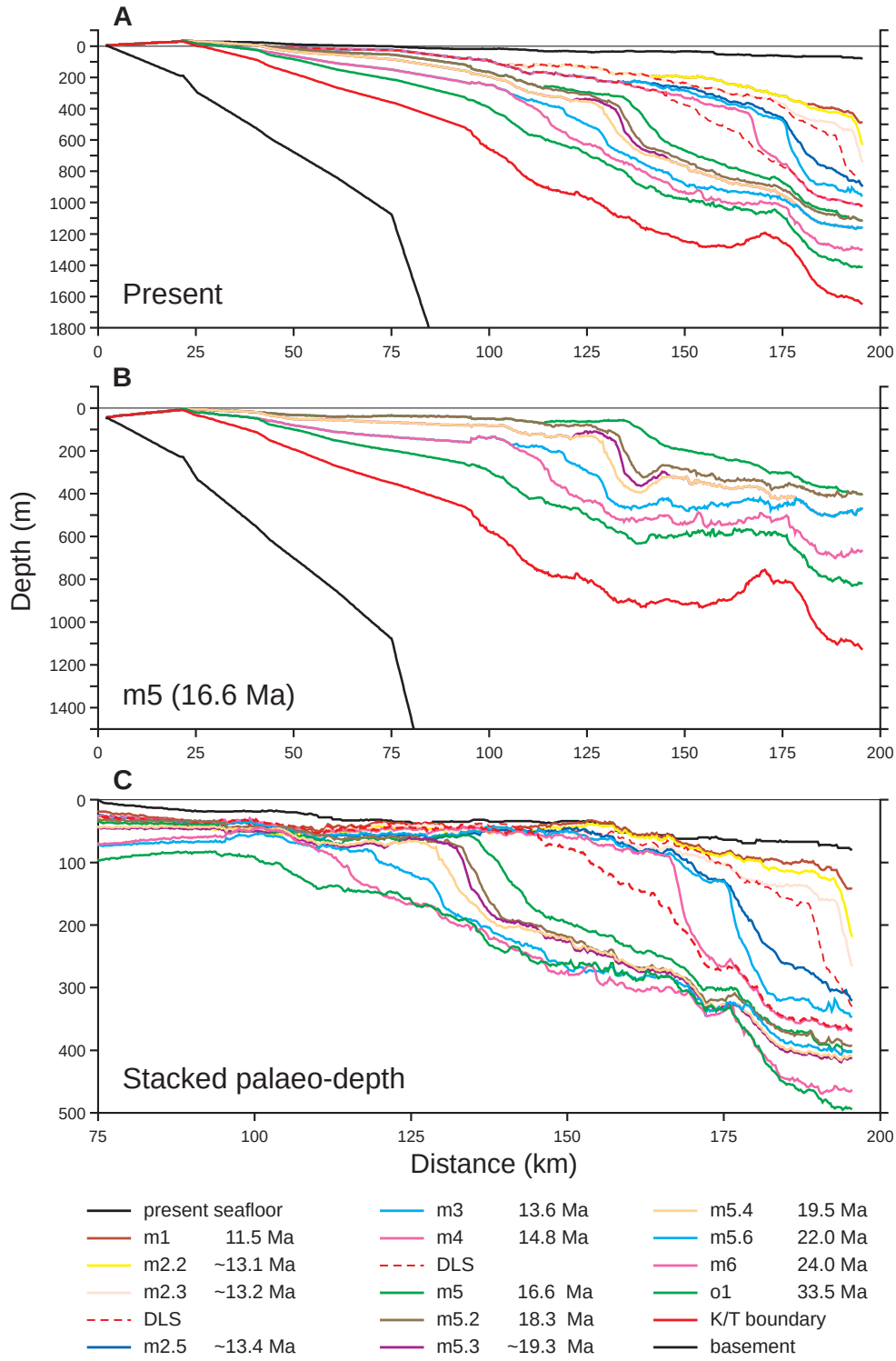

Fig. 52 Sequence boundary profiles on the New Jersey margin. (A) Tracings of 13 post-Eocene sequence boundaries, two widespread downlap surfaces, and the Cretaceous–Tertiary unconformity along profile Ew1003 (see Fig. 31). Names and ages of each are displayed in the colour code at the bottom. Reflection times have been converted to depth using a regional function of sound velocity derived from local seismic stacking velocities. (B) The same depth profiles with all sediment younger than sequence boundary m5 removed; sediment decompaction plus isostatic and flexural rebound have been calculated. (C) The depths of all sequence boundaries at the time of their formation with the added correction for estimated palaeowater depths. Note the changes in both horizontal and vertical scale. (After Steckler *et al.*, 1999.)

have advanced nearly 100 km across the underlying carbonate ramp, and now provide a relatively complete record of late Oligocene to Holocene margin evolution. Clinoforms such as these are a basic building block of many continental margins and have been the subject of considerable debate as to their imprint of eustatic change (Vail *et al*., 1977; Haq *et al*., 1987; Posamentier *et al*., 1988).

However, discussions of Tertiary evolution for the New Jersey margin must recognize that the present geometry of preserved strata is not an accurate indicator of original morphology. Subsidence, compaction, sediment loading and tectonic activity have all deformed these sediments. Backstripping removes sediments layer by layer to restore the morphology of the surface (assumed to be a former seafloor), as well as the geometry of underlying surfaces (Steckler *et al*., 1988, 1993). The shape and gradient of the past continental shelf can then be estimated, and, in particular, the height of clinoforms can be determined. Furthermore, the depth of any given clinoform rollover and its position relative to the adjacent shoreline can be evaluated.

Numerical experiments have been conducted with initial conditions based on backstripping reconstructions of margin geometries (Steckler *et al*., 1999; Syvitski *et al*., this volume, pp. 459–529). Sea-level variations were modelled to fit a sinusoidal cycle with 20-m amplitudes and 2-Myr periods, the latter being the average length of early Miocene cycles in New Jersey. These oscillations were superimposed on a long-term, post-Eocene eustatic rise of 10 m. Doubling the modelled amplitudes to 40 m causes breakdown in the smoothly varying switch from progradation to aggradation within each cycle. However, even 40 m is considerably smaller than previous estimates of 100 m and more, which were derived from sequence geometries and assumptions of lithofacies (Haq *et al*., 1987). The more modest estimates used in this Steckler *et al*. (1999) modelling effort are in accord with subsequent $\delta^{18}O$ and backstripping data based on studies from coastal-plain wells (Kominz & Pekar, 2001). Furthermore, the modelling results yield clinoforms that steepen as they prograde into deeper water, consistent with both observations.

The modern arrangement of 13 post-Eocene sequence boundaries, two widespread downlap surfaces and the Cretaceous–Tertiary unconformity are displayed in depth in Fig. 52A. Figure 52B shows a depth profile as it would have looked in the early Miocene at 16.6 Ma; all sediment younger than sequence boundary m5 has been removed, and sediment compaction, isostatic and flexural rebound have been accounted for. The true height of the m5 clinoform at 16.6 Ma is predicted in this manner to have been ~110 m. Furthermore, the m5 rollover is predicted to have been in ~60 m of water. Similar backstripped geometric models of other post-Eocene sequence boundaries (Fig. 52C) show that the relief of most clinoforms was at least this large when formed. Indeed, several of the middle Miocene sequence boundaries outline clinoform heights twice as large. This modelling illustrates that the rollover from flat-lying topsets to seaward dipping foresets typically occurs many tens of metres below sea level. This observation challenges the assumption that strata showing coastal onlap against the seaward face of a dipping clinoform are necessarily shallow-water facies.

The backstripped surfaces in Fig. 52 also show that foresets vary in steepness in an organized manner. The pattern of sigmoidal clinoforms appears to change gradually from progradation to aggradation over about six clinoforms. This corresponds as well to a gradual increase in the steepness of the foreset surfaces. If valid, this may indicate either: (i) a higher order (5–15 Myr) record of sea-level variation not yet accounted for; or (ii) a response to varying amounts of sediment supplied to the New Jersey shelf. Figure 53 shows the amount of sediment deposited on the New Jersey margin through time, based on volume calculations of the backstripped models. Note the relatively short-lived peak of sediment deposition centred at ~13 Ma and 1.5 Ma. Both of these spikes lag the times of rapid increase in global ice volume by 1–2 Ma, as indicated from increases in global $\delta^{18}O$ (Fig. 53), and suggest a link to climate-induced changes in terrestrial erosion and/or sediment delivery to the continental shelf.

Profiles show that oblique clinoforms prograded roughly 25 km across the New Jersey outer shelf in Pleistocene time, in close agreement with model simulations. Some of the sediments recovered in ODP Leg 174A cores reveal a history of deepening upwards within these deposits (Austin *et al*., 1998), consistent with the model results that these strata accumulated during a time of transgression.

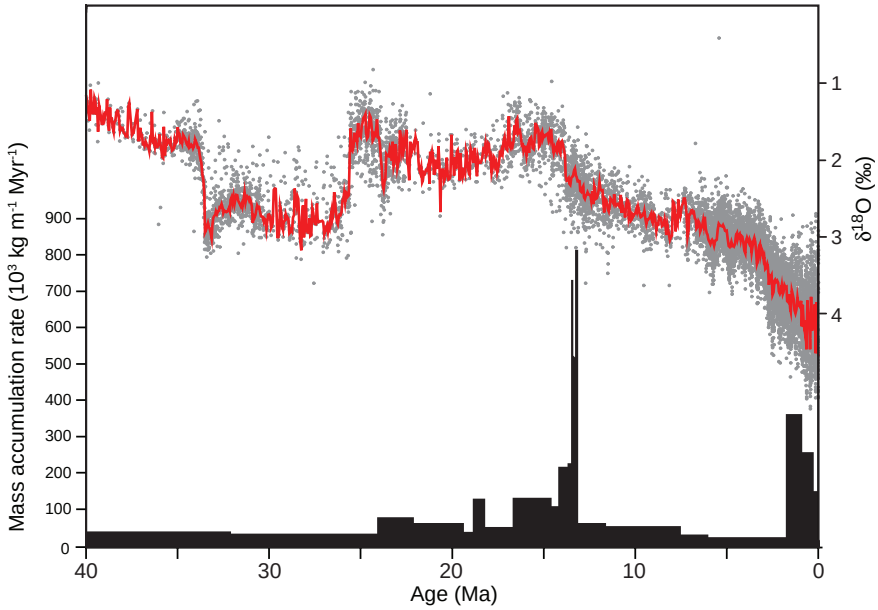

Fig. 53 Mass accumulation rate (black columns along bottom; scale at left) of sediments deposited on the New Jersey margin through time, superimposed with global values of $\delta^{18}O$ (red, right-hand scale; Zachos *et al.*, 2001). Sediment volumes were derived from calculations based on backstripped models (see Fig. 52).

This was a major surprise of ODP Leg 174A, because downstepping of eroded surfaces had suggested that these packages were formed during sea-level fall. However, modelling fails to produce the volume of oblique strata observed in two-dimensional profiles. Increasing the amplitudes of modelled sea-level fluctuations leads to more extensive sequence-boundary unconformities and, with sufficiently large fluctuations, these unconformities eventually reach the shelf edge. Most importantly, if sea-level amplitude is increased to 90 m, models predict extensive oblique clinoforms and non-marine strata overlying the preceding sequence boundary, in a position where ODP Site 1071 recovered possible lagoonal sediments of late Miocene age (Austin *et al.*, 1998). Glacio-eustatic changes implied by variations in global δO^{18} (Miller *et al.*, 1987a) are too small to support a 90-m late Miocene fall, but the drilling evidence is irrefutable: sea level was within a few metres of a clinoform top, only ~3 km from the matching rollover. Future modelling must reconcile this drilling evidence with subsidence caused by loading from sediments, water and possibly continental ice.

Oxygen isotope record

The onshore stratigraphic record can be linked to offshore sequence boundaries and to the global record of $\delta^{18}O$ (Miller & Mountain, 1994; Miller *et al.*, 1996a). A majority (nearly 30 in all) of the regionally correlated Oligocene–Neogene hiatuses documented by onshore drilling separate transgressive–regressive successions (Sugarman *et al.*, 1993; Miller *et al.*, 1997a). Basal quartz sands, shells, glauconite and organic matter deposited in 30–100 m water depths grade upward to middle neritic silts and finally to quartz sands in which biofacies indicate palaeodepths < 30 m. The succession usually ends abruptly, occasionally with evidence of erosion and subaerial exposure. These characteristics point to oscillations in sea level as a major control on coastal-plain facies successions. Geochronology based on biostratigraphic, isotopic (largely $^{87/86}Sr$ ratios) and magnetostratigraphic integration has determined the ages of roughly 10 hiatuses from latest Oligocene to mid-Miocene, and has shown they closely match the ages of inflections in global marine $\delta^{18}O$ records (i.e. inferred glacio-eustatic lowstands, Fig. 54; Sugarman *et al.*, 1997). Thus, the case for a global cause to mid-Tertiary gaps in the onshore record of New Jersey margin is very strong.

The implication that sea-level change is the cause of the Oligocene and mid-Miocene sequence boundaries (defined by facies successions) has been extended to the New Jersey slope (Miller *et al.*, 1996b). Geochronology based on biostratigraphic, isotopic and magnetostratigraphic integra-

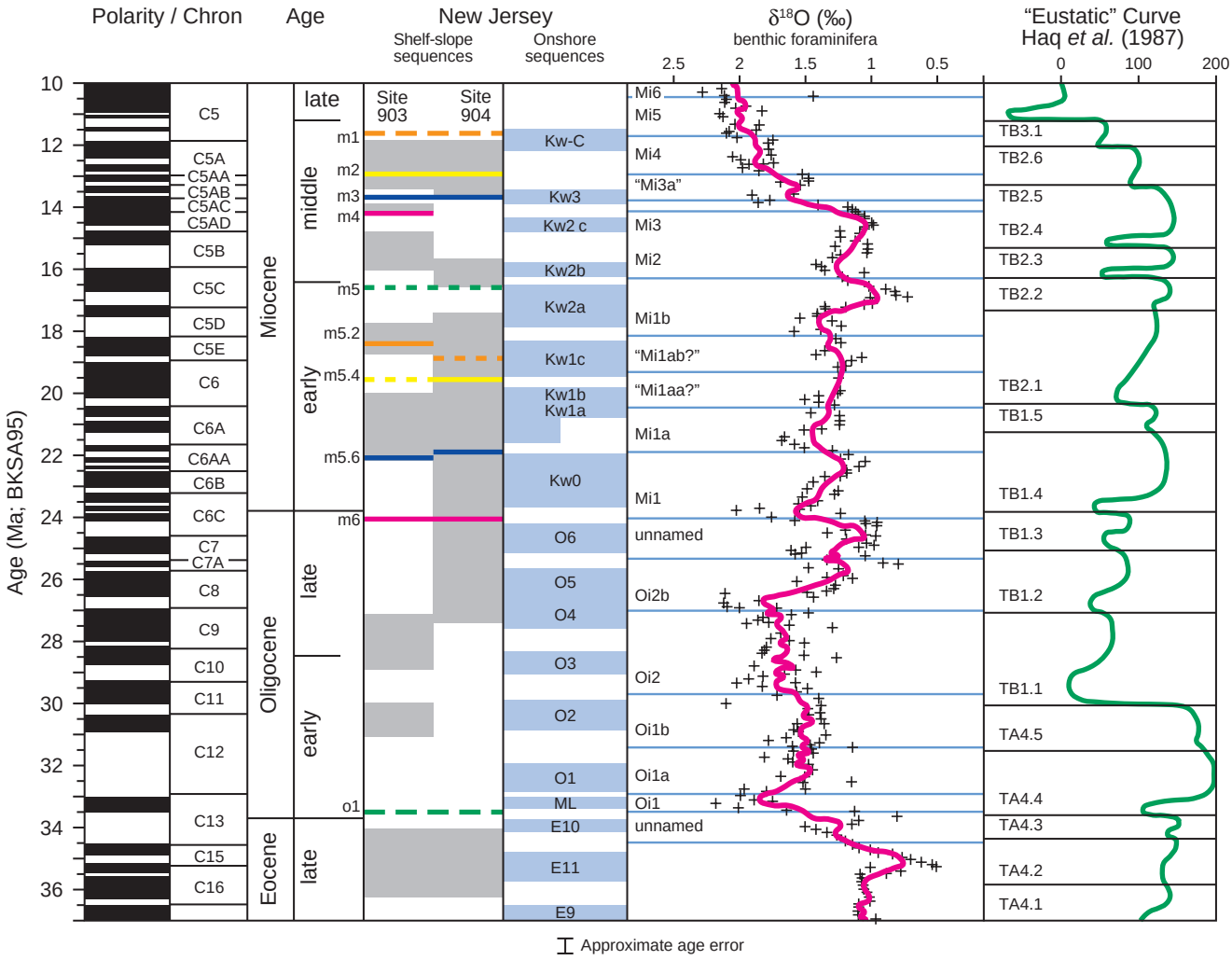

Fig. 54 Oligocene–Miocene sequences for the New Jersey margin (onshore and offshore) correlated to a composite of global $\delta^{18}O$ values and the eustatic curve of Haq *et al*. (1987). Reflector geometries tied to chronologies sampled on the slope define the offshore sequences: facies successions and erosional gaps define the onshore sequences. To a large degree, these correlate in time. The key surfaces and gaps show a close match to $\delta^{18}O$ increases, indicating growth in global ice volume. (From Miller *et al*., 1998a.)

tion strongly suggests that these surfaces formed during the time that unconformable gaps were developing onshore, and by inference the global marine record of $\delta^{18}O$ was experiencing marked changes as well. Despite the suggestion that similar numbers and ages of events onshore, offshore, and in the $\delta^{18}O$ record point to a common origin, the age comparisons implicated in Fig. 54 do not prove a causal relationship.

The ice-volume changes implied by studies on the New Jersey margin average 1.2×10^6 yr between maxima, but exhibit no clear periodicity. These events are probably composites of Milankovitch-scale (10^4–10^5-yr scale) climate cycles that have merged to yield long-term changes (Zachos *et al*., 1994). This is illustrated by a moderately high-resolution (~10^4 yr sampling; Flower & Kennett, 1995) $\delta^{18}O$ record showing that the major slope reflectors on the scale of 10^6 yr (m2 through to m5) correlate with major $\delta^{18}O$ increases, although there is higher-order variability contained in both records. Further study of New Jersey sections may continue to detect additional, smaller-scale sequences, such as some of those found onshore at the Cape May drillsite (e.g. subdivisions of Kw2a and Kw3 by de Verteuil, 1997).

SUMMARY

The long-term record: its challenges and rewards

This paper has focused on processes that build continental margins and operate on time-scales of ~20 kyr and greater. In contrast to the impact of processes that operate on shorter periods (see the other papers in this volume), long-term processes:

1 provide the opportunity to examine behaviour of the Earth system under boundary conditions very different from those of today;
2 evaluate a variety of numerical models designed to duplicate natural phenomena;
3 capture the full range of processes that have built the geological record.

Choosing to study the marine record of modern margins provides obvious advantages: sediments are less disrupted and chemically altered than are most sediments seen at outcrop; the modern depositional setting can provide analogues to the ancient environment in which the long-term record accumulated; and the logistics, cost and quality of seismic-reflection profiles are superior to those collected over land.

Gathering samples to document long-term processes inferred from seismic-reflection profiles is nonetheless a challenging task. Rotary drilling is the only technique that can reach > 100 m below seafloor, as needed to sample the long-term record. On continental shelves, these sediments are commonly sand-rich, unlithified and difficult to recover with their primary fabric still intact. Few research-based efforts have attempted to drill to substantial depths in continental margins, and where they have, the recovery has been inadequate for answering many fundamental questions concerning processes that shape the long-term record (Austin *et al*., 1998). Borehole logging provides information to fill gaps caused by incomplete core recovery, and helps to correlate two or more borehole records (Goldberg, 1997). This is accomplished by sensors lowered into an existing well or installed within the drilling assembly to measure electrical, acoustic or radiometric properties of the sediments and pore fluids. However, logging does not return a physical sample for dating or for more elaborate compositional analysis. Even with complete core recovery, the precision of absolute dating is limited by low accumulation rates, a lack of biostratigraphic markers, and poor preservation of geochemical and palaeomagnetic indexes.

Despite sampling and dating challenges, one of the primary aims in studying continental margins is to understand the causes of depositional gaps that have long been recognized throughout the geological record. Few researchers deny the existence of these widely distributed breaks, typically expressed as abrupt changes in biofacies, lithofacies and/or the angular termination of stratal surfaces. However, agreement as to their cause is far from unanimous. Debate sharpened in the 1970s when the digital revolution dramatically improved the acquisition, processing and display quality of seismic-reflection data. These images of the subsurface revealed stratal patterns in basins and continental margins throughout the world with previously unseen clarity, and classically trained stratigraphers with access to these global, high-quality subsurface data developed new ways of applying seismic-reflection profiles to the study of basin history and the search for fossil fuels. The result was an entirely new approach to interpreting the geological record – termed **seismic sequence stratigraphy**, which relies on the recognition of angular reflector terminations against basin-wide unconformities (Payton, 1977). Proponents claim this approach reveals the distribution of facies sufficiently for recognizing downward shifts in base level that are presumed to track local falls in sea level. Some researchers have taken this one step further to conclude that their records prove the existence of global, i.e. eustatic, changes in sea level every 1–2 Myr for the past 200 Ma (Vail *et al*., 1977).

Critics have pointed to the absence of a single eustatic mechanism explaining this long record (Christie-Blick, 1991), and have argued that:

1 geochronology can rarely provide the precision needed to prove this level of synchroneity;
2 numerical models show that flexural response of the **lithosphere** to sedimentary loads will generate a hiatus of distinctly different ages in different tectonic settings;
3 numerous basins show that changes in sediment supply, deltaic lobe switching, tectonism and other local processes can lead to reflector geometry that mimics the imprint of eustatic change.

Numerical modelling further demonstrates that reflector geometry, facies successions and the ultimate extraction of a eustatic signal are very sensitive to the sediment compaction history and rate of tectonic response to water and sedimentary load, and also to the regional tectonic adjustments of the underlying crust. Consequently, some researchers have claimed that the record of eustatic change in the range of 10^1 m over 10^5 yr can be overwhelmed by the magnitudes and rates of relative change produced by these other factors (Karner & Driscoll, 1997). This last argument does not deny that eustatic change affects the stratigraphic evolution of continental margins, but clearly places it among other important factors.

The Eel River Basin: difficulties in recognizing eustatic control

Studies of the Eel River Basin confirm the importance of tectonic control on margin evolution. The region surrounding the Eel River Basin has evolved over the past 80 Ma from a transcurrent to a convergent plate boundary (Atwater, 1970). The comparatively narrow shelf (defined locally as seafloor landward of the 150-m isobath) is supplied with sediment derived predominantly from the Eel River. The continental slope descends to the Cascadia Trench. An active magmatic arc plus a region of accreted terrain landward of the shoreline provide sediment to the margin. The modern Eel River margin is a classic forearc basin.

Basement subsided so rapidly in Oligocene to early Miocene time, when the Cascadia subduction zone developed off northern California, that the margin foundered and entered a lengthy period of transgression. Regression and significant sedimentary reconstruction did not begin until Pliocene time. Those processes, too, were altered substantially during 0.7–1.0 Ma, when uplift and a widespread hiatus accompanied the northward migration of the Blanco Fracture Zone along the North American–Gorda plate boundary (Orange, 1999). Since then, as much as 1 km of sediment has accumulated within the Eel River Basin, though the region is faulted and divided into deep synclines and sharp anticlines that attest to convergent plate motion (Clarke, 1987). The regional stress field has been changing since ~0.5 Ma due to the northward approach of the Mendocino Triple Junction, as expressed by rotating fault trends and basin reorientation throughout this interval (McCrory, 1989). The relatively close line spacing (5 km or less) of the STRATAFORM seismic grid provides good spatial coverage of this post-1-Ma section, but does not have the acoustic penetration to provide insight into older/deeper sedimentary units.

Complications from gas (biogenic and thermogenic) constitute a substantial challenge to documenting the long-term history of the Eel River Basin. Together with the absence of drill holes in the study area, it is apparent why detailed knowledge of controls on the long-term record in the Eel River Basin is currently limited. In particular, the age of basin-wide unconformities in the basin is not well constrained. Fourteen unconformities defined by erosional truncation, downlapping and onlapping reflectors are recognized in uplifted areas; all become conformable in adjacent synclines (Burger *et al*., 2002). Many or all of these surfaces probably mark transgressive ravinements that formed during shoreface retreat as sea level rose to flood a previously exposed or very shallow (less than storm wavebase) shelf. An observed cyclicity (~70–100 kyr) suggests that there may be a glacio-eustatic signal, but definitive age control is needed (Burger *et al*., 2001).

Despite the current lack of long-term samples, the following model of sequence-stratigraphic development has been proposed (Burger *et al*., 2002). Shelf sedimentation during highstand dominates the record and is comprised of fine-grained marine silts and muds. During regression, interfluves between rivers are areas of non-deposition and palaeosol formation; off-shelf sediment transport along the northern Eel River Basin is focused in shelf-break gullies that led into slope channels. In general, very little sediment from times of regression is likely to be found on the continental shelf. During times of trangression, incised channels are filled first, followed by a transgressive lag deposit that in interfluve areas now rests unconformably on the highstand silts and muds of the previous sequence. The recognition of ten additional surfaces incised by sharply defined channels (10–250 m deep and 100–1000 m wide) shows that local tectonism has a major influence on margin development (Burger *et al*., 2001). Each channel trends south-west from near the mouth of the Eel River and deepens towards embayments along the north side of Eel

Canyon; locations and gradients suggest that they are former river channels that cut into the shelf during shoreline regression, and have been directed toward Eel Canyon since its presumed inception at ~360 ka.

Initial attempts to model sequence development of the Eel River Basin have produced encouraging results. Depocentres transgress and regress across the shelf, but each sequence builds out to approximately the same position in each cycle, as determined by the admittedly oversimplified, uniform rates of sediment supply and margin subsidence. The largest departure between the model and observations occurs on the upper portions of the slope, where the model builds only a thin sedimentary record, and thick deposits are observed.

The New Jersey margin: eustatic imprint, with complications

Factors controlling the long-term stratigraphic development of the New Jersey Margin (NJM) are better documented than they are for the Eel River Basin, largely because they include deep sediment samples of the New Jersey margin record. The margin has evolved under a uniform and more easily documented tectonic setting, with the result that basin history can be more easily determined from seismic-sequence stratigraphy there than it can be in the Eel River Basin. The opening of the Atlantic created a rifted, passive margin along the eastern USA in Middle Jurassic time, and this plate setting has not changed to the present (Sheridan *et al*., 1988). In contrast to the post-Oligocene Eel River Basin forearc basin, rapid, shallow-water sedimentation on the New Jersey margin largely exceeded basin subsidence throughout the first 65 Myr. This resulted in a continental shelf that continued to widen as flexural loading rolled the shoreline landward (Watts & Steckler, 1979). By mid-Cretaceous time, the shelf was > 150 km wide, with its seaward limit delineated by a fringing reef that extended along the entire eastern North American continent (Jansa, 1981). The reef was overrun by siliciclastic sediment in Barremian time, and has remained buried since then. Sediment supply apparently decreased substantially during the Paleogene, and a wide, seaward-dipping ramp developed as a result. Numerical models backed by palaeowater depths of microfossils show that the seafloor above the buried mid-Cretaceous reef in Eocene time was roughly 1500 m below sea level (Steckler *et al*., 1993).

The New Jersey margin entered its present phase of margin evolution in the mid-Oligocene, when one or more rivers began building a deltaic wedge of sediment seaward across the drowned ramp (Poag, 1985). By this time, 130 Myr after rifting, thermal subsidence had diminished to a slow rate, and consequently, significant aggradation could occur only due to loading, flexure and eustatic rise. Sediment supply greatly exceeded the accommodation space provided by these three processes, and from then until Pleistocene time clinoforms prograded ~100 km across the margin (Steckler *et al*., 1999). Toes of these clinoforms reached the approximate location of the underlying Mesozoic reef in mid-Pleistocene times, and from then until the present sedimentation on the New Jersey margin has been focused on the outer shelf and upper slope. This has resulted in a substantial thickness of post-mid-Pleistocene sediment that has extended the shelf seaward ~25 km in the past 800 kyr.

Onshore drilling into marine sediments of the New Jersey Coastal Plain has documented at least 15 Oligocene to middle Miocene sequences (Miller *et al*., 1997b). Most begin with shelly, glauconitic, transgressive quartz sands deposited in 30–100 m water depths (Sugarman *et al*., 1993). These are frequently overlain by regressive, prodelta silts that coarsen upwards to the quartz sands of a nearshore or delta-front setting, followed by an apparent hiatus and then by transgressive sands of the next sequence. Shell fragments provide $^{87}Sr/^{86}Sr$ ages which demonstrate that gaps between sequences match the times of global ice increases independently inferred from the marine $\delta^{18}O$ record, thereby providing strong support for the primary role of glacio-eustasy in the arrangement of sequences on this and possibly other passive continental margins. Furthermore, seismic-sequence boundaries defined on the basis of toplap/onlap/downlap have been traced across the middle to outer shelf and tied to Oligocene–Miocene samples from the continental slope. These boundaries also correlate with the global $\delta^{18}O$ increases. In the future, in order to validate any causal link between eustasy, seismic-sequence development, and facies distribution,

samples from successions with as close to 100% recovery as possible must be collected from carefully selected locations within several sequences known to coincide with times of well-established ice-volume change. Only with this confluence of data can the seismic-sequence stratigraphic model linking stratal geometry, facies, water depth and age be properly evaluated. At present, studies from the New Jersey margin have well-documented facies successions in coastal-plain boreholes, but there are no accompanying seismic-reflection profiles to provide stratal geometry. Conversely, stratal geometries are revealed in offshore profiles, but complete samples have not yet been recovered from the crucial topset, foreset or bottomset strata that could prove or disprove the link between facies, stratal geometry and oscillations in global sea level.

Profiles across lower-to-middle Miocene clinoforms on the inner-to-middle New Jersey shelf demonstrate along-strike variability that underscores the importance of acquiring ground-truth samples (Monteverde *et al*., 2000). Isopach maps of 10 sequences, each estimated to be ~1.5-Myr duration, show lobate accumulations in some intervals, and elongated margin-parallel patterns in others. These differences are most probably due to local variations in both basement response to loading and to rates of sediment supply, but cannot be substantiated without samples that evaluate compaction history and facies. Furthermore, incised valleys across the tops of clinoforms identify ancient coastal plains, but the location of shoreline positions as well as water depths at each of the clinoform rollovers cannot be determined without samples. In contrast to margins with substantially faster rates of thermal subsidence, transgressive ravinement on the New Jersey margin has removed most seismically detectable evidence of shoreface deposits.

The variety of lower Miocene clinoform geometries raises concern that stratigraphic evolution can vary along strike to such an extent that inferences based solely on geometry lead to different conclusions depending on location within a basin. A fundamental lesson to be learned from studies of both margins is that clinoforms do not necessarily build directly seaward during times of margin growth; along-strike variations in sediment supply and lithosphere response to cooling, loading and flexure can lead to local variations in sequence development that demand a basin-wide analysis.

In direct contrast to variation along the inner New Jersey margin, clinoform development in middle-to-upper Miocene sediments of the middle-to-outer shelf was comparatively uniform. The latter deposits have been mapped using a reasonably dense (~10–15-km line spacing) grid of both academic and commercial seismic data of moderate resolution (10–20 m; Fulthorpe *et al*., 1999). Along a margin-parallel distance of several tens of kilometres, the clinoform rollover positions for mid-to-late Miocene sequences show no lobate development. This uniformity is undeniable and is made more surprising by the occurrence of incised valleys cutting into the tops of at least six mid-to-late Miocene clinoforms. These are now 5–12 m deep and 50–400 m wide, and indicate that during times of sea-level lowstand fluvial sediment traversed a coastal plain to reach the New Jersey shoreline. Either the margin was fed uniformly by other river systems without one dominating any of the others, or the mid-to-late Miocene was a time of strongly energetic shelf processes that distributed sediment along the margin so effectively that any imprint of localized sediment build-up was removed.

Progradation continued to build the New Jersey margin 25 km seaward of its position in late Miocene time. Four mid-to-late Pleistocene sequences, defined by downlap and toplap stratal geometries with no evidence of steeply dipping shoreface deposits, dominate a seismic grid (55 km × 35 km) across the modern shelf break immediately southwest of Hudson Canyon. This region was chosen for study because the scarcity of slope canyons has made shelf-to-slope correlations possible, but for this same reason it may not be typical of passive margins in general. In contrast to all preceding clinoforms described from the New Jersey margin, these developed above the shelf break established by a Mesozoic reef. Furthermore, these four Pleistocene clinoforms are distinct from all those before them in one very significant way: their foresets coincided with the continental slope that existed at that time. Previously, all Oligocene and Miocene clinoforms developed above a gently dipping ramp inherited from Eocene time. Sediment that bypassed the clinoform rollover still accumulated on the gentle grade of the Eocene

ramp, and subsequently built upward to lap onto the clinoform foresets. This was not possible once the clinoform foresets reached the true continental slope in the Pleistocene and encountered seaward gradients of 4° or more that continued to the continental rise at > 2200-m water depths. When an angle of repose was established that could retain sediment on these amalgamated clinoform foresets and continental slope, the absence of slope-cutting canyons assured that the Pleistocene upper slope was maintained as a continuously depositional setting. Consequently, a nearly uninterrupted mid-to-late Pleistocene record can now be found on the upper slope of the Hudson Apron.

All four outer-shelf Pleistocene sequences were drilled at ODP Site 1073 on the Hudson Apron in 639 m of water (Austin *et al.*, 1998), and 520 m of mid-to-late Pleistocene sediment was cored with 98% recovery. A total of 16 glacial and interglacial fluctuations of global ice volume were identified on the basis of changes in δO^{18}, yielding a geochronological proxy back to roughly 755 ka. The only time breaks that could be determined were at the very top of the section (seafloor sediments are 14.4 ka based on ^{14}C dating) and spanning Oxygen Isotope Stages 6 and 7; the latter occurred at the boundary between the shallowest two seismic sequences (McHugh & Olson, 2002). No clear hiatus could be determined from available data at the other Pleistocene sequence boundaries. Furthermore, no consistent, one-to-one correspondence was found between glacio-eustatic oscillations inferred from δO^{18} and any aspect of sequences or their boundaries. Numerous successions from mudstone to siltstone to medium sand (but with no detectable hiatus) were found within each of the four seismic sequences, suggesting oscillations of proximal/distal sediment sources without the development of stratal patterns commonly cited as indicators of sea-level change. It remains to be determined what process was responsible for the four seismic sequences; it does not appear to have been simply changes in global sea level. A likely candidate is abrupt and large changes in sediment supplied to the outer shelf. Loading and unloading effects of the Laurentide ice sheet could have amplified rates of erosion and river discharge to such an extent that sequences developed in roughly 100 kyr packages, overwhelming and encompassing any higher-order cyclicity caused by changes in the global ice budget. It remains to be seen if modelling of Pleistocene sedimentation that includes ice-sheet tectonism can duplicate the observations off New Jersey.

The long-term record – where next?

The STRATAFORM case studies of the long-term record in the Eel River Basin and New Jersey margin underscore the acute need for coring deep into continental-margin sediments. These much-needed samples would document the long-term behaviour of the Earth system in general, and would determine the evolution of these two continental margins in particular. The optimal sample locations would require three-dimensional seismic information.

Stratal discontinuities are a common feature in margin sediments and provide objective and valuable divisions of the geological record. While it is widely accepted that these discontinuities are caused by rapid changes in eustatic sea level, tectonism, sediment supply and climate, the scarcity of samples from modern shelves leaves poorly constrained the explanation of how these processes operate and interact on long time-scales. In particular, the water depth at which basin-wide unconformities develop is fundamental to understanding this complex system, and it can be established only by sampling. Morphometric, numerical and physical models of the long-term record help to identify the processes that most influence shallow-water records, but their power to isolate and explain processes is severely weakened by our limited access to long-term, shallow-water records. The Integrated Ocean Drilling Program (IODP) will continue to target the New Jersey margin in coming years. It remains to be seen if the large technological challenges to continuous core recovery can be surmounted. There is near certainty, however, that any amount of deep samples and logs from this effort will improve understanding of how the long-term stratigraphic record is built.

ACKNOWLEDGEMENTS

Most of the high-resolution reflection profiles used in this study were collected under grants N00014-95-1-0200 and N00014-96-1-0377; the vision and

long-standing support of Dr Joseph Kravitz in the Office of Naval Research, in making this work possible, is gratefully acknowledged. Samples of the long-term record offshore New Jersey have been collected by the Ocean Drilling Program. Drilling onshore New Jersey has been supported by cooperative efforts between the ODP, the New Jersey Geological Survey, the US Geological Survey, and the Continental Dynamics Program, Earth Sciences Division of the National Science Foundation. High-resolution profiles in support of ODP drilling were collected under NSF grants OCE89-11810 and OCE97-26273 from the Marine Geology and Geophysics Program, Division of Ocean Sciences. Support for acquiring detailed seismic grids across potential offshore drill sites of the New Jersey margin was provided by Joint Oceanographic Institutions, Inc. The authors thank Michael Field, Roger Flood, James Gardner, James Syvitski, and above all Charles Nittrouer for their very helpful reviews.

REFERENCES

Aalto, K.R, McLaughlin, R.J., Carver, G.A., *et al*. (1995) Uplifted Neogene margin, southernmost Cascadia–Mendocino triple junction region, California. *Tectonics*, **14**(5), 1104–1116.

Agassiz, L. (1840) *Études sur les Glaciers*. Privately published, Neuchatel, 346 pp.

Allen, D., Bergt, D., Best, D., *et al*. (1989) Logging while drilling. *Oilfield Rev*., **1**, 4–17.

Ashley, G.M., Wellner, R.W., Esker, D. and Sheridan, R.E. (1991) Clastic sequences developed during late Quaternary glacio-eustatic sea level fluctuations on a passive margin: example from the inner continental shelf near Barnegat Inlet, New Jersey. *Geol. Soc. Am. Bull*., **103**, 1607–1621.

Atwater, T. (1970) Implications of plate tectonics for the Cenozoic tectonic evolution of Western North America. *Geol. Soc. Am. Bull*., **81**, 3513–3536.

Austin, J.A., Fulthorpe, C.S., Mountain, G.S., Orange, D.L. and Field, M.E. (1996) Continental-margin seismic stratigraphy: Assessing the preservation potential of heterogeneous geological processes operating on continental shelves and slopes. *Oceanography*, **9**, 173–177.

Austin, J.A., Christie-Blick, N., Malone, M. and the Leg 174A Shipboard Party (1998) *Proceedings of the Ocean Drilling Program, Initial Reports*, Vol. 174A. Texas A & M University, Ocean Drilling Program, College Station, TX.

Bartek, L.R., Vail, P.R., Anderson, J.B., Emmet, P.A. and Wu, S. (1991) Effect of Cenozoic ice sheet fluctuations in Antarctica on the stratigraphic signature of the Neogene. *J. Geophys. Res*., **96**, 6753–6778.

Berggren, W.A., Kent, D.V., Swisher, C.C. and Aubry, M.-P. (1995) A revised Cenozoic geochronology and chronostratigraphy. In: *Geochronology, Time Scales and Global Stratigraphic Correlation* (Eds W.A. Berggren, D.V. Kent, M.-P. Aubry and J. Hardenbol), pp. 129–212. Special Publication 54, Society of Economic Paleontologists and Mineralogists,Tulsa, OK.

Bonner, S., Clark, B., Holenka, J., *et al*. (1992) Logging while drilling – a three-year perspective. *Oilfield Rev*., **4**, 4–21.

Borgeld, J.C. (1985) *Holocene stratigraphy and sedimentation on the northern California continental shelf*. Unpublished PhD dissertation, University of Washington, Seattle, 177 pp.

Brown, W.M., III and Ritter, J.R. (1971) Sediment transport and turbidity in the Eel River Basin, California. *U.S. Geol. Surv. Wat. Supply Pap*., **1986**, 70 pp.

Bruhn, C.H.L. and Walker, R.G. (1995) High-resolution stratigraphy and sedimentary evolution of coarse-grained canyon-filling turbidites from the Upper Cretaceous transgressive megasequence, Campos Basin, offshore Brazil. *J. Sediment. Res., Sect. B: Strat. Global Stud*., **65**, 426–442.

Buck, K.F., Olson, H.C. and Austin, J.A., Jr. (1999) Paleoenvironmental evidence for latest Pleistocene sea-level fluctuations on the New Jersey outer continental shelf: combining high-resolution sequence stratigraphy and foraminiferal analysis. *Mar. Geol*., **154**, 287–304.

Burger, R.L., Fulthorpe, C.S. and Austin, J.A., Jr. (2001) Late Pleistocene channel incisions in the southern Eel River Basin, northern California: implications for tectonic *vs*. eustatic influences on shelf sedimentation patterns. *Mar. Geol*., **177**, 317–330.

Burger, R.L., Fulthorpe, C.S., Austin, J.A., Jr. and Gulick, S.P.S. (2002) Lower Pleistocene to Present structural deformation and sequence stratigraphy of the continental shelf, offshore Eel River Basin, northern California. *Mar. Geol*., **185**(3–4), 249–281.

Carey, J.S., Sheridan, R.E. and Ashley, G.M. (1998) Late Quaternary sequence stratigraphy of a slowly subsiding passive margin: New Jersey Continental Shelf. *Bull. Am. Asssoc. Petrol. Geol*., **82**, 773–791.

Carver, G.A. (1987) Late Cenozoic tectonics of the Eel River Basin region, coastal northern California. In: *Tectonics, Sedimentation and Evolution of the Eel River and other Coastal Basins of Northern California* (Eds H. Schymiczek and R. Suchland), pp. 61–72. Miscellaneous Publications 37, San Joaquin Geological Society.

Cathro, D.L., Austin, J.A., Jr. and Moss, G.D. (2003) Progradations along a deeply submerged Oligocene-Miocene heterozoan carbonate shelf: how sensitive are clinoforms to sea-level variations? *Bull. Am. Assoc. Petrol. Geol.*, **87**, 1547–1574.

Christie-Blick, N. (1991) Onlap, offlap and the origin of unconformity-bounded depositional sequences. *Mar. Geol.*, **97**, 35–56.

Christie-Blick, N. and Driscoll, N.W. (1995) Sequence stratigraphy. *Ann. Rev. Earth Planet. Sci.*, **23**, 451–478.

Clarke, S.H., Jr. (1987) Late Cenozoic Geology and Structure of the Onshore-Offshore Eel River Basin, Northern California. In: *Tectonics, Sedimentation and Evolution of the Eel River and Associated Coastal Basins of Northern California* (Eds H. Schymiczek and R. Suchsland), pp. 31–40. Miscellaneous Publication 37, San Joaquin Geological Society.

Clarke, S.H., Jr. (1992) Geology of the Eel River Basin and Adjacent Region: Implications for Late Cenozoic Tectonics of the Southern Cascadia Subduction Zone and Mendocino Triple Junction. *Bull. Am. Assoc. Petrol. Geol.*, **76**, 199–224.

Couch, R.W., Victor, L.P. and Keeling, K.M. (1974) *Coastal and Offshore Earthquakes of the Pacific Northwest between 39° and 49° Latitude and 123° and 131° Longitude*. School of Oceanography, Oregon State University Press, Corvallis, OR, 67 pp.

Crouch, J.K. and S.B. Bachman (1987) Exploration potential, offshore Point Arena and Eel River basins. In: *Tectonics, Sedimentation and Evolution of the Eel River and Associated Coastal Basins of Northern California* (Eds H. Schymiczek and R. Suchsland), pp. 99–111. Miscellaneous Publication 37, San Joaquin Geological Society.

Davies, T.A. and Austin, J.A., Jr. (1997) High-resolution 3D seismic reflection and coring techniques applied to late Quaternary deposits on the New Jersey shelf. *Mar. Geol.*, **143**, 137–149.

Davies, T.A., Austin, J.A., Lagoe, M.B. and Milliman, J.D. (1992) Late Quaternary sedimentation off New Jersey: new results using 3-D seismic profiles and cores. *Mar. Geol.*, **108**, 323–343.

De Verteuil, L. (1997) Miocene dinocyst stratigraphy of the Cape May and Atlantic City boreholes. In: *Proceedings of the Ocean Drilling Program, Scientific Results 150X* (Eds K.G. Miller and S.W. Snyder), pp. 129–146. College Station, TX.

Delius, H., Kaupp, A., Muller, A. and Wohlenberg, J. (2001) Stratigraphic correlation of Miocene to Plio-/Pleistocene sequences on the New Jersey shelf based on petrophysical measurements from ODP 174A. *Mar. Geol.*, **175**, 149–165.

DeMets, C., Gordon, R.G., Argus, D.F. and Stein, S. (1990) Current plate motions. *Geophys. J. Int.*, **101**, 425–478.

Dickinson, W.R., Ingersoll, R.V. and Graham, S.A. (1979) Paleogene sediment dispersal and paleotectonics in northern California. *Geol. Soc. Am. Bull.*, **90**, 145–1528.

Diebold, J.B., Stoffa, P.L. and the LASE study group (1988) A large aperture seismic experiment in the Baltimore Canyon Trough. In: *The Geology of North America*, Vol. I-2, *The Atlantic Continental Margin* (Eds R.E. Sheridan and J.A. Grow), pp. 387–398. Geological Society of America, Boulder, CO.

Doveton, J.H. (1986) *Log Analysis of Subsurface Geology: Concepts and Computer Methods*. Wiley, New York.

Duncan, C.S. and Goff, J.A. (2001) Relict iceberg keel marks on the New Jersey outer shelf, southern Hudson Apron. *Geology*, **29**, 5, 411–414.

Duncan, C.S., Goff, J.A., Austin, J.A., Jr. and Fulthorpe, C.S. (2000) Tracking the last sea-level cycle: seafloor morphology and shallow stratigraphy of the latest Quaternary New Jersey middle continental shelf. *Mar. Geol.*, **170**, 395–421.

Ellis, D.V. (1987) *Well Logging for Earth Scientists*. Elsevier, New York, 532 pp.

Fairbanks, R.G. (1989) A 17,000-year glacio-eustatic sea level record; influence of glacial melting rates on the Younger Dryas event and deep-ocean circulation. *Nature*, **342**, 637–642.

Farre, J.A., McGregor, B.A., Ryan, W.B.F. and Robb, J.M. (1983) Breaching the shelfbreak; passage from youthful to mature phase in submarine canyon evolution. In: *The Shelfbreak; Critical Interface on Continental Margins* (Eds D.J. Stanley and G.T. Moore), pp. 25–39. Special Publication 33, Society of Economic Paleontologists and Mineralogists, Tulsa, OK.

Field, M.E. and Barber, J.H. (1993) A submarine landslide associated with shallow seafloor gas and gas hydrates off northern California. In: *Submarine Landslides: Selected Studies in the U.S. Exclusive Economic Zone* (Eds W.C. Schwab, H.J. Lee and D.C. Twichell). *U.S. Geol. Surv. Bull.*, **2002**, 151–157.

Field, M.E., Gardner, J.V. and Prior, D.B. (1999) Geometry and significance of stacked gullies on the northern California slope. *Mar. Geol.*, **154**, 271–286.

Flower, B.P. and Kennett, J.P. (1995) The middle Miocene climatic transition: East Antarctic ice sheet development, deep ocean circulation and global carbon cycling. *Palaeogeogr. Paleoclimatol. Palaeoecol.*, **108**, 537–555.

Fowler, S. and McKenzie, D.P. (1989) Gravity studies of the Rockall and Exmouth Plateau using SEASAT altimetry. *Basin Res.*, **2**, 27–34.

Fulthorpe, C.S. and Austin, J.A., Jr. (1998) Anatomy of rapid margin progradation: three-dimensional geometries of Miocene clinoforms, New Jersey margin. *Bull. Am. Assoc. Petrol. Geol.*, **82**, 251–273.

Fulthorpe, C.S. and Austin, J.A., Jr. (2004) Shallowly buried, enigmatic seismic stratigraphy on the New Jersey outer shelf: evidence for latest Pleistocene catastrophic erosion? *Geology*, **32**(1), 1013–1016.

Fulthorpe, C.S., Austin, J.A., Jr. and Mountain, G.S. (1999) Buried fluvial channels off New Jersey: did sea-level lowstands expose the entire shelf during the Miocene? *Geology*, **27**(3), 203–206.

Fulthorpe, C.S., Austin, J.A., Jr. and Mountain, G.S. (2000) Morphology and distribution of Miocene slope incisions off New Jersey: are they diagnostic of sequence boundaries? *Geol. Soc. Am. Bull.*, **112**, 817–828.

Galloway, W.E. (1989) Genetic stratigraphic sequences in basin analysis I: Architecture and genesis of flooding-surface bounded depositional units. *Bull. Am. Assoc. Petrol. Geol.*, **73**, 125–142.

Goff, J.A., Swift, D.J.P., Duncan, C.S., Mayer, L.A. and Hughes-Clarke, J. (1999) High-resolution swath sonar investigation of sand ridge, dune and ribbon morphology in the offshore environment of the New Jersey margin. *Mar. Geol.*, **161**, 307–337.

Goff, J.A., Olson, H.C. and Duncan, C.S. (2000) Correlation of side-scan backscatter intensity with grain-size distribution of shelf sediments, New Jersey margin. *Geo-Mar. Lett.*, **20**, 43–49.

Goff, J.A., Kraft, B.J., Mayer, L.A., *et al.* (2004) Seabed characterization on the new Jersey middle and outer shelf: correlatability and spatial variability of sea-floor sediment properties. *Mar. Geol.*, **209**, 147–172.

Goff, J.A., Austin, J.A., Jr., Gulick, S., *et al.* (2005) Recent and modern erosion on the New Jersey outer shelf. *Mar. Geol.*, **216**, 275–296.

Goldberg, D. (1997) The role of downhole measurements in marine geology and geophysics. *Rev. Geophys.*, **35**(3), 315–342.

Goodwin, R.H. and Prior, D.B. (1989) Geometry and depositional sequences of the Mississippi Canyon, Gulf of Mexico. *J. Sediment. Petrol.*, **59**, 318–329.

Gornitz, V., Couch, S. and Hartig, E.K. (2001) Impacts of sea level rise in the New York metropolitan area. *Global Planet. Change*, **32**, 61–88.

Grabau, A.W. (1940) *The Rhythm of the Ages*. Henri Vetch, Peking, 561 pp.

Greenlee, S.M. and Moore, T.C. (1988) Recognition and interpretation of depositional sequences and calculations of sea-level changes from stratigraphic data – offshore New Jersey and Alabama Tertiary. In: *Sea-level Changes; an Integrated Approach* (Eds C.K. Wilgus, B.S. Hastings, C.A. Ross, *et al.*), pp. 329–353. Special Publication 42, Society of Economic Paleontologists and Mineralogists, Tulsa, OK.

Greenlee, S.M., Schroeder, F.W. and Vail, P.R. (1988) Seismic stratigraphic and geohistory analysis of Tertiary strata from the continental shelf off New Jersey – calculation of eustatic fluctuations from stratigraphic data. In: *The Geology of North America,* Vol. I-2, *The Atlantic Continental Margin* (Eds R.E. Sheridan and J.A. Grow), pp. 437–444. Geological Society of America, Boulder, CO.

Greenlee, S.M., Devlin, W.J., Miller, K.G., Mountain, G.S. and Flemings, P.B. (1992) Integrated sequence stratigraphy of Neogene deposits, New Jersey continental shelf and slope: comparison with the Exxon model. *Geol. Soc. Am. Bull.*, **104**, 1403–1411.

Grow, J.A. and Sheridan, R.E. (1988) U.S. Atlantic continental margin; a typical Atlantic-type or passive continental margin. In: *The Geology of North America,* Vol. I-2, *The Atlantic Continental Margin* (Eds R.E. Sheridan and J.A. Grow), pp. 1–8. Geological Society of America, Boulder, CO.

Grow, J.A., Klitgord, K.D. and Schlee, J.S. (1988) Structure and evolution of Baltimore Canyon Trough. In: *The Geology of North America,* Vol. I-2, *The Atlantic Continental Margin* (Eds R.E. Sheridan and J.A. Grow), pp. 269–290. Geological Society of America, Boulder, CO.

Gulick, S.P. and Meltzer, A.M. (2002) Effect of the northward migrating Mendocino Triple Junction on the Eel River forearc basin, California: structural evolution. *Geol. Soc. Am. Bull.*, **114**(12), 1505–1519.

Gulick, S.P., Meltzer, A.M. and Clarke, S.H., Jr. (2002) Effect of the northward migrating Mendocino Triple Junction on the Eel River forearc basin, California: stratigraphic development. *Geol. Soc. Am. Bull.*, **114**(2), 178–191.

Gulick, S.P.S., Goff, J.A., Austin, J.A., Jr., *et al.* (2005) Basal inflection-controlled shelf-edge wedges off New Jersey track sea-level fall. *Geology*, **33**, 5, 429–432.

Hagen, R.A. and P.R. Vogt (1999) Seasonal variability of shallow biogenic gas in Chesapeake Bay. *Mar. Geol.*, **158**, 75–88.

Haller, C.R. (1980) Pliocene biostratigraphy of California. *Am. Assoc. Petrol. Geol. Stud. Geol.*, **11**, 183–341.

Haq, B.U., Hardenbol, J. and Vail, P.R. (1987) Chronology of fluctuating sea levels since the Triassic (250 million years ago to Present). *Science*, **235**, 1156–1167.

Harrison, C.G.A. (1990) Long-term eustasy and epeirogeny in continents. In: *National Research Council Studies in Geophysics: Sea-level Change*, pp. 141–158. National Academy of Sciences, Washington, DC.

Hathaway, J.C., Schlee, J., Poag, C.W., *et al.* (1976) Preliminary study of the 1976 Atlantic Margin Coring Project of the U.S. Geological Survey. *U.S. Geol. Surv. Open File Rep.*, **76–844**, 217 pp.

Hathaway, J.C., Poag, C.W., Valentine, P.C., *et al.* (1979) U.S. Geological Survey Core Drilling on the Atlantic Shelf. *Science*, **206**, 515–527.

Hays, J.D. and Pitman III, W.C. (1973) Lithospheric plate motion, sea-level changes and climatic and ecological consequences. *Nature*, **246**, 18–22.

Heller, P.L., Paola, C., Hwang, I.-G., John, B. and Steel, R. (2001) Geomorphology and sequence stratigraphy due to slow and rapid base-level changes in an experimental subsiding basin (XES 96-1). *Bull. Am. Assoc. Petrol. Geol.*, **85**, 817–838.

Holbrook, W.S. and Kelemen, P.B. (1993) Large igneous province on the U.S. Atlantic margin and implications for magmatism during continental breakup. *Nature*, **364**, 433–436

Hoskins, E.G. and Griffiths, J.R. (1971) Hydrocarbon potential of northern and central California offshore. In: *Future Petroleum Provinces of the United States, their Geology and Potential* (Ed. K.H. Kram), pp. 212–228. Memoir 15, American Association of Petroleum Geologists, Tulsa, OK.

Hovland, M. and Judd, A. (1988) *Seabed Pockmarks and Seepages: Impact on Geology, Biology and the Marine Environment*. Graham and Trotman, London, 293 pp.

Imbrie, J., Hays, J.D., Martinson, D.G., *et al*. (1984) The orbital theory of Pleistocene climate: Support from a revised chronology of the marine $\delta^{18}O$ record. In: *Milankovitch and Climate* (Eds A.L. Berger, J. Imbrie, J. Hays, G. Kukla and B. Saltzman), pp. 269–305. NATO ASI Series, Series C, Mathematical and Physical Sciences, 126, Part 1. D. Reidel, Dordrecht.

Jamieson, T.E. (1865) On the history of the last geological changes in Scotland. *Quat. J. Geol. Soc. London*, **21**, 161–203.

Jansa, L.F. (1981) Mesozoic carbonate platforms and banks of the eastern North American margin. *Mar. Geol.*, **44**, 97–117.

Karner, G.D. (1991) Sediment blanketing and the flexural strength of extended continental lithosphere. *Basin Res.*, **3**, 177–185.

Karner, G.D. and N.W. Driscoll (1997) Three-dimensional interplay of advective and diffusive processes in the generation of sequence boundaries. *J. Geol. Soc. London*, **154**, 443–449.

Keen, C.E. and Beaumont, C. (1990) Geodynamics of rifted continental margins. In: *Geology of the Continental Margin of Eastern Canada* (Eds M.J. Keen and G.L. Williams), pp. 391–472. Decade of North America Geology, Vol. I-1. Geological Survey of Canada and Geological Society of America.

Kelling, G. and Stanley, D.J. (1970) Morphology and structure of Wilmington and Baltimore submarine canyons, Eastern United States. *J. Geol.*, **78**, 637–660.

Kidwell, S.M. (1984) Outcrop features and origin of basin margin unconformities in the lower Chesapeake Group (Miocene), Atlantic coastal plain. *Am. Assoc. Petr. Geol. Mem.*, **37**, 37–57.

Kidwell, S.M. (1988) Reciprocal sedimentation and noncorrelative hiatuses in marine-paralic siliciclastics: Miocene outcrop evidence. *Geology*, **16**, 609–612.

Klitgord, K.D., Poag, C.W., Schneider, C.M. and North, L. (1994) Geophysical database of the east coast of the United States Northern Atlantic margin: cross sections and gridded database (Georges Bank basin, Long Island platform and Baltimore Canyon trough). *U.S. Geol. Surv. Open-File Rep.*, **94–637**, 189 pp.

Knebel, H.J. and Spiker, E. (1977) Thickness and age of surficial sand sheet, Baltimore Canyon trough area. *Bull. Am. Assoc. Petrol. Geol.*, **61**(6), 861–871.

Knebel, H.J., Wood, S.A. and Spiker, E.C. (1979) Hudson River: evidence for extensive migration on the exposed continental shelf during Pleistocene time. *Geology*, **7**, 254–258.

Kominz, M.A. (1984) Oceanic ridge volumes and sea-level change – an error analysis. In: *Interregional Unconformities and Hydrocarbon Accumulation* (Ed. J.S. Schlee), pp. 37–58. Memoir 36, American Association of Petroleum Geologists, Tulsa, OK.

Kominz, M.A. and Pekar, S.F. (2001) Oligocene eustasy from two-dimensional sequence stratigraphic backstripping. *Geol. Soc. Am. Bull.*, **113**, 291–304.

Kominz, M.A., Miller, K.G. and Browning, J.V. (1998) Long-term and short-term global Cenozoic sea-level estimates. *Geology*, **26**, 311–314.

Kooi, H., S. Cloetingh and J. Burrus (1992) Lithospheric necking and regional isostasy at extensional basins, 1, subsidence and gravity modeling with an application to the Gulf of Lions margin (SE France). *J. Geophys. Res.*, **97**, 17,553–17,572.

Kulm, L.D. and Suess, E. (1990) Relationship of carbonate deposits and fluid venting: Oregon accretionary prism. *J. Geophys. Res.*, **95**, 8899–8916.

Kvenvolden, K.A. and Field, M.E. (1981) Thermogenic hydrocarbons in unconsolidated sediments of the Eel River Basin, offshore northern California. *Bull. Am. Assoc. Petrol. Geol.*, **65**, 1642–1646.

Kvenvolden, K.A., G.D. Ginsburg and V.A. Soloviev (1993) Worldwide distribution of subaquatic gas hydrates. *Geo-Mar. Lett.*, **13**, 32–40.

Lagoe, M.B., Davies, T.A., Austin, J.A., Jr. and Olson, H.C. (1997) Foraminiferal constraints on very high-resolution seismic stratigraphy and late Quaternary glacial history, New Jersey continental shelf. *Palaios*, **12**, 249–266.

Lajoie, K.R., Sarna-Wojcicki, A.M. and Ota, Yuko (1982) Emergent Holocene marine terraces at Ventura and Cape Mendocino, California-indicators of high tectonic uplift rates (abstract). *Geol. Soc. Am. Abstr. Progr.*, **14**(4), 178.

Lavier, L. and Steckler, M.S. (1997) Flexural strength of the continental lithosphere: Sediment cover as the last piece of the puzzle. *Nature*, **389**, 476–479.

Lee, H.J., Locat, J., Dartnell, P., Israel, K. and Wong, F. (1999) Regional variability of slope stability: application to the Eel margin, California. *Mar. Geol.*, **154**, 305–321.

Leithold, E.L. and Blair, N.E. (2001) Watershed control on the carbon loading of marine sedimentary particles. *Geochim. Cosmochim. Acta*, **65**, 2231–2240.

Libby-French, J. (1984) Stratigraphic framework and petroleum potential of northeastern Baltimore Canyon Trough, mid-Atlantic outer continental shelf. *Bull. Am. Assoc. Petrol. Geol.*, **68**(1), 50–73.

Lorenson, T.D., McLaughlin, R.J., Kvenvolden, K.A., *et al*. (1998) Comparison of offshore and onshore gas occurrences, Eel River basin, Northern California. *U.S. Geol. Surv. Open-file Rep.*, **98**, 781.

Loutit, T.S., Hardenbol, J., Vail, P.R. and Baum, G.R. (1988) Condensed section: the key to age determination and correlation of continental margin sequences. In: *Sea Level Changes: an Integrated Approach* (Eds C.K. Wilgus, B.S. Hastings, C.G. St.C. Kendall, *et al*.), pp. 183–213, Special Publication 42. Society of Economic Paleontologists and Mineralogists, Tulsa, OK.

Lowrie, W. and Kent, D.V. (2004) Geomagnetic polarity timescale and reversal frequency regimes. In: *Timescales of the Internal Geomagnetic Field* (Eds J.E.T. Channell, D.V. Kent, W. Lowrie and J. Meert), pp. 287–298. Geophysical Monograph 145, American Geophysical Union, Washington, DC.

MacLaren, C. (1842) The glacial theory of Professor Agassiz. *Am. J. Sci.*, **42**, 346–365.

Mahradi, M. (1983) *Physical modeling studies of thin beds*. Unpublished MSc. thesis, University of Houston, 100 pp.

Martin, B.D. and Emery, K.O. (1967) Geology of Monterey Canyon, California. *Bull. Am. Assoc. Petrol. Geol.*, **51**, 2281–2304.

May, J.A., Warme, J.E. and Slater, R.A. (1983) Role of submarine canyons on shelfbreak erosion and sedimentation; modern and ancient examples. In: *The Shelfbreak; Critical Interface on Continental Margins* (Eds D.J. Stanley and G.T. Moore), pp. 315–332. Special Publication 33, Society of Economic Paleontologists and Mineralogists, Tulsa, OK.

McCrory, P.A. (1989) Late Neogene geohistory analysis of the Humboldt Basin and its relationship to convergence of the Juan de Fuca Plate. *J. Geophys. Res.*, **94**(B3), 3126–3138.

McCrory, P.A. (1995) Evolution of a trench-slope basin within the Cascadia subduction margin: the Neogene Humboldt Basin, California. *Sedimentology*, **43**, 223–656.

McCrory, P.A. (1996) Evaluation of fault hazards, northern coastal California. *U.S. Geol. Surv. Open File Rep.*, **96–656**, 87 pp.

McCrory, P.A. (2000) Upper plate contraction north of the migrating Mendocino Triple Junction, northern California: Implications for partitioning of strain. *Tectonics,* **19**(6), 1144–1160.

McGregor, B.A. (1981) Ancestral head of Wilmington Canyon. *Geology*, **9**, 254–257.

McHugh, C.M.G. and Olson, H.C. (2002) Pleistocene chronology of continental margin sedimentation: New insights into traditional models, New Jersey. *Mar. Geol.*, **185**, 389–411.

McLaughlin, R.J., Sliter, W.V., Frederiksen, N.O., Harbert, W.P. and McCulloch, D.S. (1994) Plate motions recorded in tectonostratigraphic terranes of the Franciscan Complex and evolution of the Mendocino Triple Junction, northwestern California. *U.S. Geol. Surv. Bull.*, **1997**, 60 pp.

Mederios, B.P., Karner, D.B., Muller, R.A. and Levine, J. (2000) The global ice volume record as viewed through a benthic δ^{18}O stack. *Eos (Trans. Am. Geophys. Union)* (suppl.), **81**(48), F597.

Miall, A.D. (1991) Stratigraphic sequences and their chronostratigraphic correlation, *J. Sediment. Petrol*, 61, 497–505.

Miller, K.G. and Mountain, G.S. (1994) Global sea-level change and the New Jersey margin. In: *Proceedings of the Ocean Drilling Program, Initial Reports*, Vol. 150 (G.S. Mountain, K.G. Miller, P. Blum, *et al*.), pp. 11–19. College Station, TX.

Miller, K.G., Fairbanks, R.G. and Mountain, G.S. (1987a) Tertiary oxygen isotope synthesis, sea-level history and continental margin erosion. *Paleoceanography*, **2**, 1–19.

Miller, K.G., Melillo, A.J., Mountain, G.S., Farre, J.A. and Poag, C.W. (1987b) Middle to late Miocene canyon cutting on the New Jersey continental slope; biostratigraphic and seismic stratigraphic evidence. *Geology*, **15**, 509–512.

Miller, K.G., Browning, J.V., Liu, C., *et al*. (1994) Atlantic City site report. In: *Proceedings of the Ocean Drilling Program, Initial Reports*, Vol. 150X (K.G. Miller, *et al*.), pp. 35–55. College Station, TX.

Miller, K.G., Liu, C. and Feigenson, M.D. (1996a) Oligocene to middle Miocene Sr-isotopic stratigraphy of the New Jersey continental slope. In: *Proceedings of the Ocean Drilling Program, Scientific Results*, Vol. 150 (Eds G.S. Mountain, K.G. Miller, P. Blum, *et al*.) pp. 97–114. College Station, TX.

Miller, K.G., Mountain, G.S., the Leg 150 Shipboard Party and Members of the New Jersey Coastal Plain Drilling Project (1996b) Drilling and dating New Jersey Oligocene–Miocene sequences: ice volume, global sea level and Exxon records, *Science*, **271**, 1092–1094.

Miller, K., Rufolo, S., Sugarman, P., Pekar, S., Browning, J. and Gwynn, D. (1997a) Early to middle Miocene sequences, systems tracts and benthic foraminiferal biofacies. In: *Proceedings of the Ocean Drilling Program, Scientific Results*, Vol. 150X (Eds K.G. Miller and S.W. Snyder). College Station, TX.

Miller, K.G., Browning, J.V., Pekar, S.F. and Sugarman, P.J. (1997b) Cenozoic evolution of the New Jersey coastal plain: changes in sea level, tectonics and sediment supply. In: *Proceedings of the Ocean Drilling Program, Scientific Results*, Vol. 150X (Eds K.G. Miller and S.W. Snyder), pp. 361–373. College Station, TX.

Miller, K.G., G.S. Mountain, J.S. Browning, *et al*. (1998a) Cenozoic global sea level, sequences and the New Jersey transect: results from coastal plain and continental slope drilling. *Rev. Geophys.*, **36**(4), 569–601.

Miller, K.G., P.J. Sugarman, J.V. Browning, *et al*. (1998b) Bass River site. In: *Proceedings of the Ocean Drilling Program, Initial Reports*, Vol. 174AX (K.G. Miller, P.J. Sugarman, J.V. Browning, *et al*.), pp. 5–43. College Station, TX.

Miller, K.G., Sugarman, P.J., Browning, J.V., *et al*. (1999) Ancora Site. In: *Proceedings of the Ocean Drilling Program, Initial Reports*, Vol. 174AX (Suppl.) (K.G. Miller, P.J. Sugarman, J.V. Browning, *et al*.), pp. 1–65. College Station, TX.

Milliman, J.D., Zhou, J., Li, A.C. and Ewing, J.I. (1990) Late Quaternary sedimentation on the outer and middle New Jersey continental shelf: result of two local deglaciations? *J. Geol.*, **98**, 966–976.

Mitchum, R.M., Vail, P.R. and Thompson, S., III (1977a) Seismic stratigraphy and global changes of sea level, Part 2: the depositional sequence as a basic unit for stratigraphic analysis. In: *Seismic Stratigraphy – Applications to Hydrocarbon Exploration* (Ed. C.E. Payton), pp. 53–62. Memoir 26, American Association of Petroleum Geologists, Tulsa, OK.

Mitchum, R.M., Vail, P.R. and Sangree, J.B. (1977b) Seismic stratigraphy and global changes of sea level, Part 6: stratigraphic interpretation of seismic reflection patterns in depositional sequences. In: *Seismic Stratigraphy – Applications to Hydrocarbon Exploration* (Ed. C.E. Payton), pp. 117–133. Memoir 26, American Association of Petroleum Geologists, Tulsa, OK.

Monteverde, D., Miller, K. and Mountain, G. (2000) Correlation of offshore seismic profiles with onshore New Jersey Miocene sediments. *Sediment. Geol.*, **134**, 111–127.

Morehead, M.D. and Syvitski, J.P. (1999) River-plume Sedimentation Modeling for Sequence Stratigraphy: Application to the Eel Margin, Northern California. *Mar. Geol.*, **154**, 29–42.

Mountain, G.S. (1987) Cenozoic margin construction and destruction offshore New Jersey. In: *Timing and Depositional History of Eustatic Sequences: Constraints on Seismic Stratigraphy* (Eds C. Ross and D. Haman), pp. 57–83. Special Publication 24, Cushman Foundation for Foraminiferal Research, Ithaca, NY.

Mountain, G.S., Miller, K.G., Blum, P. and the Leg 150 Shipboard Party (1994) *Proc. Ocean Drill. Program, Init. Rep.*, **150**, 885 pp.

Mountain, G.S., Damuth, J.E., McHugh, C.M.G., Lorenzo, J.M. and Fulthorpe, C.S. (1996) Origin, reburial and significance of a middle Miocene canyon, New Jersey continental slope. In: *Proceedings of the Ocean Drilling Program, Scientific Results*, Vol. 150 (Eds G.S. Mountain, K.G. Miller, P. Blum, *et al*.), pp. 283–292. College Station, TX.

Mountain, G., McHugh, C., Olson, H. and Monteverde, D. (2001) Glacioeustasy ain't what it used to be: the search for controls on stratigraphic architecture. *Eos (Trans. Am. Geophys. Union)*, 82(47), F749.

Murphy, D.P. (1993) What's new in MWD and formation evaluation. *World Oil*, **214**, 47–52.

Neidell, N.S. and Poggiagliolmi, E. (1977) Stratigraphic modeling and interpretation – geophysical principles and techniques. In: *Seismic Stratigraphy – Applications to Hydrocarbon Exploration* (Ed. C.E. Payton), pp. 417–438. Memoir 26, American Association of Petroleum Geologists, Tulsa, OK.

Niedoroda, A.W., Reed, C.W. and Swift, D.J.P., Arato, A. and Hoyanagi, K. (1995) Modeling shore-normal large-scale coastal evolution. *Mar. Geol.*, **126**, 180–200.

Nilsen, T.H. and Clarke, S.H., Jr. (1987) Geological evolution of the late Cenozoic basins of northern California. In: *Tectonics, Sedimentation and Evolution of the Eel River and other Coastal Basins of Northern California* (Eds H. Schymiczek and R. Suchland), pp. 15–29. Miscellaneous Publications 37, San Joaquin Geological Society.

Nordfjord, S., Goff, J.A., Austin, J.A., Jr. and Sommerfield, C.K. (2005) Seismic geomorphology of buried channel systems on the New Jersey outer shelf: Assessing past environmental conditions. *Mar. Geol.*, **214**, 339–364.

Nystuen, J.P. (1998) History and development of sequence stratigraphy. In: *Sequence Stratigraphy – Concepts and Applications* (Eds F.M. Gradstein, K.O. Sundvik and N.J. Milton), pp. 31–116. Special Publication 8, Norwegian Petroleum Society, Oslo.

Olsson, R.K. and Wise, S.W. (1987) Upper Paleocene to middle Eocene depositional sequences and hiatuses in the New Jersey Atlantic Margin. In: *Timing and Depositional History of Eustatic Sequences: Constraints on Seismic Stratigraphy* (Eds C. Ross and D. Haman), pp. 99–112. Special Publication 24, Cushman Foundation for Foraminiferal Research, Ithaca, NY.

Orange, D.L. (1999) Tectonics, sedimentation and erosion in northern California: submarine geomorphology and sediment preservation potential as a result of three competing processes. *Mar. Geol.*, **154**, 369–382.

Orange, D.L., Angell, M.M. and Lapp, D. (1999) Using seafloor mapping (bathymetry and backscatter) and high resolution sub-bottom profiling for both exploration and production: detecting seeps, mapping geohazards and managing data overload with GIS. *Proceedings, 30th Offshore Technical Conference*, Houston, TX.

Owens, J.P. and Gohn, G.S. (1985) Depositional history of the Cretaceous series in the U.S. coastal plain: stratigraphy, paleoenvironments and tectonic controls of sedimentation. In: *Geologic Evolution of the United States Atlantic Margin* (Ed. C.W. Poag), pp. 25–86. Van Nostrand Reinhold, New York.

Owens, J.P. and Sohl, N. (1969) Shelf and deltaic paleoenvironments in the Cretaceous–Tertiary formations of the New Jersey Coastal Plain. In: *Geology of Selected Areas in New Jersey and Eastern Pennsylvania and Guidebook of Excursions* (Ed. S. Subitsky), pp. 235–278. Rutgers University Press, New Brunswick, NJ.

Paillet, F.L., Cheng, C.H. and Pennington, W.D. (1992) Acoustic waveform logging – advances in theory and application. *Log Anal.*, **33**, 239–258.

Parker, G., Fukushima, Y. and Pantin, H.M. (1986) Self-accelerating turbidity currents. *J. Fluid Mech.*, **171**, 145–181.

Payton, C.E. (Ed.) (1977) *Seismic Stratigraphy – Applications to Hydrocarbon Exploration*. Memoir 26, American Association of Petroleum Geologists, Tulsa, OK, 516 pp.

Poag, C.W. (1977) Foraminiferal biostratigraphy. In: *Geological Studies on the COST No. B-2 well, U.S. Mid-Atlantic Outer Continental Shelf Area* (Ed. P.A. Scholle). *U.S. Geol. Circ.*, **750**, 35–36.

Poag, C.W. (1978) Stratigraphy of the Atlantic continental shelf and slope of the United States. *Ann. Rev. Earth Planet. Sci.*, **6**, 251–280.

Poag, C.W. (1980) Foraminiferal stratigraphy, paleoenvironments and depositional cycles in the outer Baltimore Canyon Trough. In: *Geological Studies on the COST No. B-3 well, U.S. Mid-Atlantic Outer Continental Shelf Area* (Ed. P.A. Scholle). *U.S. Geol. Circ.*, **833**, 44–65.

Poag, C.W. (1985) Depositional history and stratigraphic reference section for central Baltimore Canyon trough. In: *Geologic Evolution of the United States Atlantic Margin* (Ed. C.W. Poag), pp. 217–263. Van Nostrand Reinhold, New York.

Poag, C.W. (1987) The New Jersey Transect: stratigraphic framework and depositional history of a sediment-rich passive margin. In: *Initial Reports of the Deep Sea Drilling Project*, Vol. 95 (Eds C.W. Poag, A.B. Watts and the Leg 95 Shipboard Party), pp. 763–817. US Government. Printing Office, Washington, DC.

Poag, C.W. and Sevon, W.D. (1989) A record of Appalachian denudation in postrift Mesozoic and Cenozoic sedimentary deposits of the U.S. middle Atlantic continental margin. *Geomorphology*, **2**, 119–157.

Poag, C.W., Watts, A.B. and the Leg 95 Shipboard Party. (1987) *Initial Reports of the Deep Sea Drilling Project*, Vol. 95. US Government. Printing Office, Washington, DC, 817 pp.

Poag, C.W. and Ward, L.W. (1993) Allostratigraphy of the U.S. middle Atlantic continental margin – characteristics, distribution and depositional history of principal unconformity-bounded Upper Cretaceous and Cenozoic sedimentary units. *U.S. Geol. Surv. Prof. Pap.*, **1542**.

Posamentier, H.W. and Allen, G.P. (1993) Variability of the sequence stratigraphic model: effects of local basin factors, *Sediment. Geol.*, **86**, 91–109.

Posamentier, H.W. and Allen, G.P. (1999) *Siliciclastic Sequence Stratigraphy – Concepts and Applications*. Concepts in Sedimentology and Paleontology No. 7, Society of Sedimentary Geology, Tulsa, OK, 210 pp.

Posamentier, H.W. and Vail, P.R. (1988) Eustatic controls on clastic deposition II – sequence and systems tract models. In: *Sea Level Changes: an Integrated Approach* (Eds C.K. Wilgus, B.S. Hastings, C.G. St.C. Kendall, *et al.*), pp. 125–154. Special Publication 42, Society of Economic Paleontologists and Mineralogists, Tulsa, OK.

Posamentier, H.W., Jervey, M.T. and Vail, P.R. (1988) Eustatic controls on clastic deposition I – conceptual framework. In: *Sea Level Changes: an Integrated Approach* (Eds C.K. Wilgus, B.S. Hastings, C.G. St.C. Kendall, *et al.*), pp. 109–124. Special Publication 42, Society of Economic Paleontologists and Mineralogists, Tulsa, OK.

Prather, B.E. (1991) Petroleum geology of the Upper Jurassic and Lower Cretaceous, Baltimore Canyon Trough, western North Atlantic Ocean. *Bull. Am. Assoc. Petrol. Geol.*, **75**(2), 258–277.

Pratson, L.F., Ryan, W.B.F., Mountain, G.S. and Twichell, D.C. (1994) Submarine canyon initiation by downslope-eroding sediment flows; evidence in late Cenozoic strata on the New Jersey continental slope. *Geol. Soc. Am. Bull.*, **106**, 395–412.

Reynolds, D.J., M.S. Steckler and B.J. Coakley (1991) The role of the sediment load in sequence stratigraphy: the influence of flexural isostasy and compaction, *J. Geophys. Res.*, **96**, 6931–6949.

Ruch, P., Mirmand, M., Jouanneau, J.M. and Latouche, C. (1993) Sediment budget and transfer of suspended

sediment from the Gironde Estuary to Cap Ferret Canyon. *Mar. Geol.*, **111**, 109–119.

Ruddiman, W.F., Raymo, M.E., Martinson, D.G., Clement, B.M. and Backman, J. (1989) Pleistocene evolution: northern hemisphere ice sheets and north Atlantic Ocean. *Paleoceanography*, **4**(4), 353–412.

Savin, S. (1977) The history of the Earth's surface temperature during the past 100 million years, *Ann. Rev. Earth Planet. Sci.*, **5**, 319–355.

Schlee, J.S. (1981) Seismic stratigraphy of the Baltimore Canyon Trough. *Bull. Am. Assoc. Petrol. Geol.*, **65**, 26–53.

Schwab, W.C., Denny, J.F., Foster, D.S., *et al.* (2002) High-Resolution Quaternary Seismic Stratigraphy of the New York Bight Continental Shelf. *U.S. Geol. Soc. Open-File Rep.*, **02-152**.

Sclater, J.G. and P.A. Christie (1980) Continental stretching: an explanation of the post Mid-Cretaceous subsidence of the Central North Sea basin. *J. Geophys. Res.*, **85**, 3711–3739.

Sheridan, R.E., Gradstein, F. and the Leg 76 Shipboard Party (1983) *Initial Reports of the Deep Sea Drilling Project*, Vol. 76. US Government. Printing Office, Washington, DC, 947 pp.

Sheridan, R.E., Grow, J.A. and Klitgord, K.C. (1988) Geophysical data. In: *The Geology of North America*, Vol. I-2, *The Atlantic Continental Margin* (Eds R.E. Sheridan and J.A. Grow), pp. 177–195. Geological Society of America, Boulder, CO.

Sheridan, R.E., Ashley, G.M., Miller, K.G., *et al.* (2000) Offshore-onshore correlation of upper Pleistocene strata, New Jersey coastal Plain to continental shelf and slope. *Sediment. Geol.*, **134**, 197–207.

Sheriff, R.E. (1977) Limitations on resolution of seismic reflections and geologic detail derivable from them. In: *Seismic Stratigraphy – Applications to Hydrocarbon Exploration* (Ed. C.E. Payton), pp. 3–14. Memoir 26, American Association of Petroleum Geologists, Tulsa, OK.

Sheriff, R.E. (1985) Aspects of seismic resolution. In: *Seismic Stratigraphy II – an Integrated Approach to Hydrocarbon Exploration* (Eds O.R. Berg and E.G. Woolverton), pp. 1–10. Memoir 39, American Association of Petroleum Geologists, Tulsa, OK.

Sloss, L.L. (1963) Sequences in the cratonic interior of North America, *Geol. Soc. Am. Bull.*, 74, 93–114.

Song, G.S., Ma, C.P. and Yu, H.S. (2000) Fault-controlled genesis of the Chilung sea valley (northern Taiwan) revealed by topographic lineaments. *Mar. Geol.*, **169**, 305–325.

Spinelli, G.A. and Field, M.E. (2001) Evolution of continental slope gullies on the northern California margin, *J. Sediment. Res.*, **71**(2), 237–245.

Stanford, S.D., Ashley, G.M. and Brenner, G.J. (2001) Late Cenozoic fluvial stratigraphy of the New Jersey Piedmont: a record of glacioeustasy, planation and incision on a low-relief passive margin. *J. Geol.*, 109, 265–276.

Stanley, D.J. and Kelling, G. (1978) *Sedimentation in Submarine Canyons, Fans and Trenches*. Dowden, Hutchinson and Ross, Stroudsburg, PA, 382 pp.

Steckler, M.S. and Watts, A.B. (1982) Subsidence history and tectonic evolution of Atlantic-type continental margins. In: *Dynamics of Passive Margins* (Ed. R.A. Scrutton), pp. 184–196. Geodynamic Series, No. 6, American Geophysical Union, Washington, DC.

Steckler, M.S., A.B. Watts and J.A. Thorne (1988) Subsidence and basin modeling at the U.S. Atlantic passive margin. In: *The Geology of North America*, Vol. I-2, *The Atlantic Continental Margin* (Eds R.E. Sheridan and J.A. Grow), pp. 399–416. Geological Society of America, Boulder, CO.

Steckler, M.S., D.J. Reynolds, B.J. Coakley, B.A. Swift and R.D. Jarrard (1993) Modeling passive margin sequence stratigraphy. In: *Sequence Stratigraphy and Facies Associations* (Eds H.W. Posamentier, C.P. Summerhayes, B.U. Haq and G.P. Allen), pp. 19–41. Special Publication 18, International Association of Sedimentologists. Blackwell Scientific Publications, Oxford.

Steckler, M.S., G.S. Mountain, K.G. Miller and N. Christie-Blick (1999) Reconstruction of Tertiary progadation and clinoform development on the New Jersey passive margin by 2-D backstripping. *Mar. Geol.*, **154**, 399–420.

Stille, H. (1924) *Grundfragen der vergleichenden Tektonik*. Borntraeger, Berlin, 443 pp.

Sugarman, P.J. and Miller, K.G. (1997) Correlation of Miocene sequences and hydrogeologic units, New Jersey Coastal Plain, *Sediment. Geol.*, **108**, 3–18.

Sugarman, P.J., Miller, K.G., Owens, J.P. and Feigenson, M.D. (1993) Strontium isotope and sequence stratigraphy of the Miocene Kirkwood Formation, Southern New Jersey, *Geol. Soc. Am. Bull.*, **105**, 423–436.

Sugarman, P., McCartan, L., Miller, K., *et al.* (1997) Strontium-isotopic correlation of Oligocene to Miocene sequences, New Jersey and Florida. In: *Proceedings of the Ocean Drilling Program, Scientific Results*, Vol. 150X (Eds K.G. Miller and S.W. Snyder), pp. 147–159. College Station, TX.

Swift, D.J.P., Moir, R. and Freeland, G.L. (1980) Quaternary rivers on the New Jersey shelf: relation of seafloor to buried valleys. *Geology*, **8**, 276–280.

Syvitski, J.P.M., Pratson, L. and O'Grady, D. (1999) Stratigraphic predictions of continentnal margins for

the US Navy. In: *Numerical Experiments in Stratigraphy: Recent Advances in Stratigraphic and Sedimentologic Computer Simulations* (Eds J.W. Harbaugh, W.L. Watney, E.C. Rankey, *et al*.), pp. 219–236. Special Publication 62, Society of Economic Paleontologists and Mineralogists, Tulsa, OK.

Teller, J.T. (1987) Proglacial lakes and the southern margin of the Laurentide ice sheet. In: *North America and Adjacent Oceans during the Last Deglaciation* (Eds W.F. Ruddiman and H.E. Wright), pp. 39–69. Geological Society of America, Boulder, CO.

Tittman, J. (1991) Vertical resolution of well logs – recent developments. *Oilfield Rev*., **3**, 24–28.

Tucker, P. and Yorston, H. (1973) *Pitfalls in Seismic Interpretation*. Monograph Series, No. 2, Geophysicists Society of Exploration, 50 pp.

Tushingham, A.M. and Peltier, W.R. (1991) ICE–3G: a new global model of late Pleistocene deglaciation based upon geophysical predictions of post glacial relative sea level change, *J. Geophys. Res*., **96**, 4497–4523.

Twichell, D.C. and Roberts, D.G. (1982) Morphology, distribution and development of submarine canyons on the United States Atlantic continental slope between Hudson and Baltimore canyons. *Geology*, **10**, 408–412.

Twichell, D.C., Knebel, H.J. and Folger, D.W. (1977) Delaware River: evidence for its former extension to Wilmington Submarine Canyon. *Science*, **195**, 483–485.

Uchupi, E., Driscoll, N., Ballard, R.D. and Bolmer, S.T. (2001) Drainage of late Wisconsin glacial lakes and the morphology and late Quaternary stratigraphy of the New Jersey – southern New England continental shelf and slope. *Mar. Geol*., **172**, 117–145.

Ulicny, D., Nichols, G. and Waltham, D. (2002) Role of initial depth at basin margins in sequence architecture: field examples and computer models. *Basin Res*., **14**(3), 347–360.

Vail, P.R. (1987) Seismic stratigraphy interpretation using sequence stratigraphy. Part 1: seismic stratigraphy interpretation procedure. In: *Atlas of Seismic Stratigraphy*, Vol. 1 (Ed. A.W. Bally), pp. 1–10. Studies in Geology, No. 27, American Association of Petroleum Geologists, Tulsa, OK.

Vail, P.R., Mitchum, Jr. R.M. and Thompson, S. III, (1977) Seismic stratigraphy and global changes of sea level, Part 4: Global cycles of relative changes of sea level. In: *Seismic Stratigraphy – Applications to Hydrocarbon Exploration* (Ed. C.E. Payton), pp. 83–98. Memoir 26, American Association of Petroleum Geologists, Tulsa, OK.

Van Hinte, J.A., Wise, S.W. and the Leg 93 Shipboard Party (1987) *Initial Reports of the Deep Sea Drilling Project*, Vol. 93. US Government. Printing Office, Washington, DC, 1423 pp.

Van Waggoner, J.C., Posamentier, H.W., Mitchum, R.M., *et al*. (1988) An overview of the fundamentals of sequence stratigraphy and key definitions. In: *Sea-level Changes; an Integrated Approach* (Eds C.K. Wilgus, B.S. Hastings, C.A. Ross, *et al*.), pp. 39–45. Special Publication 42, Society of Economic Paleontologists and Mineralogists, Tulsa, OK.

Von der Borch, C.C., Grady, A.E., Aldam, R., *et al*. (1985) A large-scale meandering submarine canyon; outcrop example from the late Proterozoic Adelaide Geosyncline, South Australia. *Sedimentology*, **32**, 507–518.

Walther, J. (1894) *Einleitung in die Geologie als Historische Wissenschaft, Bd. 3, Lithogenesis der Gegenwart*, pp. 535–1055. G. Fischer Verlag, Jena.

Watts, A.B. (1988) Gravity anomalies, crustal structure and flexure of the lithosphere at the Baltimore Canyon Trough. *Earth Planet. Sci. Lett*., **89**, 221–138.

Watts, A. and Steckler, M.S. (1979) Subsidence and eustasy at the continental margins of eastern North America. In: *The Continental Margins and Paleoenvironments: Deep Drilling Results in the Atlantic Ocean* (Eds W. Talwani and W. Ryan), pp. 273–310. Maurice Ewing Symposium 3, American Geophysical Union, Washington, DC.

Watts, A.B. and Thorne, J.A. (1984) Tectonics, global changes in sea-level and their relationship to stratigraphic sequences at the U.S. Atlantic continental margin. *Marine Petrol. Geol*., **1**, 319–339.

Watts, A.B., Karner, G.D. and Steckler, M.S. (1982) Lithospheric flexure and the evolution of sedimentary basins. In: *The Evolution of Sedimentary Basins* (Eds Sr. P. Kent, M.H.P. Bott, D.P. McKenzie and C.A. Williams). *Philos. Trans. Roy. Soc. London*, **305A**, 249–281.

Weed, E.G.A., Minard, J.P., Perry, W.J., Rhodehamel, E.C. and Robbins, E.I. (1974) *Generalized pre-Pleistocene geologic map of the northern United States Atlantic continental margin*, Map I–861 (scale 1:1,000,000). Miscellaneous Geological Investigation Series, US Geological Survey.

Wheatcroft, R.A., Borgeld, J.C., Born, R.S., *et al*. (1996) The anatomy of an oceanic flood deposit. *Oceanography*, **3**(9), 158–162.

Widess, M.B. (1973) How thin is a thin bed? *Geophysics*, **38**(6), 1176–1180.

Wonham, J.P., Jayr, S., Mougamba, R. and Chuilon, P. (2000) 3D sedimentary evolution of a canyon fill (lower Miocene-age) from the Mandorove Formation, offshore Gabon. *Mar. Petrol. Geol*., **17**, 175–197.

Wood, L.J., Ethridge, F.G. and Schumm, S.A. (1993) The effects of rate of base-level fluctuation on coastalplain,

shelf and slope depositional systems; an experimental approach. In: *Sequence Stratigraphy and Facies Associations* (Eds H.W. Posamentier, C.P. Summerhayes, B.U. Haq and G.P. Allen), pp. 43–53. Special Publication 18, International Association of Sedimentologists. Blackwell Scientific Publications, Oxford.

Woodward-Clyde Consultants (1980) *Evaluation of the Potential for Resolving the Geologic and Seismic Issues at the Humboldt Bay Power Plant Unit No. 3*. Unpublished Final Report Prepared for Pacific Gas and Electric Company, 309 pp.

Yun, J.W., Orange, D.L. and Field, M.E. (1999) Subsurface gas offshore of northern California and its link to submarine geomorphology. *Mar. Geol.*, **154**, 357–368.

Zachos, J.C., Stott, L.D. and Lohmann, K.C. (1994) Evolution of early Cenozoic marine temperatures. *Paleoceanography*, **9**, 353–387.

Zachos, J.C., Pagani, M., Sloan, L., Thomas, E. and Billups, K. (2001) Trends, rythyms and aberrations in global climate 65 Ma to Present. *Science*, **292**, 686.